KTH ROYAL INSTITUTE OF TECHNOLOGY

UNIVERSITA' DEGLI STUDI DI PADOVA

Degree Project in Medical Engineering

Second Cycle, 30 credits

Stockholm, Sweden 2023

Pilot Study on Working Memory:

Investigating Single Trial Decoding to Find the Best Stimulus and Target for a Future Personalized Neurofeedback

Author: Erik Gasparini

Supervisors: Luca Tonin and Herman Pawel

KTH ROYAL INSTITUTE OF TECHNOLOGY

SCHOOL OF ENGINEERING SCIENCES IN CHEMISTRY, BIOTECHNOLOGY AND HEALTH

UNIVERSITA' DEGLI STUDI DI PADOVA

DIPARTIMENTO DI INGEGNERIA DELL'INFORMAZIONE

Pilot Study on Working Memory: Investigating Single Trial Decoding to Find the Best Stimulus and Target for a Future Personalized Neurofeedback

Pilotstudie om arbetsminne: Undersökning av enstaka provavkodning för att hitta den bästa stimulansen och det bästa målet för en framtida personlig neurofeedback

Authors

Erik Gasparini
Master of Science Thesis in Medical Engineering
Advanced level (second cycle), 30 credits
TRITA-CBH-GRU-2023:148

Place for Project

School of Engineering Sciences in Chemistry , Biotechnology and Health (CBH)
KTH Royal Institute of Technology
SE-141 86 Huddinge, Stockholm, Sweden
http://www.kth.se/cbh

Examiner

Matilda Larsson - KTH Royal Institute of Technology

Supervisor

Pawel Herman - KTH Royal Institute of Technology
Luca Tonin - Università degli Studi di Padova

Reviewer

Maksims Kornevs - KTH Royal Institute of Technology

Abstract

A standard Neurofeedback approach to mitigate the working memory decline in some fragile groups (elderly, subjects affected by stroke or Alzheimer's disease) can be suboptimal for some patients. The goal of this research is to investigate which visual stimulus (among colour, geometrical shape, direction, and symbol) is the most suited for each of the six healthy participants and which brain areas are the most discriminative, during the maintenance of a presented stimulus in a retro-cue-based working memory experiment. In order to identify the most discriminative stimulus, the single-trial classification accuracies of some Support Vector Machines, trained on the theta, alpha and beta electroencephalography power bands, have been compared; while, in order to identify the most involved brain regions, three machine learning feature reduction techniques have been explored: the first based on a massive univariate analysis, the second based on multivariate filtering and wrapping, and the last one based on Frequency-based Common Spatial Pattern. The results have shown that the univariate approach, more than the others, managed to clearly identify for each participant at least one preferential type of stimulus and a brain region of discriminative electrodes during the maintenance of the stimulus. These promising results can be interpreted as a further step to optimize the Neurofeedback working memory enhancement through a personalised approach.

Keywords

Visual working memory; Personalised neurofeedback; Visual stimulus; Targeted brain region.

Sammanfattning

En vanlig Neurofeedback-metod för att mildra försämringen av arbetsminnet i vissa bräckliga grupper (äldre, patienter som drabbats av stroke eller Alzheimers sjukdom) kan vara suboptimal för vissa patienter. Målet med denna forskning är att undersöka vilken visuell stimulans (blandat färg, geometrisk form, riktning och symbol) som är mest lämpad för var och en av de sex friska deltagarna och vilka hjärnområden som är mest diskriminerande under upprätthållandet av en presenterad stimulus i ett retro-cue-baserat arbetsminnesexperiment. För att identifiera den mest diskriminerande stimulansen har klassificeringsnoggrannheten i enstaka försök för vissa Support Vector Machines, tränade på theta-, alfa- och beta-elektroencefalografi-effektbanden, jämförts; medan, för att identifiera de mest inblandade hjärnregionerna, har tre tekniker för reducering av maskininlärningsfunktioner utforskats: den första baserad på en massiv univariat analys, den andra baserad på multivariat filtrering och inpackning, och den sista baserad på Frequency-based Common Rumsligt mönster. Resultaten har visat att det univariata tillvägagångssättet, mer än de andra, lyckades tydligt identifiera för varje deltagare åtminstone en föredragen typ av stimulans och en hjärnregion av diskriminerande elektroder under upprätthållandet av stimulansen. Dessa lovande resultat kan tolkas som ett ytterligare steg för att optimera förbättringen av Neurofeedback- arbetsminnet genom ett personligt tillvägagångssätt.

Nyckelord

Visuellt arbetsminne; Personlig neurofeedback; Visuell stimulans; Riktad hjärnregion.

Acknowledgements

Alla conclusione di questa avventura, che ha riservato molti eventi inaspettati, desidero esprimere la mia profonda gratitudine a tutte le persone che mi hanno accompagnato lungo questo importante tratto della mia vita.

Innanzitutto, vorrei ringraziare il mio Relatore a Stoccolma, il professor *Herman Pawel*. La sua presenza è stata il fulcro del mio soggiorno svedese, e desidero ringraziarlo di cuore per avermi aiutato a delineare il percorso che desidero intraprendere nella mia futura carriera professionale. Inoltre, desidero estendere i miei ringraziamenti alla dottoressa *Charles Chernik* e a tutti i membri del *Karolinska Institutet* che ci hanno fornito l'equipaggiamento necessario per la raccolta dei dati. Senza la loro preziosa collaborazione, il progetto non sarebbe stato completato con successo. Vorrei inoltre esprimere la mia gratitudine al mio Scientific Reviewer, il dottor *Maksims Kornevs*, la cui guida e gentilezza mi hanno sostenuto durante i momenti più difficili. Infine, desidero ringraziare il mio relatore a Padova, il professor *Luca Tonin*, per la sua attenta supervisione che ha permesso di curare dettagliatamente l'elaborato finale.

In secondo luogo, vorrei rivolgere un sentito ringraziamento a tutti i compagni che ho incontrato durante il mio soggiorno a Stoccolma. In particolare, desidero menzionare *Noè Bernandes*, *Jinya Kimura* e *Kento Tsuboi*, che sono stati compagni preziosi in numerose serate. Vorrei anche ringraziare il gruppo del *THS-Main*, in particolare *Emanuele D'Allestro*, con il quale abbiamo organizzato molti eventi indimenticabili. Infine, vorrei esprimere la mia gratitudine a tutti gli amici che mi hanno sostenuto durante la mia assenza. In particolare, vorrei ringraziare *Taras Rashkevych*, *Marco Rosson*, *Fabio Strappazzon* e *Mario Semperbon*, nonché i miei due compagni di avventura più stretti: *Alessio Buda* e *Marco Pinamonti*. Grazie di cuore, ragazzi, senza di voi probabilmente sarei impazzito (o almeno più di quanto non lo sia ora).

Desidero quindi ringraziare mio fratello *Ruben*, che è stato sempre vicino a me in modo incondizionato. Vorrei esprimere la mia gratitudine anche a mia madre *Francesca*, mio padre *Luigi*, mia sorella *Alba*, alla mia splendida principessina *Eva* e alla nonna *Giovanna*, per il sostegno e il calore che mi hanno donato in questi mesi.

Infine, desidero dedicare un ringraziamento speciale alla mia bellissima ragazza *Elisa Querinuzzi*. Se sono sopravvissuto a questa esperienza, è solo merito tuo. Queste brevi parole non saranno mai sufficienti per esprimere l'amore e il rispetto che provo per te. Ti amo.

Acronyms

WM	Working memory
VWM	Visual working memory
EEG	Electroencefalography
fMRI	Functional magnetic resonance imaging
iEEG	Intracranial electroencephalography
MEG	Magnetoencephalography
EOG	Electroculogram
MVPA	Multivariate pattern analysis
ICA	Independent Component Analysis
PSD	Power Spectral Density
FDR	False Discovery Rate
FS	Fisher Score
mrmr	Minimum Redundancy Maximum Relevance
MIQ	Mutual Information Quotient
KS	Kendall's Tau Score
FCSP	Frequency Common Spatial Pattern
ADHD	Attention Deficit in Hyperactivity Disorders

Contents

List of Figures

List of Tables

Chapter 1

Introduction

Leaving an item at the supermarket after shopping has happened to everyone, forgetting the keys at home while answering the phone can be annoying, but finding yourself in the middle of a room without knowing why you entered could be a different case. It can indicate a Working memory (WM) decline. Working memory is a very important cognitive function that allows the temporally storing of information for further processing [1]. Therefore, it is an essential function to perform planning, reasoning, problem-solving, and reading comprehension [2]. Nonetheless, some brain disorders such as Schizophrenia, Alzheimer's disease, and major depression have been associated with deficits in this cognitive function [3, 4, 5, 6]. Despite some approaches, such as neuromodulation and neurofeedback [7, 8], having managed to promisingly mitigate this decline [9], almost 30% of the participants did not result in improvements with these techniques. Therefore, some authors [10, 11] highlighted the necessity to define for each patient a personalised stimulus and targeted brain region to reduce the number of non-responders. Indeed, the identification of individual-specific stimuli and relative discriminative regions could maximise the classifiers' capability of decoding task-related brain activities and, therefore, improve the clinical outcome.

The **goal** of this research is to investigate whether some Electroencefalography (EEG) related differences across subjects are present during the working memory maintenance of an item (after its disappearance) depending on the visual stimulus (among colour, geometrical shape, direction, and symbol), and to define which are the most discriminative areas in a single trial classification. To answer these questions,

six healthy participants have been involved in a working memory experiment based on a retro-cue paradigm. These differences have been assessed considering the single-trial performances, especially in terms of generalisability, of some Machine Learning models, and by investigating the position of the EEG electrodes responsible for such discrimination. The tested models were Support Vector Machines mainly trained on the theta, alpha, and beta powers of the pre-processed signals, while the discriminative areas have been investigated using three different methods: the first has been based on a mass univariate approach, the second has been based on a multivariate technique that exploits filtering and wrapping to reduce the number of features, and the final one has been based on a spatial filter. Not only future neurorehabilitation research could benefit from these findings to comprehend the importance of a personalised approach, but also neurocognitive experts could benefit from this comparison across stimuli as a first step to study the volitional control of working memory with Neurofeedback during cognitive tasks.

The rest of the present document has been organised following this structure: firstly, in the *Background* section, the choice of the EEG as the acquisition method (compared to the other classical methods), and the differences between an averaged approach and single-trial decoding have been described. Secondly, in the *Methodology* section, the experimental paradigm, the pre-processing, and the processing steps have been listed. Moreover, the three explored machine learning techniques have been explained in a more detailed way. Then, in the *Results* section, the behavioural and physiological performances have been reported, specifically describing one random participant as a representation of the obtained results. Finally, in the *Discussion* section, the coherence with previous results and the importance of the individualised analysis have been highlighted. Whilst the limitations of the study have been discussed in the *Future Work* section, and a final summary has been reported in the *Conclusion* section.

Chapter 2

Background

Working memory refers to the capability of a brain system to temporarily store and manipulate the information necessary for such complex cognitive tasks as language comprehension, learning, and reasoning [1]. Visual working memory (VWM) acts in the same way: maintaining and processing visual information [12]. While VWM decline has been associated with age [13], early stages of Alzheimer's disease [14], or as a consequence of brain injury [15, 16] or stroke [17, 18]; some novel techniques such as Neuromodulation [19, 20] or Neurofeedback [21] has shown some benefits for healthy elderly [22] and young [23] subjects; and for patients who suffer from Mild Cognitive Impairment [24]. Hence, more and more attention has been given to the study of these techniques as possible treatments for mitigating WM neural decline [22, 24]. Neurofeedback, specifically, is a technique that allows subjects to self-regulate their brain activity in a closed-loop scenario relying on humans' learning abilities and on brain plasticity by activating reinforcement learning networks [25]. This modulation can be achieved during a cognitive task through real-time visual and/or audio information about brain waves as feedback [22] (Figure 2.0.1). Therefore, cerebral activity is recorded during a cognitive task through a non-invasive system (such as EEG), and some features (such as electrode powers) are used to classify among experimental conditions. Finally, the features are reported, depending on the classifier outputs, through visual (such as filling bars or moving circles) or auditory (such as changing continuous tones) feedback. This neurocognitive training technique has already been adapted to other clinical applications [21]: for the treatment of attention deficit hyperactivity disorders, anxiety, depression, epilepsy, insomnia, drug addiction, schizophrenia, learning disabilities, dyslexia, and dyscalculia. Despite all

these findings in different areas, most of the benefits have been shown at a group level; some authors [10, 11] pointed out the presence of almost 30% of Neurofeedback non-responders for VWM enhancement, highlighting the necessity to have individual-specific targets (both in terms of cerebral area under investigation and suited feedback) in order to achieve proper individualised benefits [26].

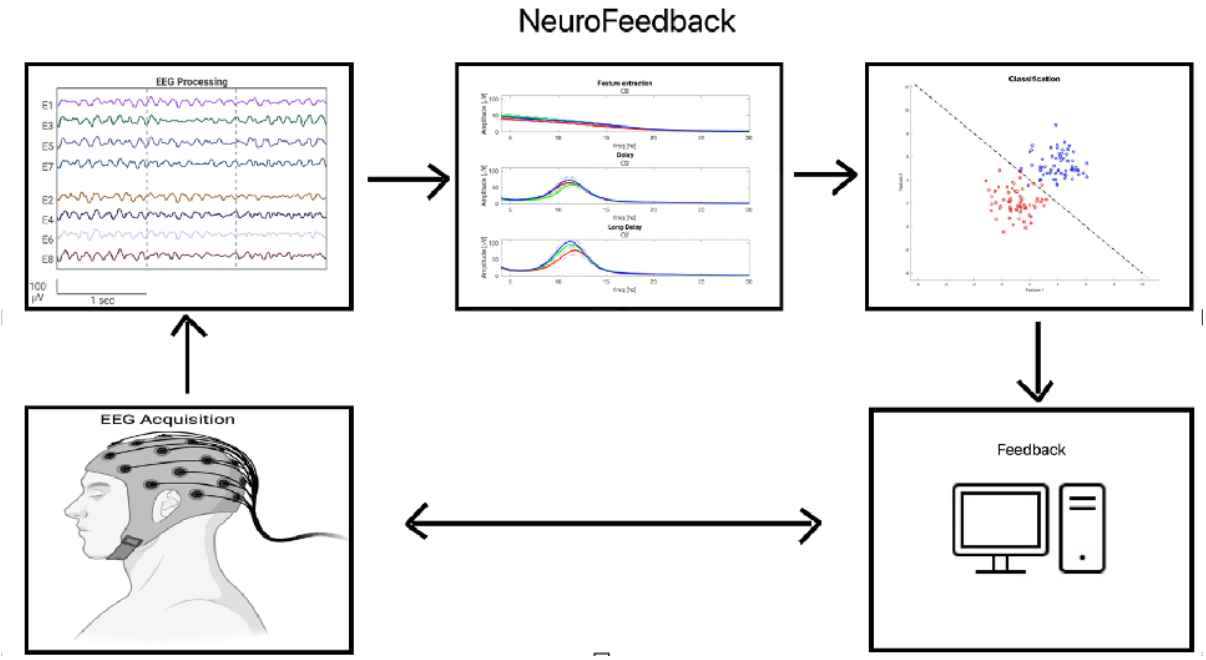

Figure 2.0.1: Neurofeedback scheme – the EEG signals have been acquired, pre-processed, and the extracted features have been used to train a classifier. The classification performances have been reported to the participant in real-time.

The traditional methodologies to investigate the brain areas active during a visual working memory task are Functional magnetic resonance imaging (fMRI), Intracranial electroencephalography (iEEG), Magnetoencephalography (MEG), and EEG). fMRI is a spread technique in neuroimaging, and it is commonly applied to determine which brain areas have changed their concentration of Deoxy and Oxy haemoglobin (BOLD signal) over an interval of time; hence, it relies on the assumption that activations of specific brain regions are followed by a difference in the blood supply. In the VWM context, this technique has been used, for example, to predict if a group of participants is going to remember or forget the targeted item [27]. The main advantage of fMRI is the optimal spatial resolution (2mm); In contrast, the low temporal resolution (seconds), the high cost, the neurovascular coupling, and possible experimental constraints (due to the MRI scanner) lead it to be not the best candidate to follow the brain activity during neurofeedback. iEEG acquisitions on monkeys have

revolutionised the current understanding of working memory through the decoding of the activity of single neurons or groups of neurons (Local Field Potential [28]). These high temporal and spatial resolution data acquisitions have allowed overcoming the classical view of working memory as led by the sustained activity of neurons within the prefrontal cortex [29]; revealing high dynamicity of the representation over time [30], and "activity-silent" configuration in which the memory could be maintained during silent phases due to short-term plasticity [31]. However, the insertion of such electrodes in the human brain requires surgical operations, and the high risk of infections allows the implantations only for medical reasons (to detect epileptic seizures [32]). MEG and EEG are non-invasive recording methodologies sensitive to the electromagnetic synchronous activity of large populations of cortical neurons. Even if these scalp measures are not a unique representation of the generating sources [33], scalp topographies can be compared to different spatial patterns generated by different neuronal populations [34]. Both have a high temporal resolution, while the better spatial resolution of MEG is counterbalanced by its high cost, and by the instrument dimensions that bring it to be hardly used on large populations or in out-of-lab environments. Despite the low spatial resolution, the low signal-to-noise ratio, and the high inter and intra-subject variability of the EEG, some experiments managed to build reliable classifiers to predict subject-specific performances in working memory tasks [9, 35, 36]. Considering its low cost and portability [37], it resulted to be the optimal candidate for the purpose of this analysis.

Some previous iEEG, fMRI, MEG and EEG studies have permitted the decoding of specific objects information from neural activity. Colour and Orientation encoding information has been invasively recorded from many cortical areas of macaques, and in non-invasive electrophysiological acquisitions from macaques and monkeys [38]. The encoding of the items with non-invasive techniques has been reached mainly with Multivariate pattern analysis (MVPA), investigating the time-by-time classifier performances. This methodology has been used to successfully decode orientation [39, 40, 41], location, frequency, motion orientation, colour [42, 43, 44, 45], and colour and luminance [46]. It is important to note, that spatial stimuli (orientation, location, frequency, and motion orientation) have been shown to be strongly susceptible to eye movements (spatial biases in micro-saccades), leading to biased results [47, 48]. Some fMRI studies tried to individuate the active brain regions with different VWM stimuli. *Lee S. and Baker C. (2016)* [49], for example, reviewed some fMRI studies highlighting

the general role of the Visual Cortex during WM maintenance for different stimuli, but also the presence of some Frontal and Parieto-Occipital activations for specific stimuli (Position and Direction). Whilst *Christophel T. et al.* [50] showed the role of the same brain areas to decode shapes during VWM maintenance. About MEG and EEG, only a few works have compared the encoding of different visual stimuli like *Hajonides et al. (2021)* [51] (in his Supplementary Materials section) who found above-chance decoding during the stimulus encoding of colour, but not of orientation after averaging all contralateral posterior electrodes. Moreover, *Ratcliffe et al. (2022)* [52] were able to classify objects against scenes during the encoding (mainly driven by Parieto-Posterior regions) and maintenance (mainly driven by Centro-Posterior regions functionally coupled with Fronto-Medial Theta). Even fewer papers have examined the possibility of decoding both encoding and maintenance among different stimuli. *Bocincova A. and Johnson J. (2019)* [53] investigated both Colour and Orientation decoding to follow the temporal evolution of these two activities for task-relevant and irrelevant features in WM. It resulted in above-chance classification for task-relevant features during the encoding of colour and orientation, but only orientation was above chance during the maintenance period (mainly due to the total power of the alpha band).

All these previous studies have focused on disentangling group-level differences. For this reason, to improve the signal-to-noise ratio, they have averaged several trials in the same subject and the classifier performances across subjects. Trial averaging is a great strategy to reveal phase-locked activity (present during encoding), but it is not appropriate for the induced activity (Figure 2.0.2, left) that is present during maintenance. *Nobre A. and Ede F.* [54] pointed out the issues that can be born from assuming trial-wise variability as noise, and treating its average as a prototypical reflection of the underlying dynamics because the same averaged representation can arise from different causes such as changes in amplitudes, rate, or duration (Figure 2.0.2, right). Furthermore, this average approach among subjects could have hidden individual differences in the perceiving and maintaining of the items, for example, *Zimmer H. and Fisher B.* [55] showed differences in behavioural capacities during a visual WM task with Chinese people compared to German. Nonetheless, the better performances for the first group were limited in distinguishing changes in characters' shape, but not in other aspects of these symbols such as colour or font type.

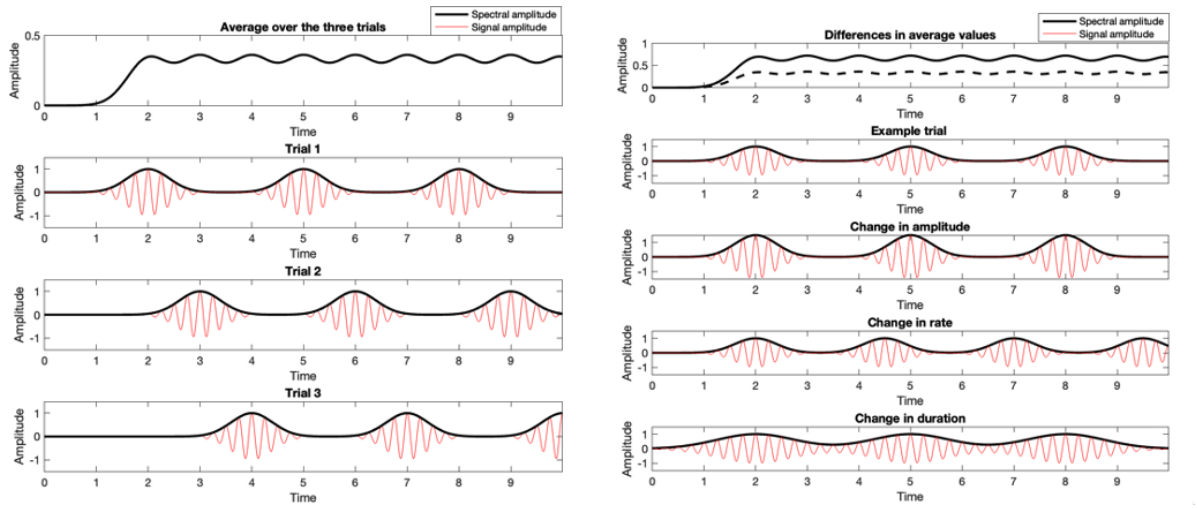

Figure 2.0.2: Averaging of non-phase-locked activity (Left) and differences in the average representation due to different causes (Right).

With the purpose of identifying decodable EEG correlates of working memory maintenance in an experimental paradigm involving different visual stimuli for future neurofeedback personalised approach, this work differs from previous related papers for:

1. Working at a single trial level (without averaging trials) as in real-time neurofeedback.
2. Treating each subject independently and not as a part of a population, identifying for each participant the different performances in colour, geometrical shape, orientation, and character decoding.
3. Targeting not only the possibility to decode the stimulus, but also investigating which brain areas are the main drivers of the decoding.

Chapter 3

Methodology

The methodology section has been written following the scheme in Figure 3.0.1. Firstly, the experimental design has been described in *"3.1 Experiment Design"*; Secondly, the considered behavioural parameters have been explained in *"3.2 Behavioural Performances"*, whilst the physiological data have been pre-processed as expressed in *"3.3 Data Preprocessing"* and processed following what stated in *"3.4 Power Spectral Density Estimate"*. Finally, the extracted features have been used in support vector machine classifiers *"3.5 Classification"* to investigate the differences across subjects or within the same subjects in *"3.6 Cross Subjects Generalisation"* and the different methodologies to identify the significant areas have been explained in *"3.7 Subject Specific Feature Selection"*.

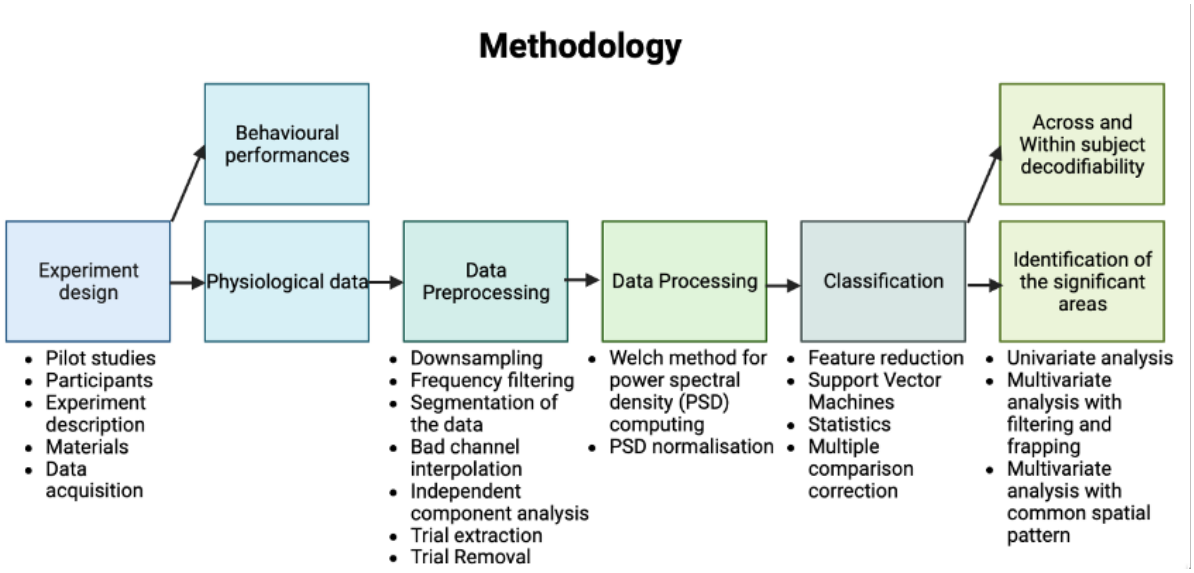

Figure 3.0.1: Methodology scheme.

3.1 Experiment Design

3.1.1 Pilot Studies

This experiment has been designed based on two pilots (more details available in the 10. Appendix | Pilots) that have explored:

a The effect of the duration of the experiment (see *"B.1 Interview on the Feasibility of the Experimental Design"* and *"B.2 Behavioural Performances"* - *"B. Appendix | Pilots)*.

b The visual fatigue of the participants (see *"B.1 Interview on the Feasibility of the Experimental Design"* and *"B.3 Eye-Artefact and ICA Component Removal"* - *"B. Appendix | Pilots)*.

c The effects of different mental modalities on the performances of the classifiers and on the most discriminative areas (see *"B.5 Subject 14 – Effects of Different Mental Modalities - Univariate Analysis"* - *"B. Appendix | Pilots)*.

The duration of the experiment is an essential decision to ensure the goodness of the results. In fact, the dimensions of the dataset are important to build a reliable classifier to distinguish among items [51], but a long experiment could tire the participants leading to a decrease in the performances and in the quality of the data. For the same reason, a good trade-off between the intensity of the stimuli and visual fatigue should be reached. In fact, *Sutter et al. (2021)* [46] showed the performances in colour decoding during encoding as dependent on luminance. Finally, investigating the effects of different mental modalities is essential to ensure reliable results in this analysis. This was assessed, for example, by *Hajonides et al. (2021)* [51] considering the posterior activity contralateral to the object as a probe of the object identification (without verbal labelling). This approach is not feasible with the current analysis because the stimuli have been presented in the centre of the screen to minimise eye movement confounders. The reason for this discrimination between object identification and its verbal labelling is under the assumption that different discriminant areas are expected depending on if the memorisation is mainly driven by object remembering or by verbal labelling [49]. The mental modalities reported by each participant during the real experiment have been listed in *"A.1 Mental Strategies"* – 9. Appendix | Real experiment.

3.1.2 Participants

All 6 participants are young (mean:24, std:4) men, right-handed, without any pathological condition, with normal or corrected-to-normal vision, and without colour impairment (assessed by the book "Ishihara Test for colour deficit"). They have been recruited without monetary compensation. Before the experiment started, they completed 5 trials per type of stimulus (20 total trials) to increase their confidence in the experimental paradigm (to understand the importance, see "10.1 Interview on the feasibility of the experimental design" - *"B. Appendix | Real Experiment)*.

3.1.3 Experiment Description

Each participant undertook 4 sessions with different visual stimuli (colour, geometrical shape, direction, and symbols) in the same order. Even though some learning effects have been associated with task training [56], the decision to keep them in the same order has been made to ensure comparison among subjects. Between sessions, the subject had enough time to rest, and the following part started with his decision. Each session was composed of 3 blocks of 30 trials. Among the trials, a pause of 30 seconds was present, and the participant could decide when to start the next block. Each trial had a global duration of 8.5 sec for a total time of the session which was below 15 minutes (summarised in Figure 3.1.1. This amount of time has been considered short enough to avoid the effects of participant fatigue (See *"B.2 Behavioural Performances"* - *"B. Appendix | Pilots)*. Each trial was based on a retro cue paradigm, in which 2 objects were presented and a retro cue will have informed on which object will have been tested. Hence, each trial was composed of the same sequence of events (summarised in Figure 3.1.2):

1. Fixation: 500 msec with a white cross in the centre of the screen.
2. First stimulus: 300 msec with the first stimulus in the centre of the screen.
3. First delayed period: 1200-1400 msec (jittered interval) with a white cross in the centre of the screen, during which the participants were asked to memorise the First stimulus, thinking mainly at the stimulus itself and less about its verbal label (See *"B.5 Subject 14 – Effects of Different Mental Modalities - Univariate Analysis "* - *"B. Appendix | Pilots)*.
4. Second stimulus: 300 msec with the second stimulus in the centre of the screen.

5. Second delayed period: 1200-1400 msec (jittered interval) with a white cross in the centre of the screen, the same as 2), but thinking about the second stimulus.

6. Retro-Cue: 300 msec with a white number in the centre of the screen. "1" or "2" indicated which stimulus will have been probed.

7. Third delayed period: 2000 msec with a white cross in the centre of the screen, the same as 2), but thinking about the cued stimulus.

8. Response: 1500 msec in which both the stimuli were presented, and the participant had to indicate which was the cued item pressing up or down depending on its position on the screen. After the response, the stimuli disappeared. If the participant did not answer in this time interval, the answer would have been marked as "NaN". Importantly, participants were asked to non-answer if they did not remember the cued item.

9. Rest: The total time of the trial was fixed at 8500 msec, so after the response the subject could rest before the beginning of the following trial.

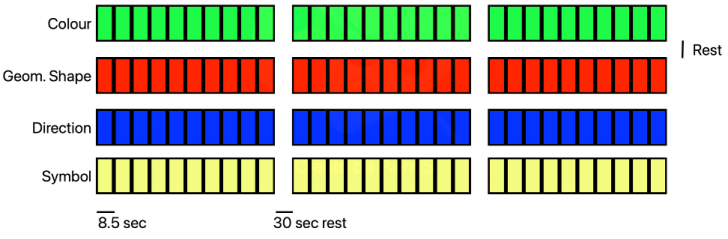

Figure 3.1.1: Experimental design, 4 sessions with 3 blocks or 30 trials each.

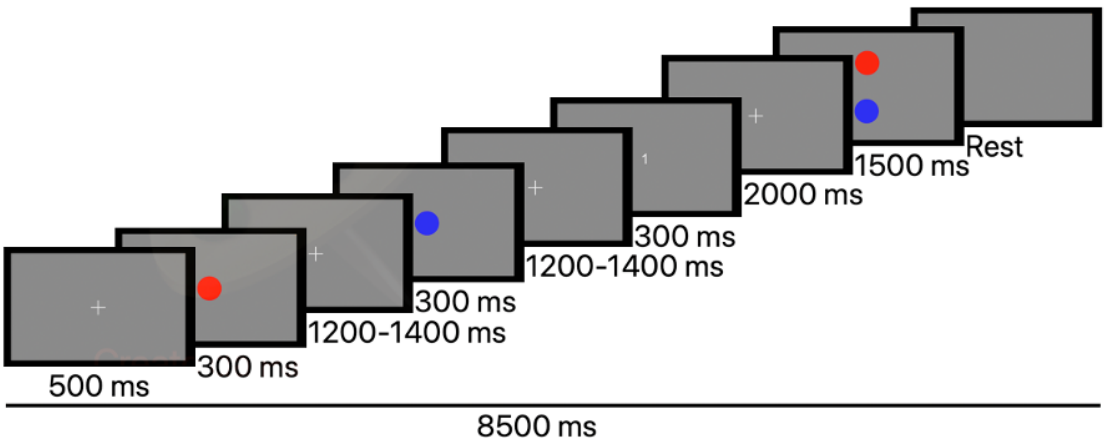

Figure 3.1.2: Single-trial design | Example with colour, the cued item was the first item (red circle), so the participant had to press up.

Considering the design of the experiment, 3 objects have been presented in each session. Therefore, for each of the 5 time intervals under investigation (presentation of the first stimulus, first short delay, second stimulus, second short delay, and the final long delay), at most 30 samples have been collected for each object.

Artefacts that are confounded with one stimulus could be considered the main source of discriminability for a classifier [37]. This could be, for example, when one item is perceived as more tiresome compared to another. Some common EEG artefacts can include eye blinks, eye movements [57, 58] and muscle movements [37]. To avoid these possible confounders, participants were asked to blink, move their eyes, and move (only if necessary) during the period between the response and the fixation of the following trial. To ensure this, the subjects were recorded with an eye tracker and four electrodes were placed to measure the Electroculogram (EOG). To reduce the predictability of the objects, the appearance of the two presented items has been randomly shuffled for each trial. Hence, they have been equally distributed among trials and between the first and second stimuli. For the same reason, also the cues ("1" or "2") and the position of the cued item ("up" or "down") have been equally distributed. Finally, to avoid anticipatory potentials [59], the first and second delayed periods were jittered; and, to avoid the effects of possible lateralisation during the third delay period due to motor anticipatory potentials [60], the subjects were asked to press the keyboard with both hands.

3.1.4 Materials

The experiment was run on a DELL E2422H monitor (1920x1080 resolution, refresh rate of 60 Hz, 53x30 cm), colour profile D6500. The participant had his head placed on a chin rest which was 60 cm distant from the screen. The presented stimuli have been created by MATLAB Psychophysics Toolbox Version 3 [61]. The trial background was grey [RGB: $128, 128, 128$], while the cross and the cue were white [RGB: $230, 230, 230$], with a dimension of $2.86°$ of visual angle. All the stimuli had a dimension of $5.24°$ of visual angle and were:

1. Circles of different colours: Red [RGB: $230, 40, 40$], Green [RGB: $40, 230, 40$], and Blue [RGB: $40, 40, 230$].

2. White [RGB: $230, 230, 230$] geometrical shapes: Triangle, Square, and Pentagon.

3. White [RGB: $230, 230, 230$] and black [RGB: $0, 0, 0$] square oriented gratings: $60°$, $180°$ and $300°$. Other parameters were contrast=1, phase=$90°$, and spatial frequency=5.

4. White [RGB: $230, 230, 230$] symbols: '□', '□', and .'□' These characters have been obtained with the UTF-8 codes ($1341, 1355, 1500$) respectively.

The position of the stimuli during the response part was centred on an invisible circle with $2.62°$ of visual angle. The cued item was placed in a position randomly extracted at $60° - 120°$ or $240° - 300°$, whilst the uncued item was placed opposite to it (Figure 3.1.3).

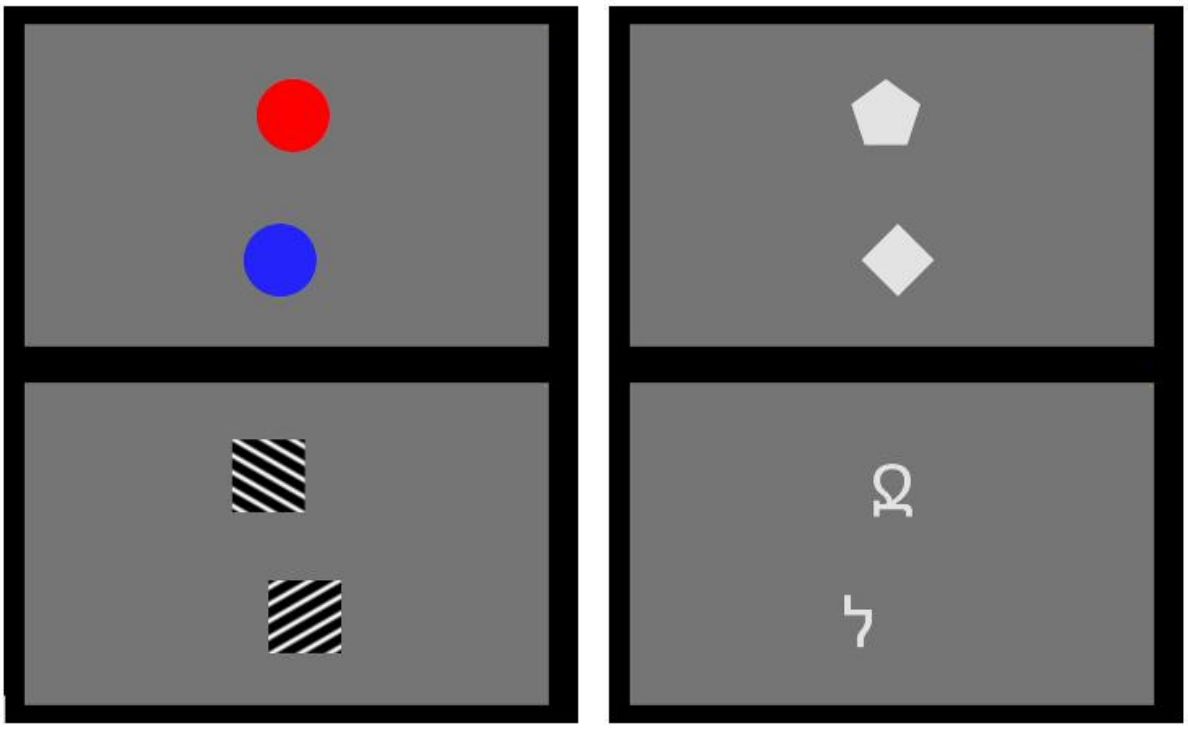

Figure 3.1.3: Example of response for the sessions of Colour (Up-Left), Shape (Up-Right), Direction (Bottom-Left) and Symbol (Bottom-Right).

3.1.5 Data Acquisition

The EEG signals have been acquired with BioSemi Active Two equipment, with 64 Ag/AgCl electrodes placed following the international 10/20 system (American Electroencephalographic Society, 1994), with a sampling rate of 2048 Hz. Six additional electrodes have been placed on the skin of participants: numbers 65 and 66 on the left and right Mastoid respectively; numbers 67 and 68 were placed 1 cm distant from left and right eyes to follow the horizontal movements; and numbers 69 and 70

above and below the right eye to monitor the vertical movements. Eye movements have been registered by GP3 Eye Tracker with a sampling rate of 60 Hz.

3.2 Behavioural performances

The probability of a correct random answer during the response phase is 50%. To ensure all the analyses are related only to the real cognitive process, participants were asked not to answer if they did not remember the item, and only the trials that led to the correct answer have been considered. Task accuracy, number of non-responses, and response time have been registered for each participant to monitor their behavioural cognitive performances and to quantify the perceived cognitive load among the sessions.

3.2.1 Fatigue and Willingness to Repeat

To ensure the protocol can be applied in real scenarios, participants were asked to report their level of visual and general fatigue before and after the experiment on a scale from 1 to 10 where 1 is related to a low level of fatigue and 10 to a high level of fatigue. Moreover, they were asked if they would have been in favour of repeating it in the future.

3.3 Data Preprocessing

The collected data have been processed with MATLAB R2021a and EEGLAB toolbox (v. 2022.1). The signals of the 64 active electrodes have been referenced to the algebraic average of the left and right mastoid, and an EEGLAB cap template (Standard-10-20-Cap81.ced) has been taken as the location for the channels. From this file, the unused electrodes have been removed, and their sequence has been sorted according to the acquisition configuration file of the EEG system. The analysis of the signals taken from the 64 active electrodes will be described in more detail in the next session. It includes downsampling, temporal filtering, artefact removal (Segmentation, Bad channel interpolation, and Independent Component Analysis (ICA) decomposition), trial extraction and trial rejection. The data pre-processing has been described in a detailed way because it can influence a lot the results, especially when the data are not averaged as in our analysis. *Bocincova A. and Johnson J. (2019)* [53], for example,

tested that the decoding of orientation during maintenance was no longer possible using raw data, even if the decoding was above chance during encoding.

Importantly, EOG signals have not been exploited during these analyses, because the number of trials with eye-related artefacts was expected to be big enough to exclude the possibility of trial removal in dependence on ocular activity (see *"B.3 Eye-Artefact and ICA Component Removal"* - *"B. Appendix | Pilots)*. Moreover, also eye-tracker data have not been explored because they were missing for the second session of subject 22, and the fourth session of subject 26.

3.3.1 Downsampling

The data has been downsampled from 2048 to 512 Hz. This is a common practice used to reduce the high-frequency noise and the computational cost for the following analysis [37]. This step has been judged as not critical considering 2 milliseconds short enough to study the dynamic of the ongoing processes.

3.3.2 Frequency Filtering

The expected activations for a WM task are mainly in the medium (theta and alpha) and high-frequency bands (beta and gamma) [53]. Nonetheless, considering the purpose of a single-trial classification (so without the possibility to mediate across trials), the noise is expected to be very high. The EEG power spectral density follows the 1/f power law [62]; therefore, the signal-to-noise ratio is expected too low in the gamma band to extract reproducible results. Hence, the following analysis is mainly focused on theta (4-8 Hz), alpha (8-13 Hz), and beta (13-30 Hz) bands. To remove very high and low frequencies, a 4-order Butter Bandpass filter with 0.5 and 40 Hz [53, 63] as cut-off frequencies have been applied. Filtfilt() MATLAB function has been used to produce a zero-phase filter to avoid introducing temporal shifts. The low cut-off frequency of 0.5 Hz has been decided instead of lower ones (like 0.01 Hz) because otherwise the slow temporal shift would have been considered as the main source of variability for ICA decomposition. However, some possible temporal peak shifts are not critical for this power analysis.

3.3.3 Segmentation of the Data

From the whole data, only the parts of stimulus presentations and delayed periods are under investigation. Hence, only the portions of data from the first stimulus appearance to the end of the long delay have been conserved to avoid misinterpretation or artefact injection during artefact removal.

3.3.4 Bad Channel Interpolation

Bad channels have been examined considering both their standard deviation and their time series. As expected, the standard deviation of the frontal electrodes is generally higher due to eye-related artefacts. After these considerations and the visual inspection of the time series, only the P2 channel of subject 23 has been interpolated through a spherical interpolation (pop_interp() eeglab function). This deviation was systematic for all his sessions, possibly because the electrode has been not placed correctly during the acquisition

3.3.5 Independent Component Analysis

Infomax ICA algorithm (pop_runica() eeglab function) has been applied to decompose the signal and delete possible artefacts. This algorithm has been considered more stable (reliably across runs) than fastICA [64] to detect eye artefacts, even though more computationally expensive. For each subject, the specific components to remove have been chosen by visual inspection of the ICA-component time course, spectral content, and topographic map. ICA is not an algorithm that can be used for online applications, but trial rejection would have brought an imbalance of data across sessions, considering the opposite effects of learning and patients' fatigue (see *"B.3 Eye-Artefact and ICA Component Removal"* - *"B. Appendix | Pilots)*. Once identified the neural correlates (the target) and the stimulus (the feedback) that are suited for each participant, a shrunk trial can be used. Moreover, some pilot participants reported having automatically learned when to blink over trials or with training (see "*"B.1 Interview on the Feasibility of the Experimental Design"*. An example of eye-artefact (inside the red rectangle) removed through acICA decomposition is reported in Figure 3.3.1 (pre-ICA reconstruction on the left, and post-ICA reconstruction on the right), which reported trial 5 (identified as 105) of the first session of subject 26.

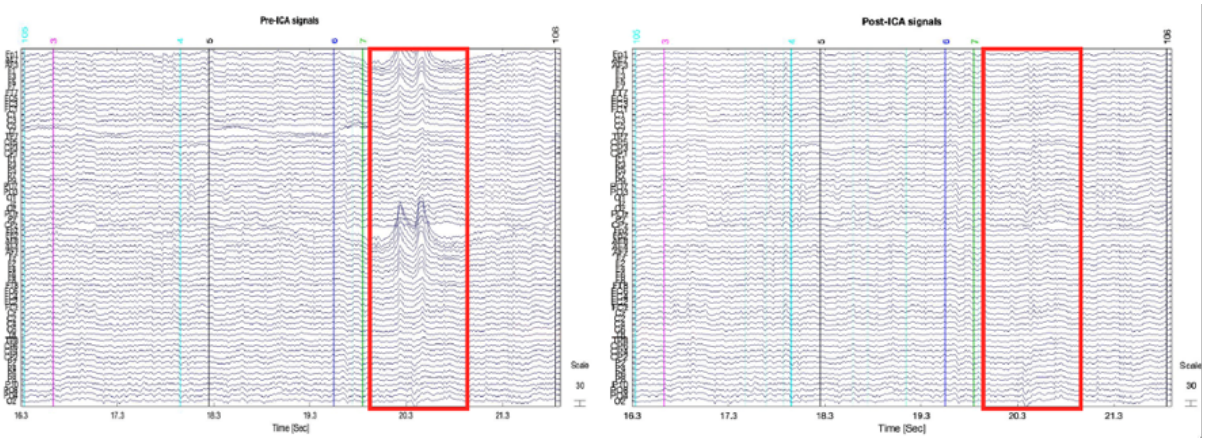

Figure 3.3.1: Example of eye-artefact (in the red block) removed through ICA. Before (Left) and after (Right) ICA reconstruction. Subject 26, Session 1, trial 5 (identified as 105).

3.3.6 Trial Extraction

The data obtained from ICA reconstruction has been segmented into three categories: stimulus presentation, short-delayed period, and long-delayed period. The segmentation has been performed to ensure that the following processing (e.g., power spectral density (PSD) computing) would not interfere with the classifier performances due to residual effects (i.e., considering the temporal sequence of stimulus presentation and short delay period, compute the power spectral density along the whole period would have increased the correlation between their powers biasing the cross-interval classifier performances). With this procedure, the data have been segmented to obtain periods of 300 msec for the stimulus presentation, 1000 msec for the short delay, and 2000 msec for the long delay. Some authors have used longer segments before PSD to avoid edge effects, and to normalise the post-stimulus activity with the pre-stimulus baseline [46]. For this analysis, edge effects have not been considered critical because no other filtering steps have been applied. On the other hand, pre-stimulus baseline normalisation has not been considered due to the structure of the experimental design: in fact, a rest period was present only at the beginning of the trial and the duration of the whole trial (8.5 sec) was too long to consider it as a stable baseline. Moreover, it has been a period with a lot of eye-related artefacts (participants stopped to blink at the appearance of the white cross).

3.3.7 Trial Removal

To examine the possibility of undesired components resistant to ICA decomposition, all the trials have been visually inspected before and after ICA reconstruction. If a trial had some resistant artefacts that were present in all the subpart (stimulus presentations, short and long delays), it was removed before ICA reconstruction to avoid artefact injection; while if it had some resistant artefacts that were present only in some subparts, those parts were removed after ICA reconstruction. Table 3.3.1 reports the Mean absolute [and percentage relative to the number of correct trials] and the standard deviation values across sessions for each participant and experimental time segments (Stimulus Presentation (SP), Short Delay (SD), and Long Delay (LD)). As can be seen, subject 22 has the highest number of rejected trials.

Table 3.3.1: Mean Absolute value [Percentage with respect to the number of correct trials] $\pm$ Standard Deviation of rejected portions of trials (SP=Stimulus Presentation, SD=Short Delay, LD=Long Delay) for each subject.

Subject ID	**Mean [%] $\pm$ Std rejected SP**	**Mean [%] $\pm$ Std rejected SD**	**Mean [%] $\pm$ Std rejected LD**
21	$0.0[0] \pm 0.0$	$0.3[0.2] \pm 0.5$	$0.3[0.4] \pm 0.5$
22	$18.3[10.3] \pm 4.5$	$21.5[12.1] \pm 7$	$10.5[11.9] \pm 3.4$
23	$1.8[1] \pm 1.0$	$1.0[0.6] \pm 2.0$	$0.5[0.6] \pm 1.0$
24	$0.5[0.3] \pm 1.0$	$0.5[0.3] \pm 1.0$	$0.0[0.0] \pm 0.0$
25	$2.0[1.1] \pm 2.3$	$1.8[1.0] \pm 1.5$	$0.5[0.6] \pm 0.6$
26	$0.0[0] \pm 0.0$	$0.0[0] \pm 0.0$	$0.0[0] \pm 0.0$

3.4 Power Spectral Density Estimate

Endogenous cerebral activity is not expected to be phase locked. For this reason, Event-Related Potentials or Evoked power activities have not been considered in this pipeline, differently from all previous work [42, 46, 51]. This primary analysis was focused on the stable frequency components over time, even if WM maintenance is considered a highly dynamic process [30]. The static power spectral density estimate is based on the strong assumptions of the stationarity of the ongoing processes.

3.4.1 Welch Method

To extract the power in the desired bands, the Welch method [65] has been applied to estimate the power spectral density. This method mitigates the leakage effects by averaging overlapping segments of the same window [66]. For the stimulus presentation, a window of 125 msec and an overlap of 62.5 msec has been used; whilst for the delayed period, a window of 500 msec and an overlap of 250 msec has been applied. The PSD has been computed on equispaced support (with steps of 0.05 Hz) of frequencies from 1 to 40 Hz, but only the data from 4.1 to 30 Hz have been used for the following analysis (518 frequency points).

3.4.2 Power Spectral Density Normalisation

The power spectral density has been normalised by the total power from 4.1 to 30 Hz. It has been obtained by integrating the PSD in this frequency interval. This normalisation has been applied to avoid the effects of possible outliers during the creation of the decision boundaries of the classifiers. Figure 3.4.1 represents the grand average (averaging among all the trials within the specific object) for each object (columns of the figure) of the power in theta (left), alpha (centre), and beta (right) in each time interval (rows of the figure) for the first session of Subject 26.

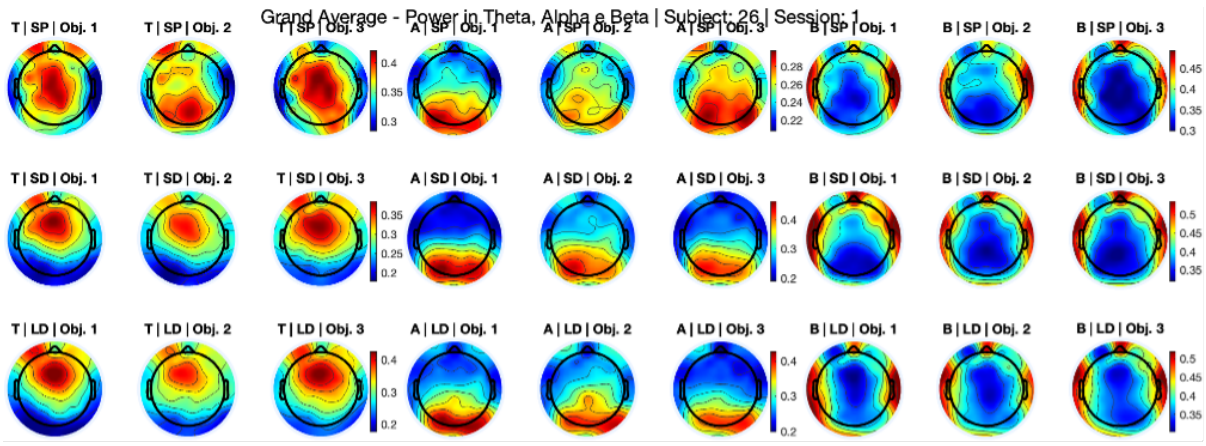

Figure 3.4.1: Example of Grand Average – Power in Theta (T), Alpha (A), and Beta (B) during Stimulus Presentation (SP), Short Delay (SD), and Long Delay (LD) | Subject 26 | Session 1.

3.5 Classification

In order to identify some possible reliable individual-specific neural correlates, some classical Machine Learning steps of feature reduction, classifier training and testing in an independent dataset, and statistical analysis have been performed. The train test stratified division is essential to avoid the model overfitting on the training set. Therefore, to allow the generalizability of the model in unseen data, the dataset has been divided following the traditional 70/30 train test division.

3.5.1 Feature Reduction

Feature reduction is an important step to reduce the noise for the classifier [37, 67]; more important the aim of this work is to find some possible reliable neural correlates. A classic methodology to perform feature reduction is to perform a 5-fold cross-validation in the training set, in order to avoid circularity issues [37]. This means that the training set is divided into 5 stratified folds and, for each of the five iterations, only one fold is considered as the validation set, while the others as the training set (Figure 3.5.1).

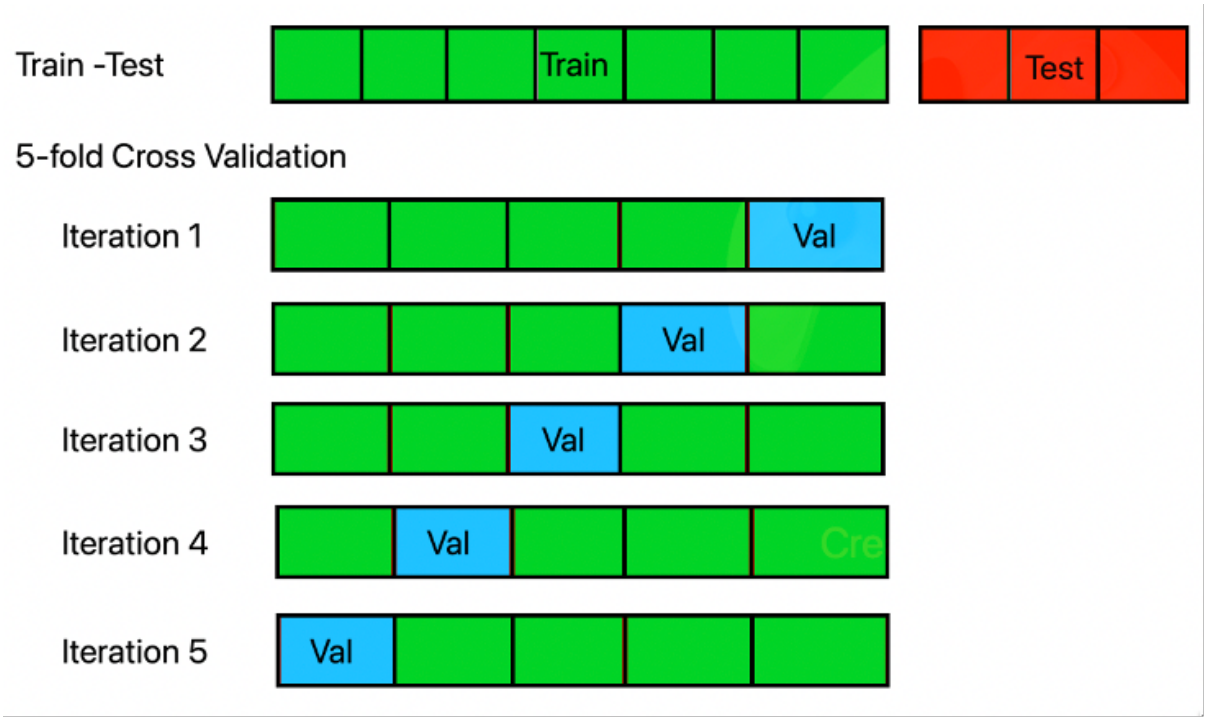

Figure 3.5.1: 5-fold Cross Validation scheme after train test division (70/30).

3.5.2 Support Vector Machine

Among Linear classifiers, such as Support Vector Machine (SVM) [68] and Linear Discriminant Analysis, the second has been discarded because it relies on the assumption of homoscedasticity of the distributions [69], even if it is commonly applied in these analyses [51, 52, 53] due to its low computational training time. Moreover, SVM generally provides better performances compared to other classifiers when dealing with many features [36, 37].

A Support Vector Machine is a discriminant algorithm that maximises the separation between two classes. Considering $X_1, X_2, ..., X_n$ the training data, b the bias, and W the classifier weights; the highest separation is achieved by minimising the cost function $J(W)$ (3.1), subject to the constraint (3.2).

$$J(W) = \frac{1}{2} * ||W||^2 \tag{3.1}$$

$$Y_i(W' * X_i - b) \geq 1; \forall i = 1, \ldots, n \tag{3.2}$$

Indicating the class label with $\omega \in \Omega$, the classification rule is obtained by (3.3) where the class $k \in \Omega$ is discriminant against the rest [70].

$$\omega \begin{cases} \in k & if\ W^T \geq b \\ \notin k & if\ W^T < b \end{cases} \tag{3.3}$$

For this analysis, the MATLAB function fitcsvm() has been applied with the default parameters.

3.5.3 Statistics

Considering the limited number of samples in this design, the performances of the classifiers have been evaluated using a non-parametric permutation test. In fact, with small datasets, the general threshold of chance level is more than 50% for binary [71] or 33% for ternary classification. To overcome this issue, the permutation test generates a null distribution from N random permutations of the data of the same dataset. The final p-value has been obtained considering the number of chance classifiers (trained and tested on shuffled data) which performs better than the real classifier (trained

and tested on the real data) divided by the number of permutations (N). The only assumption of this test is the data point independence [71]. The p-value has been evaluated by comparing the accuracies of the chance classifiers with the test accuracy. For this analysis, 1000 permutations have been applied, so the final sensitivity of the p-value is 0.001.

3.5.4 Multiple Comparison Correction

The Multiple Comparisons Problem is typical of EEG-MEG data because, due to the high number of statistical comparisons, it is not possible to control the so-called family-wise error rate (FWER) [72]. In this field, a common approach to overcome this issue is the Clustering correction under the assumption of spatial correlation across electrodes, and of time-frequency correlation across time-frequency samples [72]. This correction methodology cannot be applied in the current analysis, due to the calculation of the powers in large and not-overlapping frequency bands. Another classical methodology is the Bonferroni correction, but it relies on the assumption of the independence of the tests which is not coherent with the present correlation across channels. Therefore, also considering the limited number of statistical tests, False Discovery Rate (FDR) correction has been applied only during the univariate analysis (described below).

3.6 Cross Subjects Generalisation

From a Neuroscientific perspective, all five time intervals are under investigation (considering that the neural circuits related to the second stimulus may be different when the first is kept in memory).

In order to identify for each participant and session whether the extracted features were able to discriminate the specific objects, some ternary classifiers have been trained for each time interval of interest. Considering the total number of features extracted for each participant and time interval (33152 features = 64 channels x 518 frequencies) with a dataset which has at most 30 trials per item, the features have been reduced by calculating the powers in the specific bands by integrating the normalised PSD from 4.1 to 8 Hz for the theta band, from 8.1 to 13 Hz for the alpha band, and from 13.1 to 30 Hz for the beta band. With this step, the number of features has been reduced to 192 (64

channels x 3 frequency bands). Moreover, 8 brain areas have been considered in this first analysis corresponding to the Left and Right Frontal, Central, Parieto-Occipital, and Temporal regions (Figure 3.6.1). Therefore, the powers have been averaged in each region, reducing the number of features to 24 (8 brain areas x 3 frequency bands). Finally, the data have been log transformed to increase the Gaussianity.

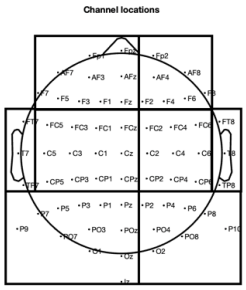

Figure 3.6.1: Channel division in Brain regions: Left and Right Frontal, Central, Temporal, and Parieto-Occipital areas.

In a ternary classification with SVM, two possible configurations can be exploited. In a "1vsAll" configuration, three classifiers (one for each class) are considered. Each of these classifiers is trained considering one class as the first class and all the other classes as the second one (Figure 3.6.2, Right, Up). On the other hand, in a "1vs1" configuration, three classifiers (one for each couple) are considered. Each classifier is trained considering these couples (Figure 3.6.2, Right, Down). A "1vs1" approach has been used in this section, considering it more like the following analysis (which is based on binary classifiers for each pair of objects).

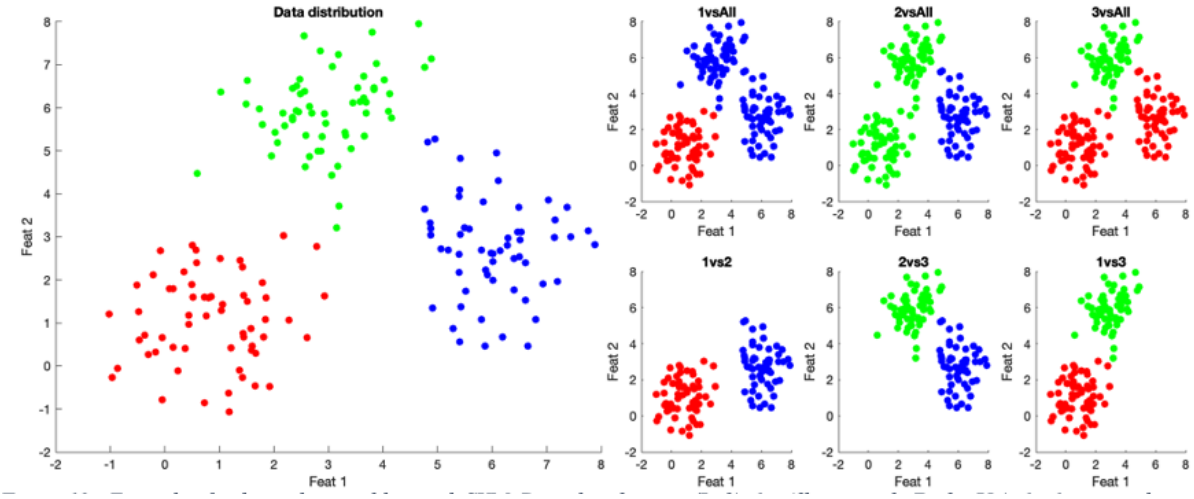

Figure 3.6.2: Example of a three-class problem with SVM. Data distributions (Left), 1vsAll approach (Right, Up), 1vs1 approach (Right, Down).

3.6.1 Across Subjects Analysis

To understand if some common representations were shared across participants, for each session and time interval a 3-fold cross-subject validation has been applied (therefore, for each iteration the classifier has been trained on four subjects and tested in the remaining two). For the statistical analysis, the mean cross-subjects test accuracy has been compared to the N mean cross-subjects random test accuracies.

3.6.2 Within Subjects Analysis

Working at the participant level, for each session a ternary classifier has been trained in a time interval and tested in another one. Moreover, the performances within the same time interval have been evaluated through a stratified 5-fold cross-validation. Also in this condition, for the statistical analysis, the mean cross-validation test accuracy has been compared to the N mean cross-validation random test accuracies. To test the possibility of different mental representations depending on the sequence of events, the mean cross-validation test accuracies of the first and second stimulus presentation, and of the first and second delay periods have been compared through a parametric paired-sample t-test or a non-parametric Wilcoxon Rank Sum test, depending on the Gaussianity of the distribution, assessed through a Lilliefors test.

3.7 Subject Specific Feature Selection

From a Rehabilitation perspective, only three of the five-time intervals are under investigation (presentation of the stimulus, short delay, and long delay), considering the objective of distinguishing the specific object independently on the order of the events. Moreover, to enhance the treatments of working memory, only the two delayed periods are the most significant even if the final long period could have been affected by the cue and some anticipatory potentials [59]. Nonetheless, to keep into account possible different brain representations related to the sequence of the events, the samples of the stimulus presentation and short delay have been pooled in a stratified way in each partition (train-test division or cross-validation if present) of the datasets. Hence, the number of samples of these time intervals has been equally partitioned. Finally, it is important to point out, that the lower number of trials for the long delay

(30 trials at most per object), led to that analysis being less reliable compared to the other time intervals (60 trials at most per object).

In order to identify some possible reliable individual-specific neural correlates, for each time interval and for each object comparison (1vs2, 2vs3, and 1v2), three different classification methodologies have been explored: a mass univariate analysis, a multivariate analysis based on Filtering and Wrapping methods, and a multivariate analysis based on Frequency Common Spatial Pattern (FCSP) [73]. The univariate analysis offers the advantage of immediate interpretability of results; in contrast, the high number of statistical tests requires important Multiple Comparison Corrections, and it is generally less robust to noise compared to multivariate approaches [74]. On the other hand, the physiological meaning of the multivariate analysis is not trivial. In fact, only for linear models, the reconstruction of the activation patterns can be reached through Weight Projection from classifier weights [74], or through the interpretation of the activation patterns of the CSP filter. Importantly, a weakness of weight projection is that the reliability of the patterns depends on the performances of the classifier [37].

3.7.1 Univariate Analysis

For the univariate analysis, for each electrode, the powers in the specific bands have been calculated in the theta, alpha and beta bands. Then, the data have been log transformed to increase the Gaussianity. After the train-test division, only the 10 features that had provided the best mean validation accuracy were kept (Figure 3.7.1). This number of 10 has been chosen to reduce the computational time and the number of statistical comparisons, under the assumption that the best features (selected by the CV mean validation accuracy) are the best to describe the dataset. This analysis has been performed under the hypothesis that each channel has the same probability to be significant, even if the most robust results are expected to be related to clusters of significant activity.

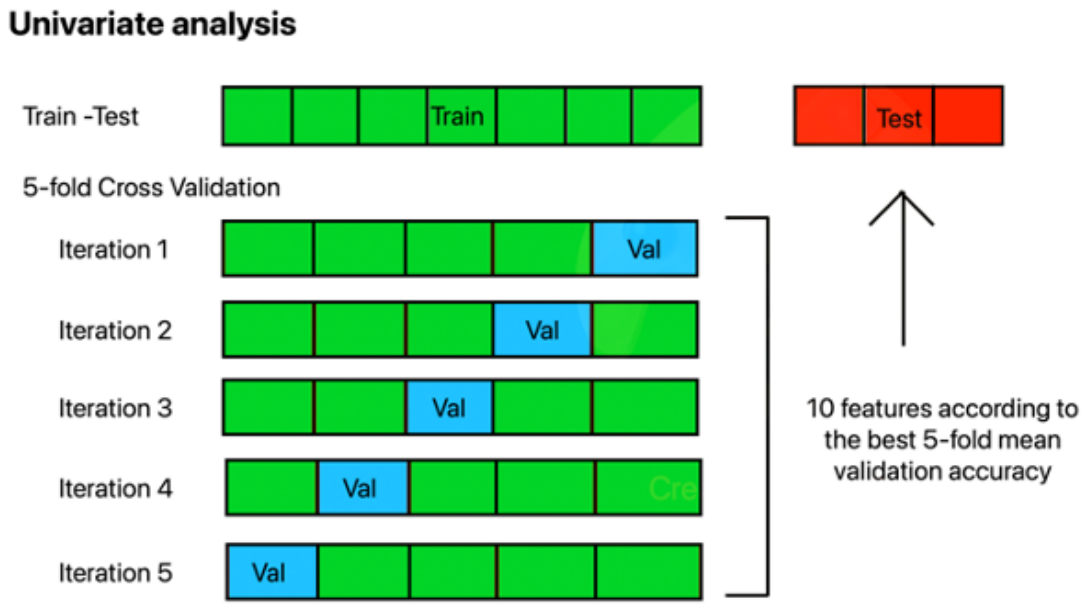

Figure 3.7.1: Univariate analysis scheme, from the cross-validation, the 10 features with the highest mean validation accuracy have been selected.

3.7.2 Multivariate Analysis, Filtering and Wrapping

For this multivariate analysis, the powers in the specific common bands (theta, alpha, and beta) have been calculated as for the univariate analysis and the data have been log-transformed. After the train-test division, filtering methods have been applied in the training set to extract a subset of discriminating features. In particular, only the 10 features which provide the best Fisher Score (FS), Minimum Redundancy Maximum Relevance (mrmr), or Kendall's Tau Score (KS) were kept. These scores are common filtering methods for continuous data and categorical responses [67]. After this first discrimination, a stratified 5-fold cross-validation has been applied in the training set to extract the wrapped features from Linear Support Vector Machines. The decided wrapping algorithm has been a forward sequential feature selection with a Loss function that minimised the SVM-Cross-Validation validation error [36] (Figure 3.7.2).

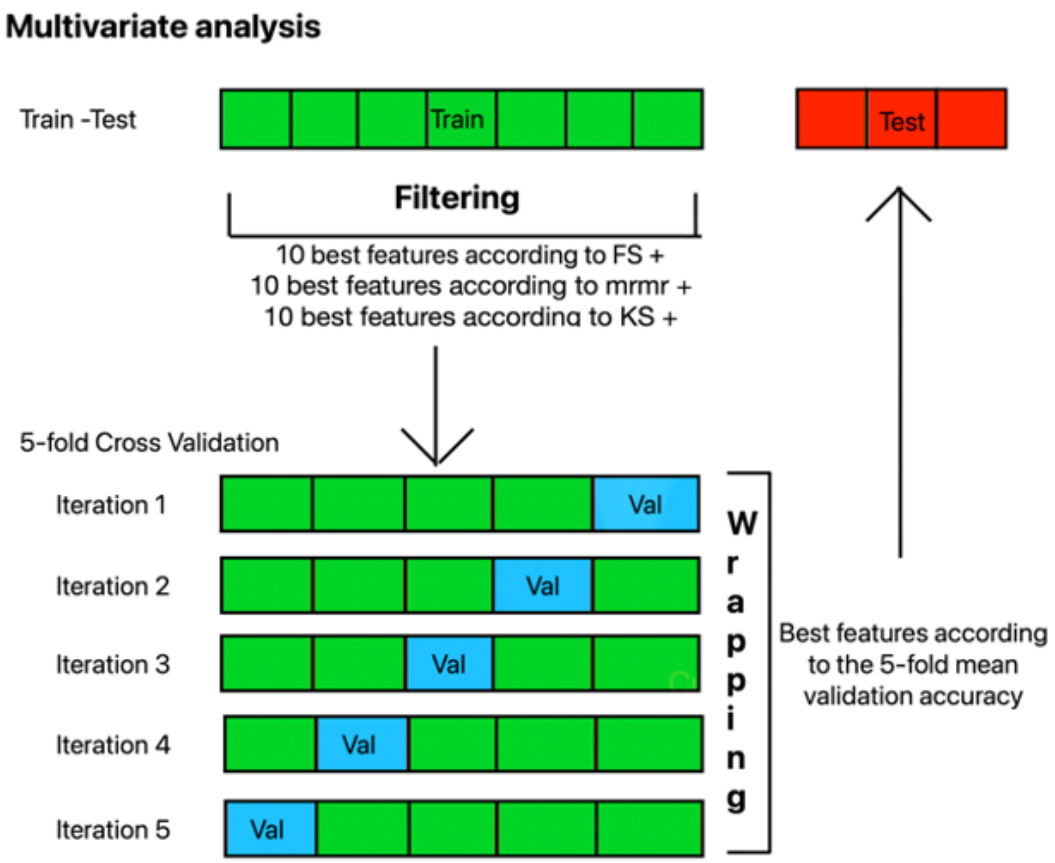

Figure 3.7.2: Multivariate analysis scheme, after the filtering on the training set and the wrapping on the cross-validation of the training set, the selected features have been tested in the test set.

Fisher Score

Fisher Score is a measure of distinctiveness between two classes a and b. For each feature k, a score is calculated following (3.4). Where $\mu_{a,k}$ represents the mean value obtained from class a for the feature k, while $\sigma_{a,k}$ represents the standard deviation value obtained from class a for the feature k.

$$FS_k = \frac{\mu_{a,k} - \mu_{b,k}}{\sqrt{{\sigma_{a,k}}^2 + {\sigma_{b,k}}^2}}; \tag{3.4}$$

The most discriminant features have been considered those which had the highest FS_k.

Minimum Redundancy Maximum Relevance

Minimum Redundancy Maximum Relevance is a score based on Mutual Information. The mutual information (I) between the discrete random variables X and Z is defined as (3.5).

$$I(X,Z) = \sum_{i,j} P(X = x_i, Z = z_i) \ln \left(\frac{P(X = x_i, Z = z_i)}{P(X = x_i) * P(Z = z_i)} \right) \tag{3.5}$$

Indicating with V_x: the relevance of feature x with respect to a response variable y (3.6), and W_x: the redundancy of feature x with respect to a response variable y and the set of features S (3.7). This algorithm calculates for each feature x the Mutual Information Quotient (MIQ) as expressed in (3.8).

$$V_x = I(x,z) \tag{3.6}$$

$$W_x = \frac{1}{|S|} \sum_{z \in S} I(x,z) \tag{3.7}$$

$$MIQ_x = \frac{V_x}{W_x} \tag{3.8}$$

The features which have been considered more discriminant and less redundant have been those which had the highest MIQ$_x$.

Kendall's Tau

Kendall's Tau is a Parametrical statistic test that counts the number of (i,j) pairs, for $i < j$, for which $X_{a,i}$–$X_{a,j}$ and $Y_{a,i}$–$Y_{a,j}$ have the same sign. For the a column Xa in matrix X and the a column Ya in matrix Y, KS can be calculated through (3.9), (3.10), (3.11). Where n is the number of columns of X and Y.

$$\xi(X_{a,i}, X_{a,j}, Y_{a,i}, Y_{a,ij}) = \begin{cases} 1 \; if \; (X_{a,i}, X_{a,j}) * (Y_{a,i}, Y_{a,j}) > 0 \\ 0 \; if \; (X_{a,i}, X_{a,j}) * (Y_{a,i}, Y_{a,j}) = 0 \\ -1 \; if \; (X_{a,i}, X_{a,j}) * (Y_{a,i}, Y_{a,j}) < 0 \end{cases} \tag{3.9}$$

$$K_{a,b} = \sum_{i=1}^{n-1} \sum_{j=i+1}^{n} \xi(X_{a,i}, X_{a,j}, Y_{a,i}, Y_{a,j}) \tag{3.10}$$

$$\tau_{a,b} = \frac{2K_{a,b}}{n(n-1)} \tag{3.11}$$

The features which have been considered more discriminants have been those with the lowest p-value.

3.7.3 Multivariate Analysis, Frequency Common Spatial Pattern

For the multivariate analysis with FCSP, after the train-test division, the training set has been used to determine the projection matrix V [73] (Figure 3.7.3). Considering the matrices of the normalised Power Spectral Density (PSD) coefficients from 4.1 to 30 Hz (after the subtraction of the mean PSD for each channel and trial): $X1$ with dimensions (num_trials1 (=$k1$) x num_channels x num_frequencies) and $X2$ with dimensions (num_trials2 (=$k2$) x num_channels x num_frequencies). For each trial i and class (1 or 2), the normalised spatial covariance matrices have been calculated through (3.12), in order to compute the mean spatial covariance matrices (3.13), and the overall spatial covariance matrix (3.14).

$$C_{1,i} = \frac{X_{1,i} * X_{1,i}^T}{Tr(X_{1,i} * X_{1,i}^T)} \qquad C_{2,i} = \frac{X_{2,i} * X_{2,i}^T}{Tr(X_{2,i} * X_{2,i}^T)} \tag{3.12}$$

$$\overline{C_1} = \frac{1}{k_1} \sum_{i=1}^{k_1} C_{1,i} \qquad \overline{C_2} = \frac{1}{k_2} \sum_{i=1}^{k_1} C_{2,i} \tag{3.13}$$

$$\overline{C} = \overline{C_1} + \overline{C_2} \tag{3.14}$$

After the eigenvalue decomposition of $\overline{C}$ (3.15 and the whitening process (3.16, the common eigenvectors can be calculated through (3.17, and the CSP projection matrix V (num_channels x num_channels) have been obtained with (3.18).

$$\overline{C} = U_o * \Sigma * U_o^T \tag{3.15}$$

$$P = \sqrt{\Sigma^{-1}} * U_o^T \tag{3.16}$$

$$S_1 = U * \Sigma_1 * U^T \qquad S_2 = U * \Sigma_2 * U^T \qquad with\ \Sigma_1 + \Sigma_2 = \mathbb{I} \tag{3.17}$$

$$V = U^T * P \tag{3.18}$$

This matrix has been applied to filter each trial i of the data X (num_trialstotal x num_channels x num_frequencies) obtaining Z (matrix of the spatially filtered signals) through (3.19).

$$Z = V * X \tag{3.19}$$

For each trial, only the first (=$z1$) and the last column (=$z2$) of Z^T were kept (corresponding to the most discriminative features for one class and for the other); then, the final features ($f1$ and $f2$) have been obtained from the log-transformation of the normalised variance over the frequencies (3.20).

$$f_i = ln\left(\frac{var(z_i)}{\sum_{j=1}^{2} var(z_j)}\right) \tag{3.20}$$

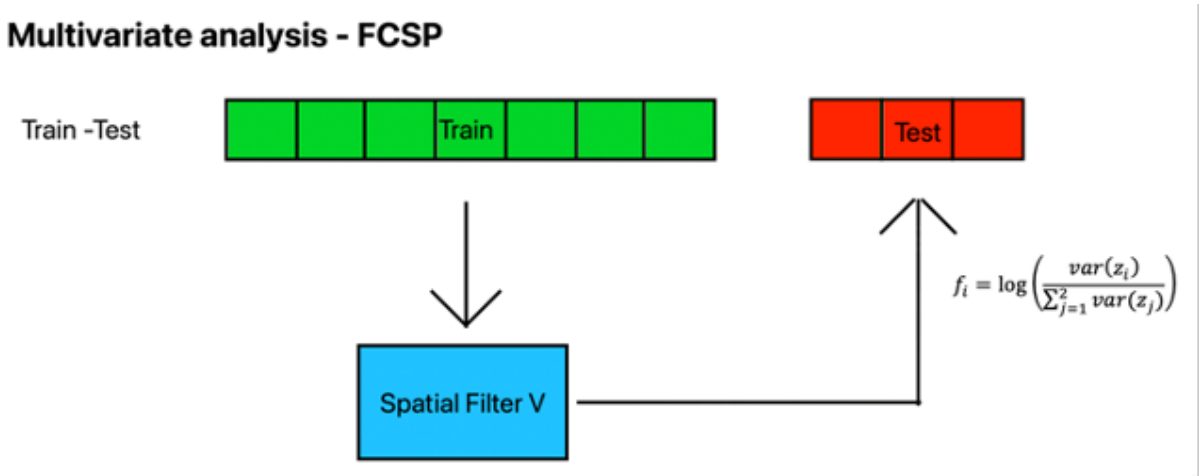

Figure 3.7.3: Multivariate analysis scheme, after the creation of the projection matrix V on the training set, the test data has been filtered and the log relative variance has been extracted.

Chapter 4

Results

4.1 Behavuoiral Performances

For each session and participant, accuracies, number of non-responses, and response time have been reported in Figure 4.1.1. These behavioural data have been summarised in Table 4.1.1 which describes the participant performances across sessions, while in Table 4.1.2 the performances during each session (across participants) have been reported. Some individual differences can be highlighted across participants, for example, subjects 22 and 23 achieved the highest accuracies and the smallest response time, while subject 24 has the lowest accuracy and the longest response time. On the other hand, these parameters have proved to be enough stable across sessions.

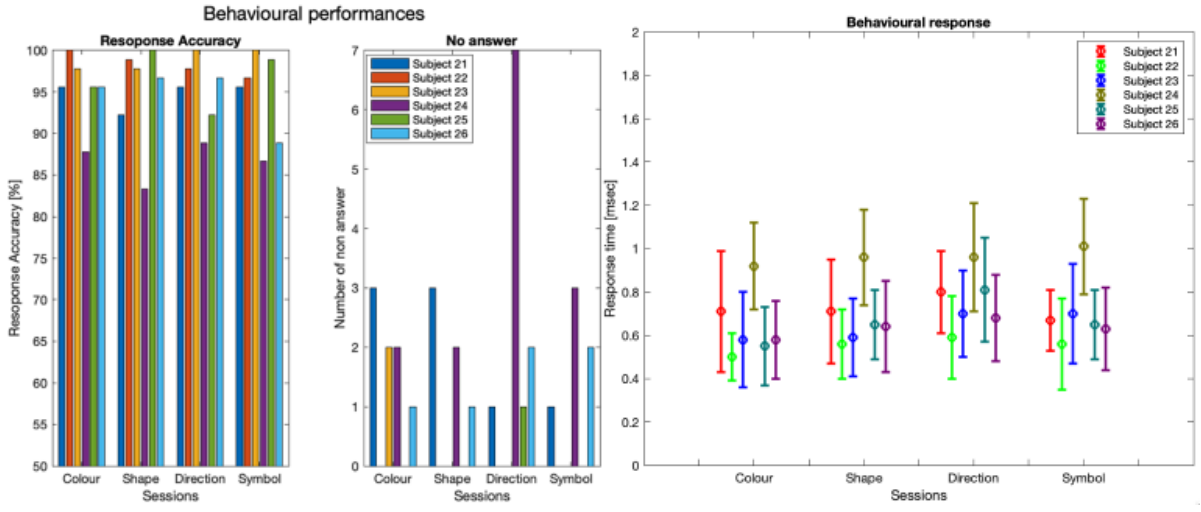

Figure 4.1.1: Behavioural Accuracy and Number of Non-Responses (Left) and Response Time (Right) among subjects and sessions.

Table 4.1.1: Behavioural Accuracy, Number of Non-Responses, and Response Time for each Participant across sessions.

Subject ID	**Accuracy [%] Mean ± Std**	**NaN Mean ± Std**	**Resp. Time [sec] Mean ± Std**
21	$94,8 \pm 1.7$	2.0 ± 1.2	0.7 ± 0.1
22	$98,4 \pm 1.4$	0.0 ± 0.0	0.6 ± 0.0
23	$98,9 \pm 1.3$	0.5 ± 1.0	0.6 ± 0.1
24	$86,7 \pm 2.4$	3.5 ± 2.4	1.0 ± 0.0
25	$96,7 \pm 3.5$	0.3 ± 0.5	0.7 ± 0.1
26	$94,5 \pm 3.8$	1.5 ± 0.6	0.6 ± 0.0

Table 4.1.2: Behavioural Accuracy, Number of Non-Responses, and Response Time for each Session across participants.

	S1 Mean ± Std	**S2 Mean ± Std**	**S3 Mean ± Std**	**S4 Mean ± Std**
Accuracy [%]	95.4 ± 4.1	94.8 ± 6.3	95.2 ± 4.01	94.5 ± 5.5
NaN	1.3 ± 1.2	1.0 ± 1.3	1.8 ± 2.6	1.0 ± 1.3
Response Time [Sec]	0.6 ± 0.2	0.7 ± 0.1	0.8 ± 0.1	0.7 ± 0.2

4.1.1 Fatigue and Willingness to Repeat

The level of visual and general fatigue has been assessed on a scale from 1 to 10 (Table 4.1.3); where 1 represents no fatigue and 10 is a high level of fatigue.

Table 4.1.3: Level of Visual and General Fatigue, and Favourability to repeat the experiment in the future.

Subject ID	Level of Visual Fatigue	Level of General Fatigue	Favourable to Repeat in the Future
21	3.0–4.5	6.0–5.0	*Yes*
22	2.5–9.0	3.0–7.0	*No*
23	4.0–6.0	4.0–5.0	*Yes*
24	4.5–6.0	3.0–5.0	*Yes*
25	1.5–2.5	2.0–2.5	*Yes*
26	2.0–4.0	2.0–3.0	*Yes*

4.2 Cross Subjects Generalisation

4.2.1 Across Subjects Analysis

Figure 4.2.1 illustrates the mean test 3-fold cross-subjects validation test accuracy for each session. No statistically significant performances have been reached in none of the comparisons.

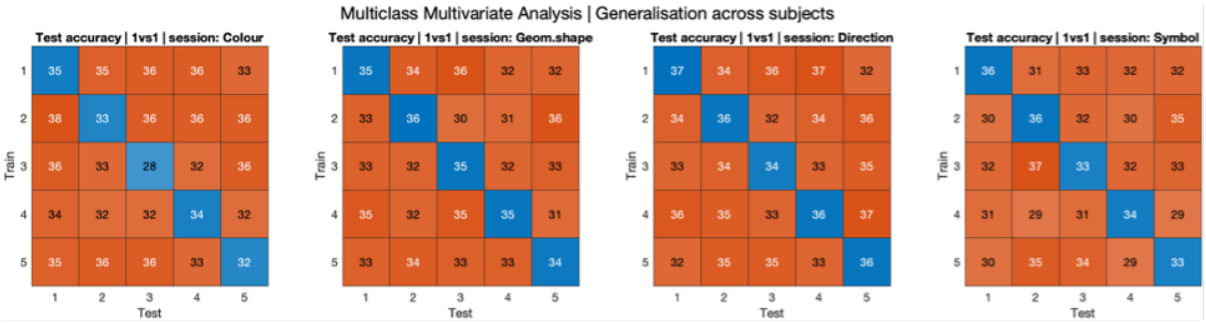

Figure 4.2.1: Mean 3-fold cross-subjects validation test accuracy for each session.

4.2.2 Within Subjects Analysis

Figure 4.2.2 describes the performances of each participant (rows of the image) and session (column of the image). The rows of each matrix represent the time intervals in which the classifier has been trained, while the columns of each matrix represent the time intervals in which the classifier has been tested. When the dataset was the same (the diagonal of the matrices), the mean 5-fold cross-validation test accuracy has

been reported. The significant performances (p-value<0.05) have been represented with a white star in the top right corner of each comparison. Within the same time interval, some above-chance classifications have been highlighted especially during the session with direction as the stimulus. Instead, across the different time intervals, some significant performances have been reported with different patterns across participants.

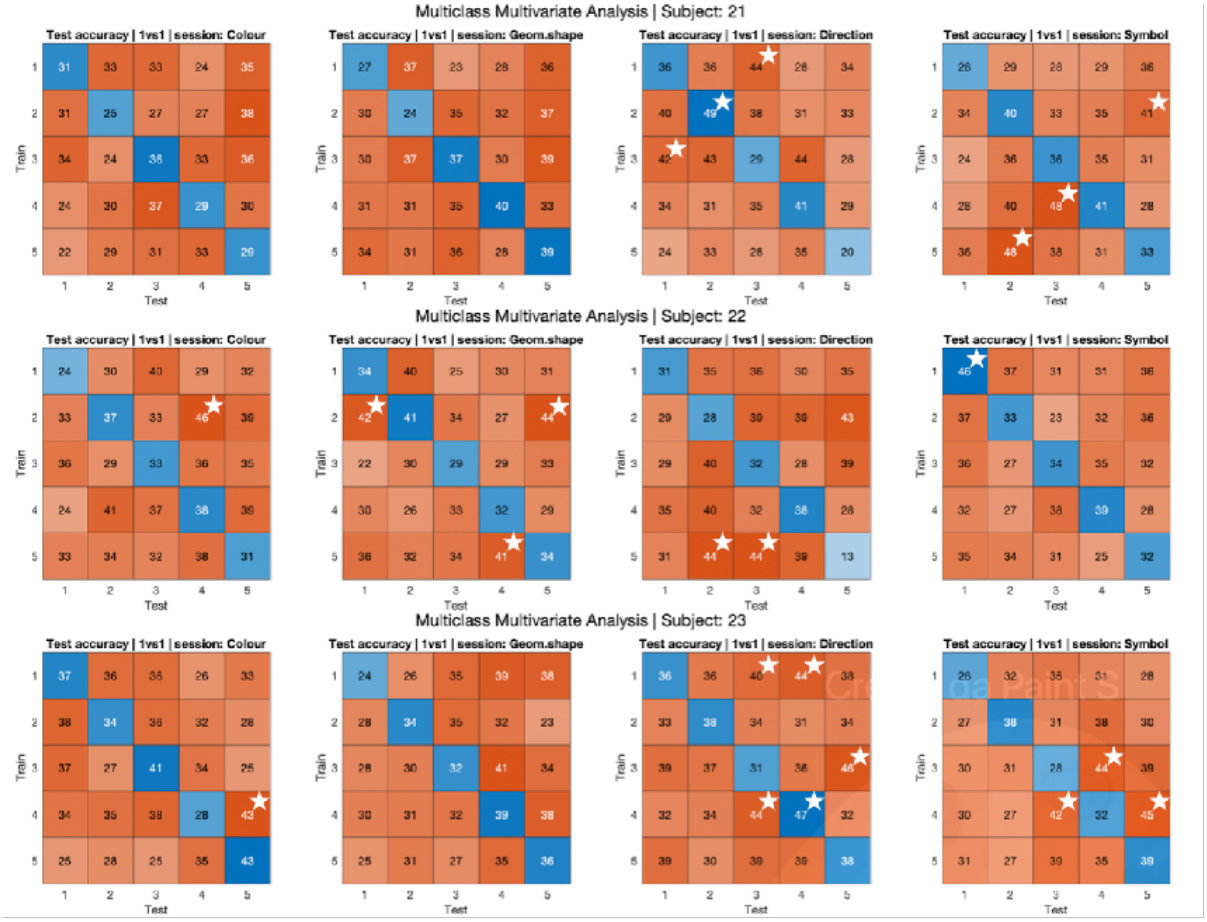

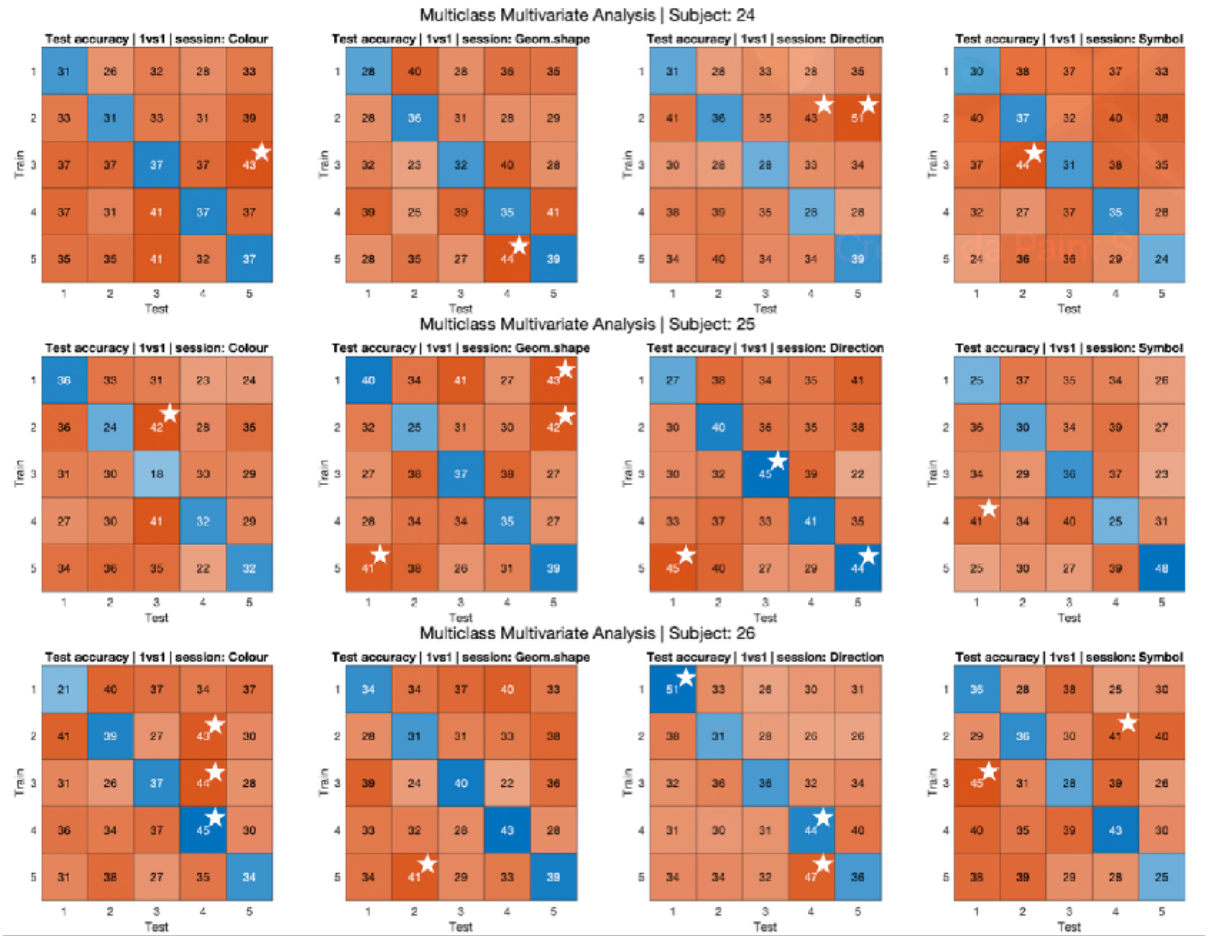

Figure 4.2.2: For each subject (row) and each session (column) a 5x5 matrix reports: the mean 5-fold cross-validation test accuracy on the diagonal, and the test accuracy of the classifier trained of the i time interval and tested in the j time interval in the i,j. position. The white stars indicate the accuracies with a p-value<0.05.

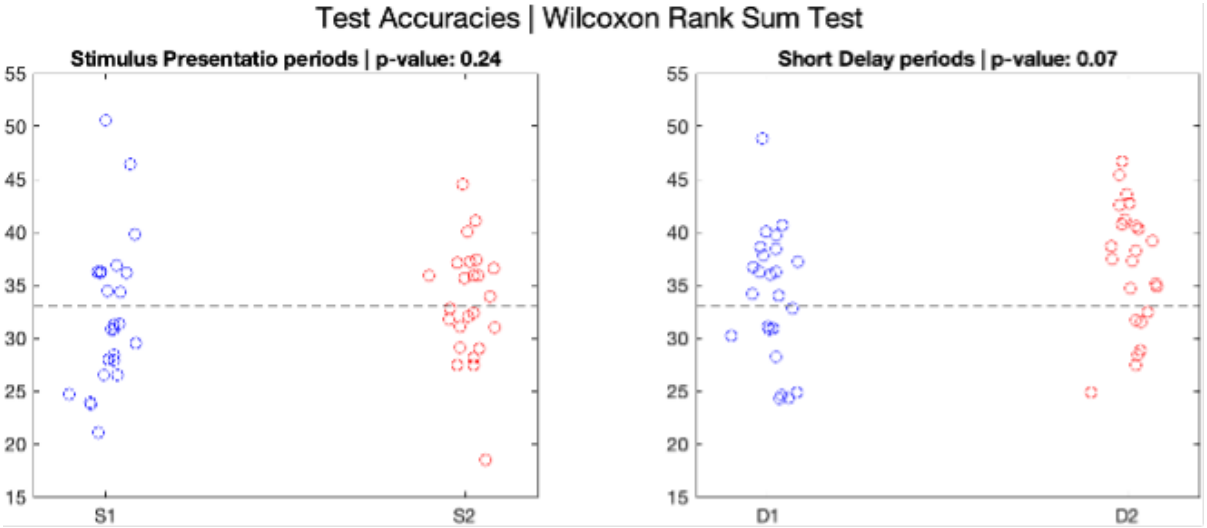

Figure 4.2.3: Test accuracies comparisons between the first (S1) and second (S2) Stimulus Presentation, and the first (D1) and second (D2) Delay periods. Black dashed lines indicate the theoretical chance level with three classes.

4.3 Subject Specific Feature Selection

The following analysis will describe in detail the physiological performances of one random subject (ID:26) for each of the three classification methods and each session. Each figure reports the analysis related to the three-time segments (stimulus presentation, short delay, and long delay; rows of the figures) and each of the three object comparisons (1vs2, 2vs3, and 1vs3; columns of the figures). A detailed description of each subject is available in *"A.2 Identification of significant areas"* - *"A. Appendix | Real experiment)*.

4.3.1 Univariate Analysis

For each figure, the test accuracies (bar plots) of each of the 10 features selected according to the Cross-Validation mean validation and their topographical distribution (topographical scalp plots) have been reported. In the topographical representation, the symbol "." indicates the selected discriminant channels and bands, while "*" represents the ones (among these discriminant features) which are statistically significant (significance threshold of α=0.05) after the FDR correction. The channels have been evaluated in theta, alpha or beta band; therefore, the channels have been represented depending on their frequency bands (green=theta, red=alpha, blue=beta, dark yellow=theta+alpha, light blue= alpha+beta, violet=theta+beta, black=thata+alpha+beta).

During the colour session (Figure 4.3.1), a significant area can be identified in the Frontal region during the short delays, mainly driven by alpha activity; while the long delay has been decoded by Frontal alpha and Temporo-Parietal-Occipital theta. Whilst, during the geometrical shape session (Figure 4.3.2), Parieto-Occipital theta activity is responsible for the decoding during the stimulus presentation and the short delay. Similarly, during the geometrical direction session (Figure 4.3.3) some Parieto-Occipital theta activity is responsible for the decoding during the short and long delay. Finally, during the symbol session (Figure 4.3.4) some Frontal beta activity can decode the stimulus presentation, while a massive Parieto-Occipital activity (mainly in beta) is responsible for the decoding during all the three-time intervals.

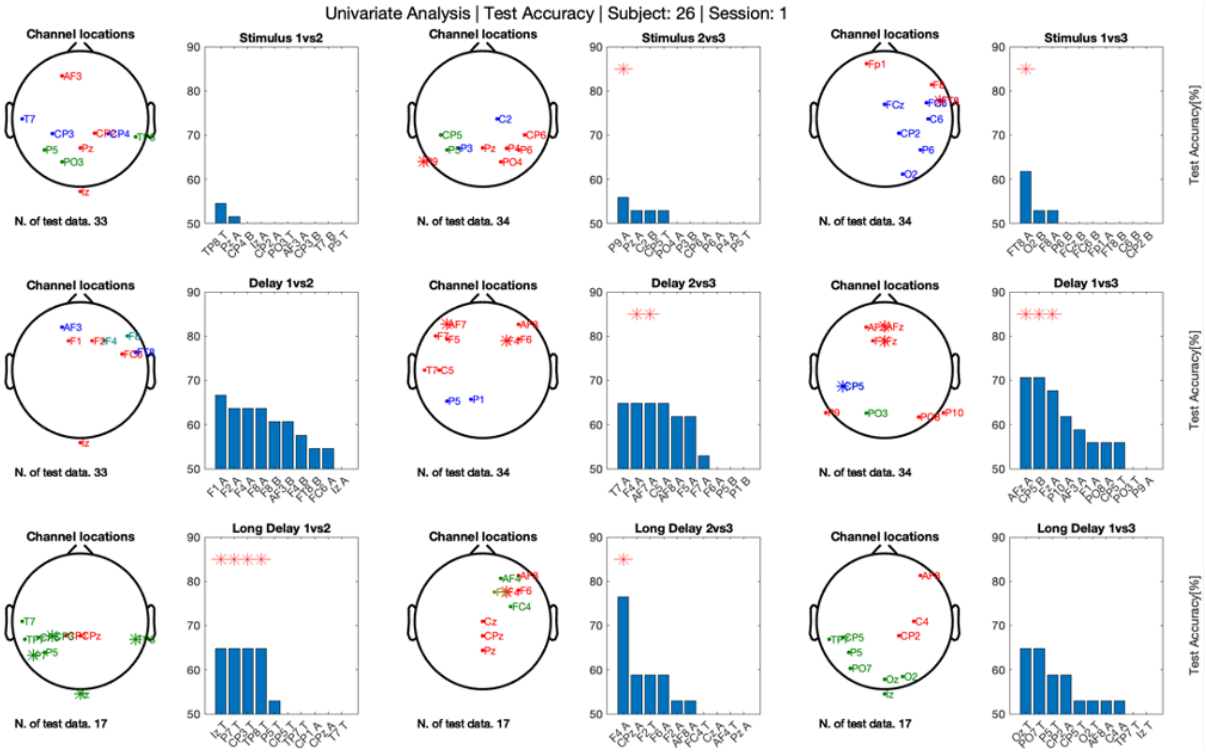

Figure 4.3.1: Test Accuracy and Meaningful channel representation | Subject 26 | Session 1 | Univariate analysis.

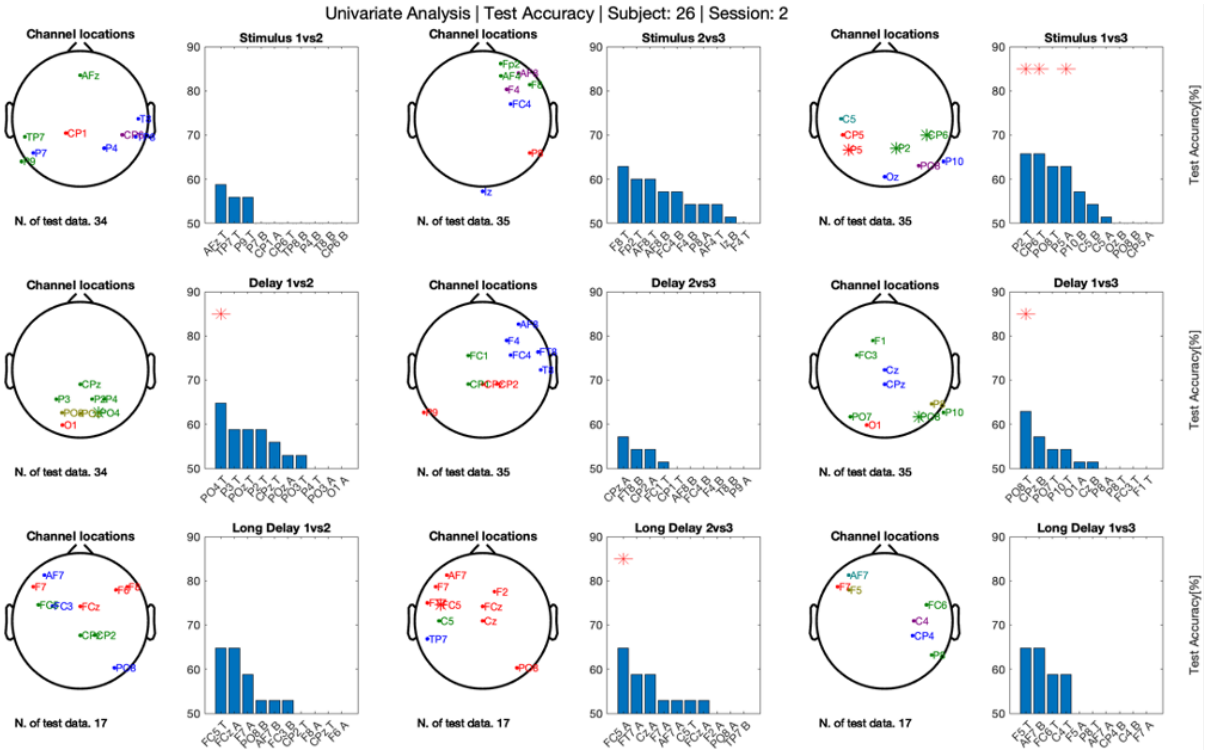

Figure 4.3.2: Test Accuracy and Meaningful channel representation | Subject 26 | Session 2 | Univariate analysis.

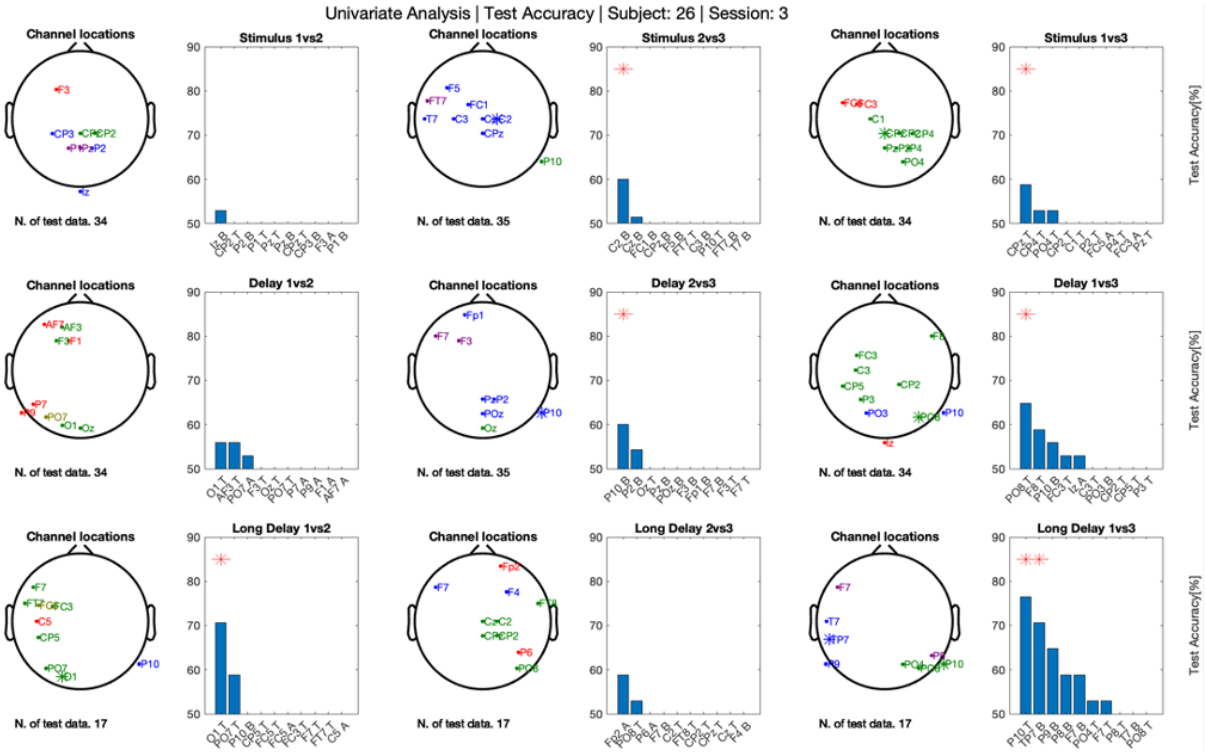

Figure 4.3.3: Test Accuracy and Meaningful channel representation | Subject 26 | Session 3 | Univariate analysis.

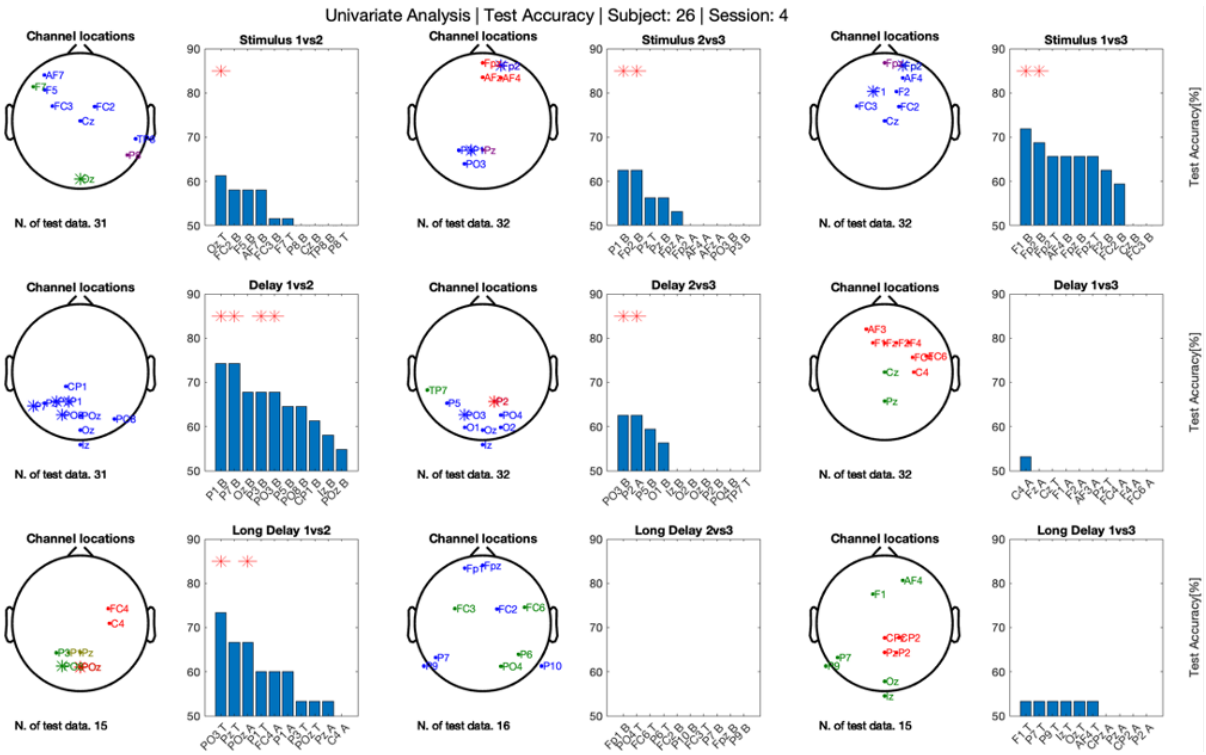

Figure 4.3.4: Test Accuracy and Meaningful channel representation | Subject 26 | Session 4 | Univariate analysis.

4.3.2 Multivariate Analysis, Filtering and Wrapping

Considering the same subject as before as an example; The following representation is very similar to the previous one with the difference that only the subset of wrapped features has been considered, and the significance has not been corrected by multiple comparisons (considering that only 1 statistical test has been used for each comparison). Moreover, over the topographical representation, the reconstruction of the activation patterns has been reached through Weight Projection from classifier weights [74]. In fact, the activation pattern A_test can be reconstructed following (4.1).

$$A_{test} = Cov(X_{test}) * w \tag{4.1}$$

Where A_test is the NxM matrix of the test data (N: number of trials; M: number of features) and w is the vector of the classifier weights. If some channels have been selected in different bands, their activation patterns have been summed.

During the colour session (Figure 4.3.5), some above-chance classification has been reached only during the long delay by the Occipital region. Whilst, during the shape session (Figure 4.3.6), only the Occipital region has been considered significant during the stimulus presentation. While, during the direction session (Figure 4.3.7), the mixed activity of the Frontal and Occipital regions has been responsible for the decoding of the long delay. Finally, during the symbol session (Figure 4.3.8), the Parieto-Occipital region allowed the above-chance decoding of the long delay.

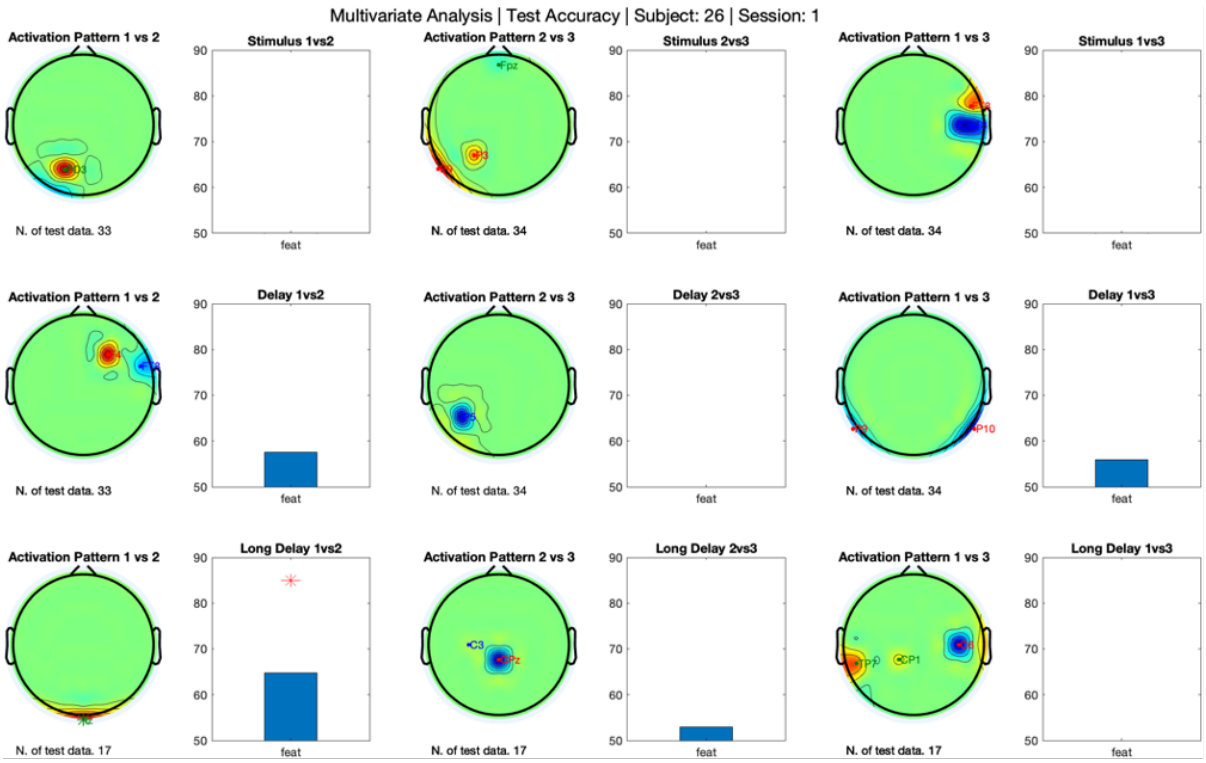

Figure 4.3.5: Test Accuracy and Meaningful channel representation | Subject 26 | Session 1 | Multivariate analysis.

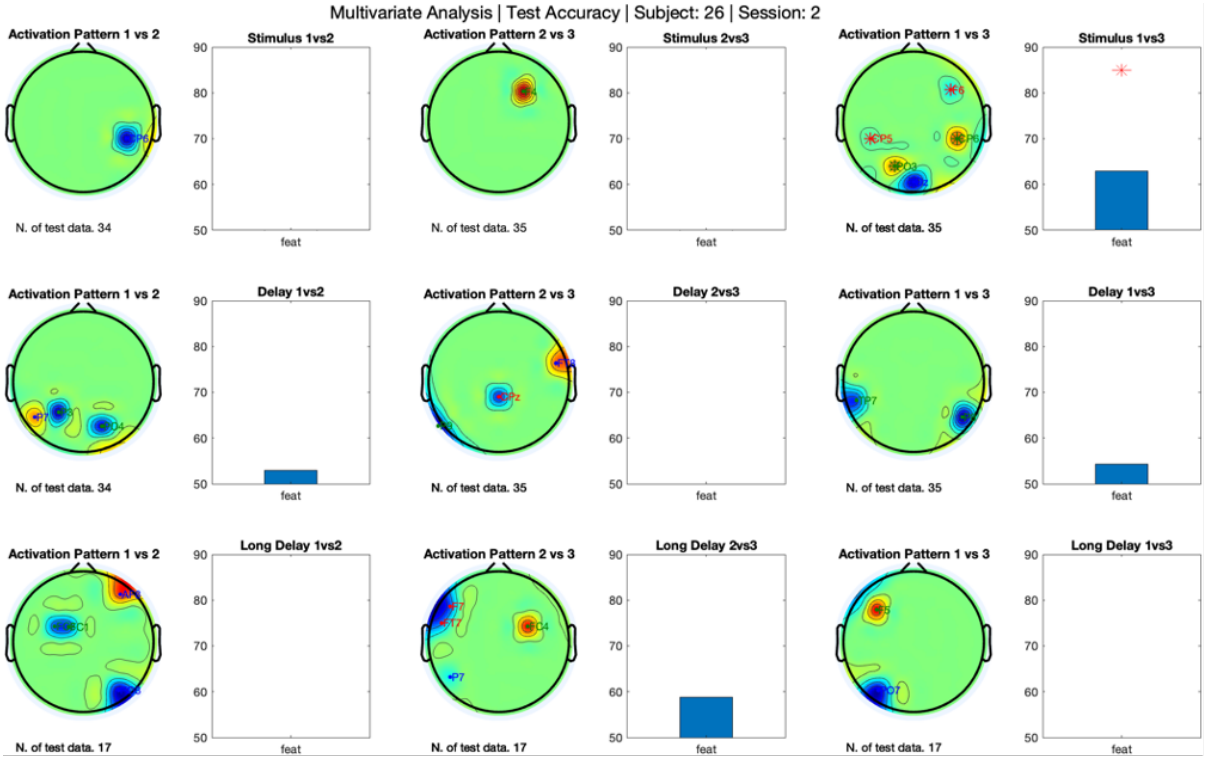

Figure 4.3.6: Test Accuracy and Meaningful channel representation | Subject 26 | Session 2 | Multivariate analysis.

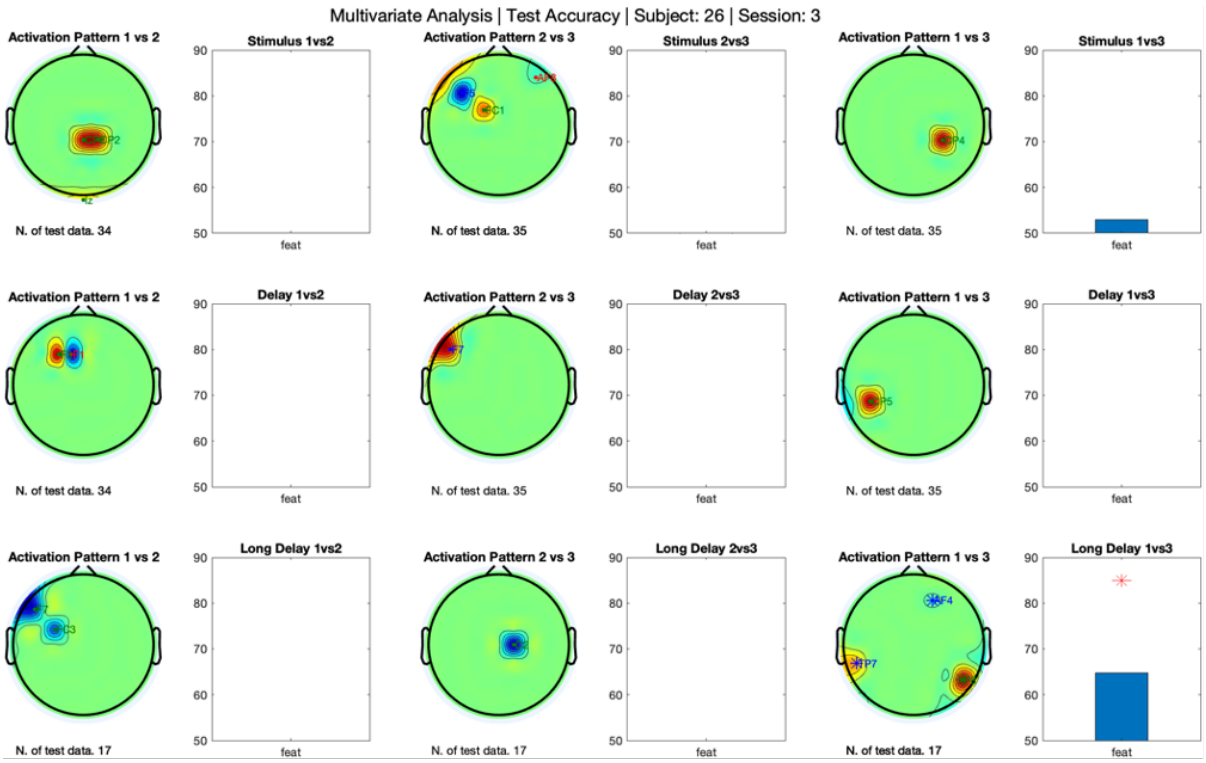

Figure 4.3.7: Test Accuracy and Meaningful channel representation | Subject 26 | Session 3 | Multivariate analysis.

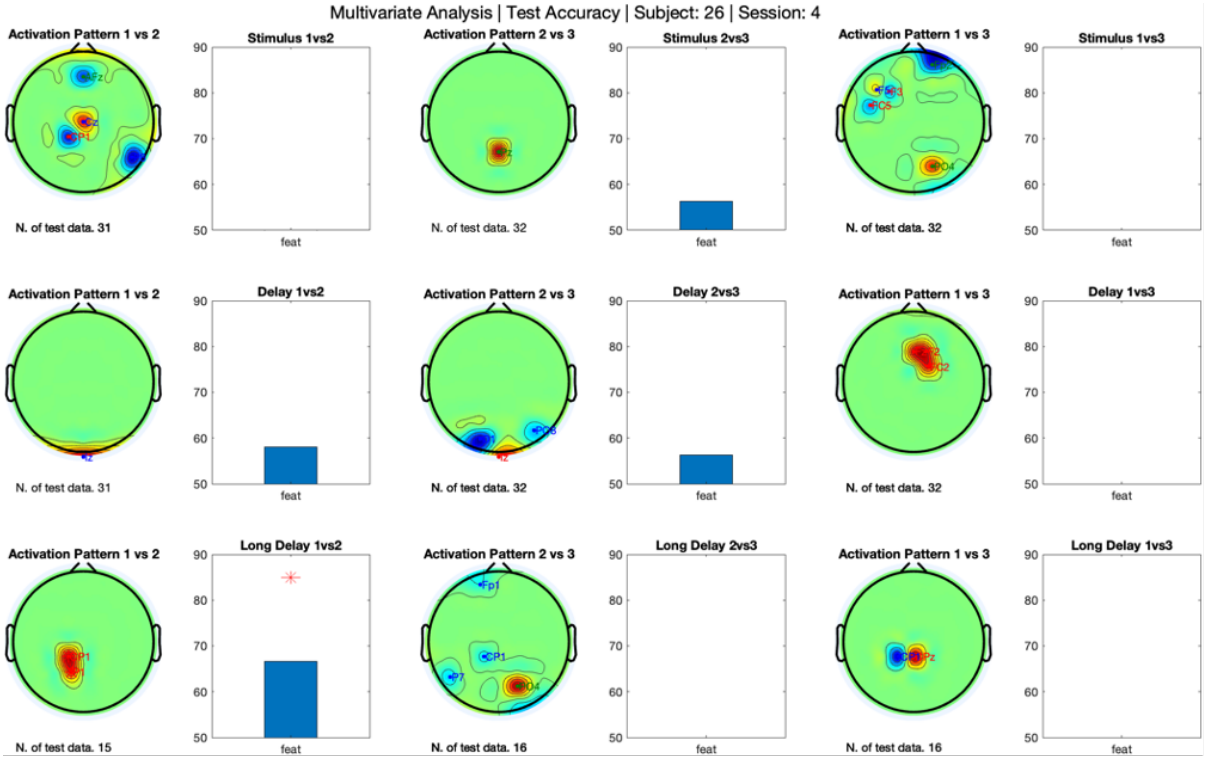

Figure 4.3.8: Test Accuracy and Meaningful channel representation | Subject 26 | Session 4 | Multivariate analysis.

4.3.3 Multivariate Analysis, FCSP

Considering the same subject as before as an example; The following representation is very similar to the previous one with the difference that only the most discriminative features for one class and for the other have been considered. Moreover, over the topographical representation, the reconstruction of the activation patterns has been reached projecting the absolute difference between the first and the last column of the Common Spatial Patterns V^{-1}.

During the colour session (Figure 4.3.9), the above-chance classification has been reached during the short and long delay by the central region. Whilst, during the shape session (Figure 4.3.10), the Frontal region has been considered significant during the stimulus presentation and the Central during the short delay. While, during the direction session (Figure 4.3.11), no statistically significant test accuracies have been reached. Finally, during the symbol session (Figure 4.3.12), the Temporal region allowed the above-chance decoding of the short delay.

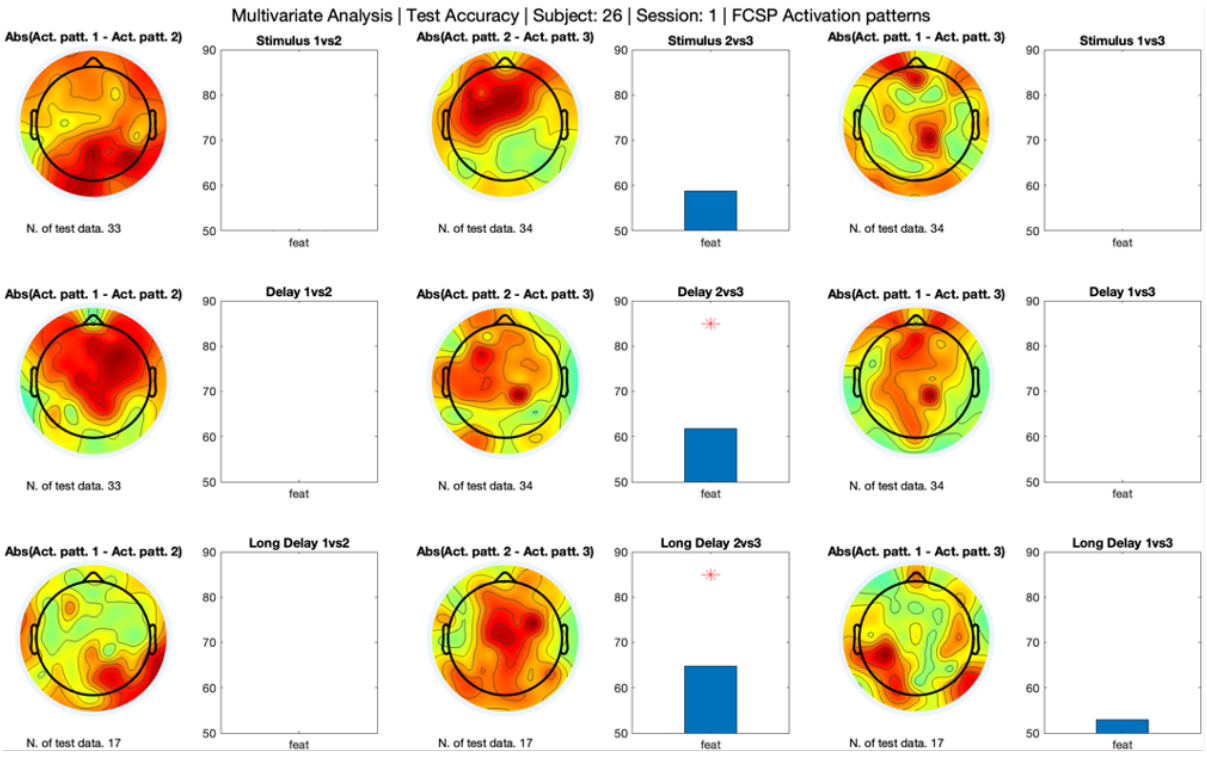

Figure 4.3.9: Test Accuracy and Meaningful channel representation | Subject 26 | Session 1 | Multivariate analysis | FCSP.

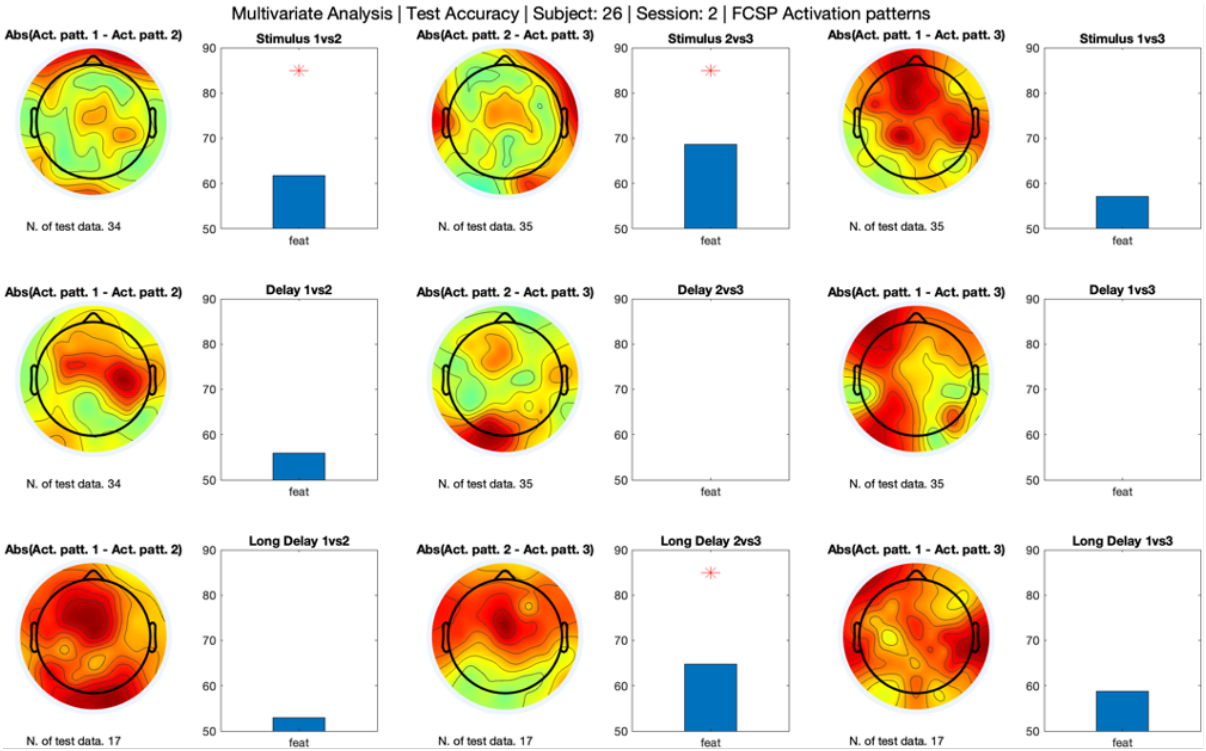

Figure 4.3.10: Test Accuracy and Meaningful channel representation | Subject 26 | Session 2 | Multivariate analysis | FCSP.

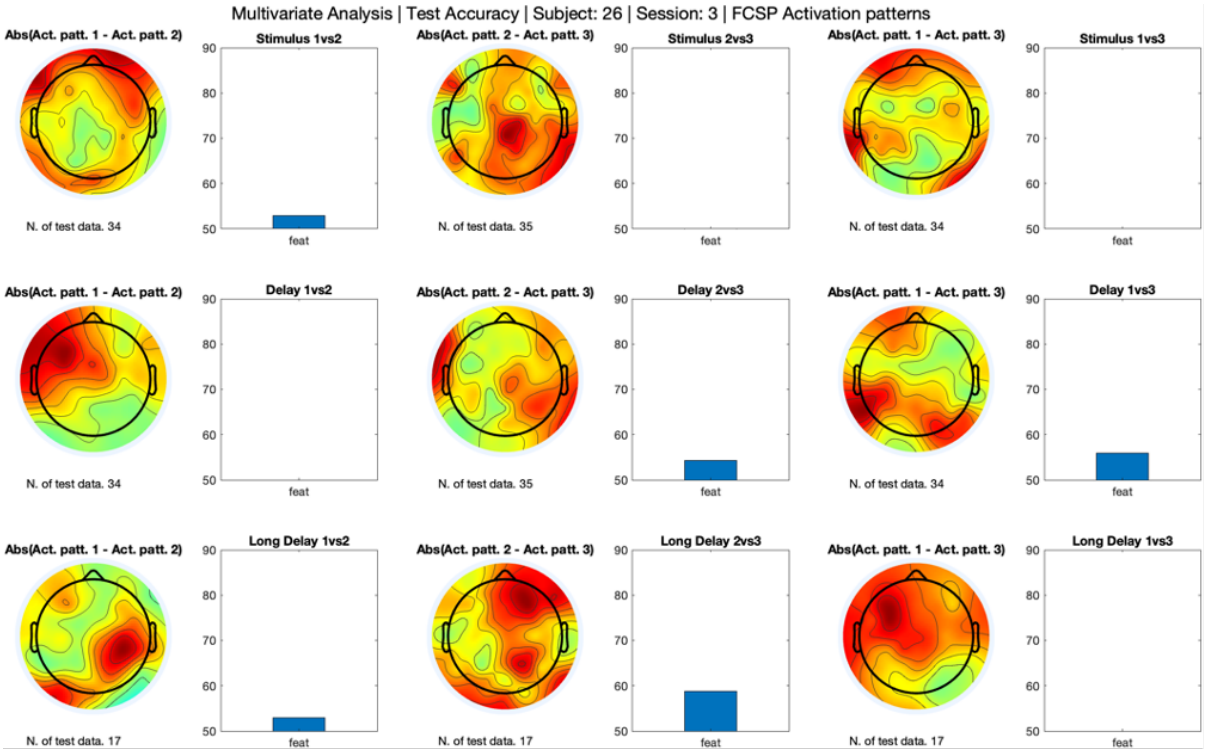

Figure 4.3.11: Test Accuracy and Meaningful channel representation | Subject 26 | Session 3 | Multivariate analysis | FCSP.

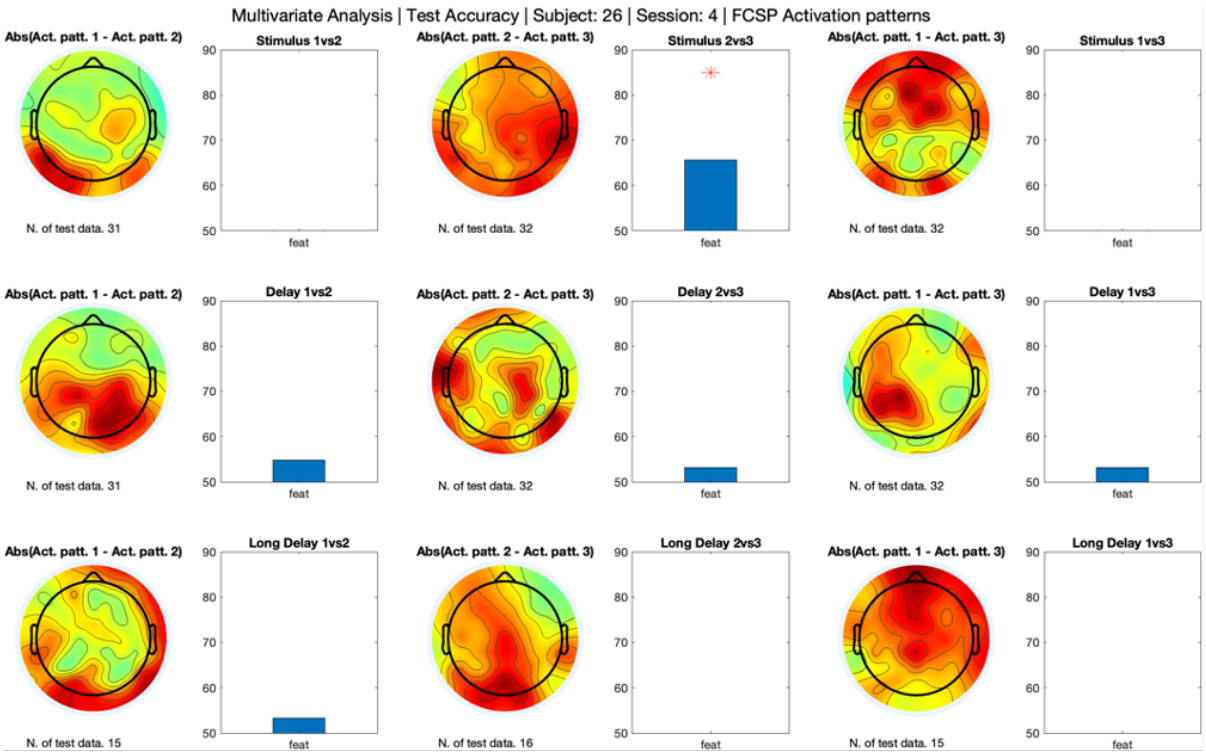

Figure 4.3.12: Test Accuracy and Meaningful channel representation | Subject 26 | Session 4 | Multivariate analysis | FCSP.

4.3.4 Univariate Analysis, General View

The results of the univariate analysis can be summarised in the following figures. All the selected features in at least one of the 3 comparisons (1vs2, 2vs3, and 1vs3) have been reported with a representation of their test accuracy p-value. If the same channel and band have been selected in more than one comparison, the lowest p-value has been taken as the final p-value. The reported value is complementary to the p-value (1-p).

For each time interval, some clusters of significant brain areas across subjects can be identified (blue rectangles in the following images). These clusters have been defined if the test accuracies have been found significant for at least 3 subjects within the same brain region. Therefore, during the stimulus presentation (Figure 4.3.13), two clusters of Occipital activity (especially in theta and beta) can be recognised for the symbol session; while the Frontal regions have been the main drivers for almost all sessions (mainly in alpha for the colour, whilst in theta for the direction and the symbol sessions) during the short delay (Figure 4.3.14); finally, only two clusters of theta Fronto-Central activity can be highlighted during the sessions of

colour and symbol during the long delay (Figure 4.3.15). In this final case, these results should be cautiously interpreted due to the more limited number of samples per comparison.

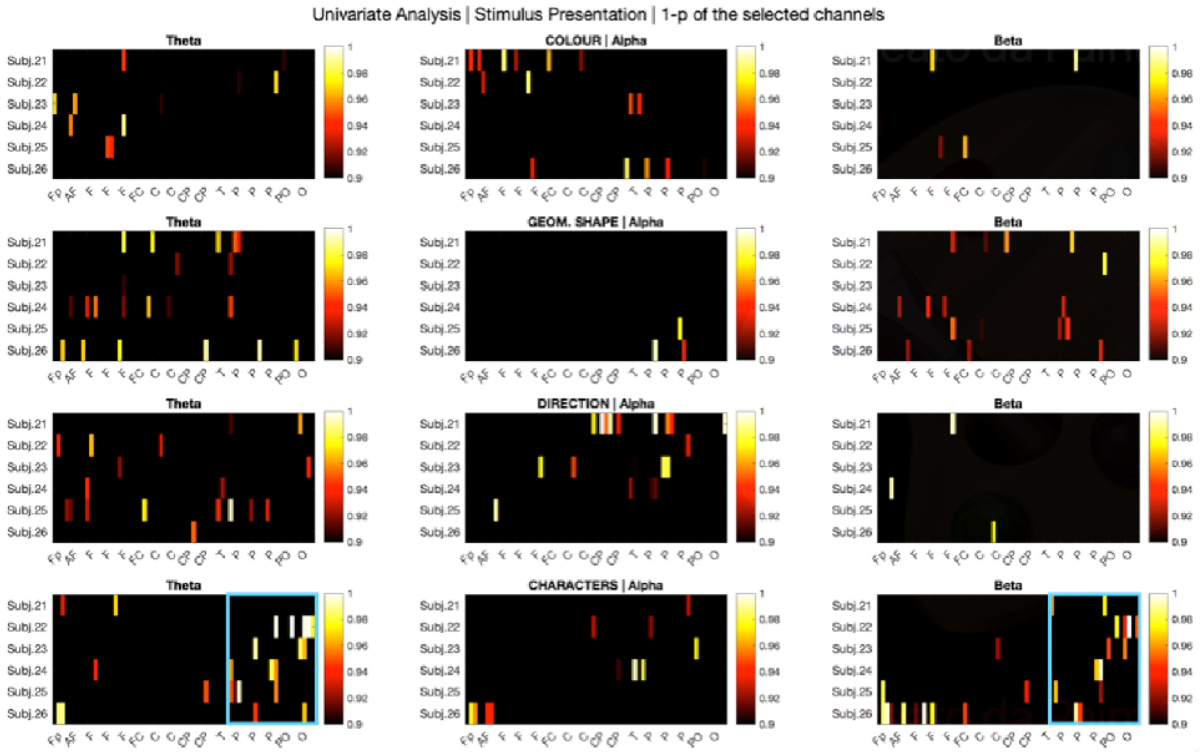

Figure 4.3.13: (1-p) of the selected channels from the univariate analysis for each subject and all together | Stimulus Presentation.

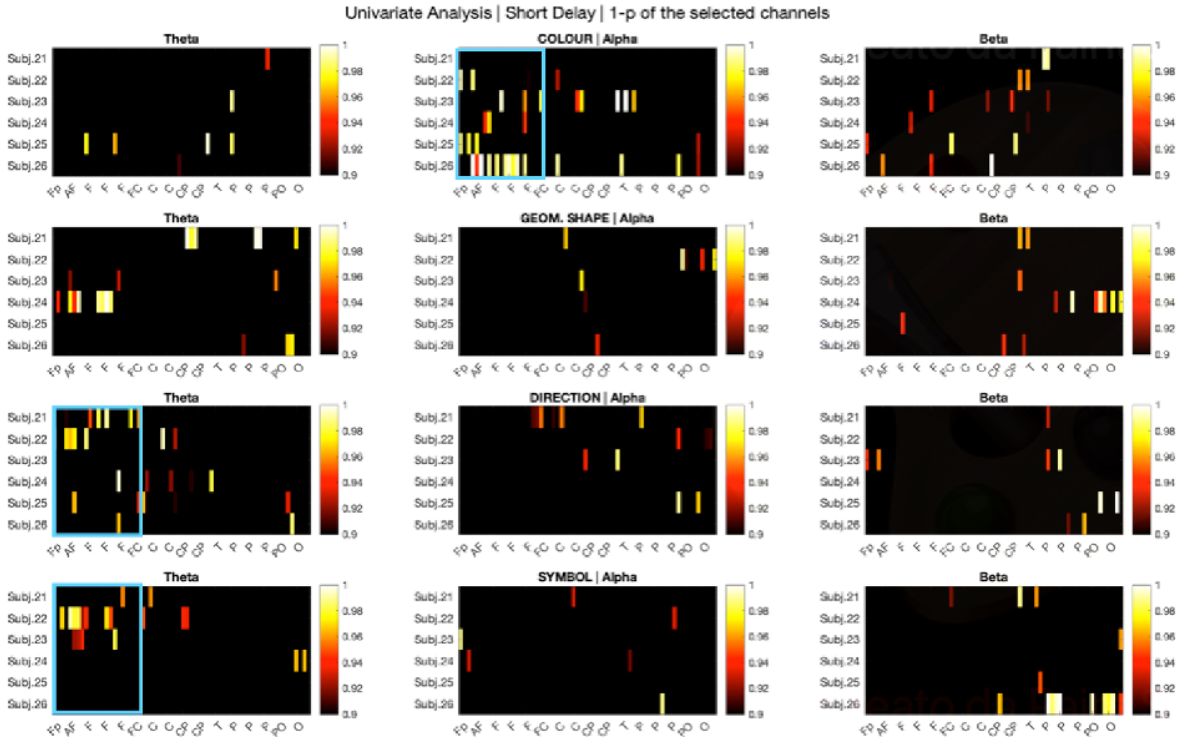

Figure 4.3.14: (1-p) of the selected channels from the univariate analysis for each subject and all together | Short Delay.

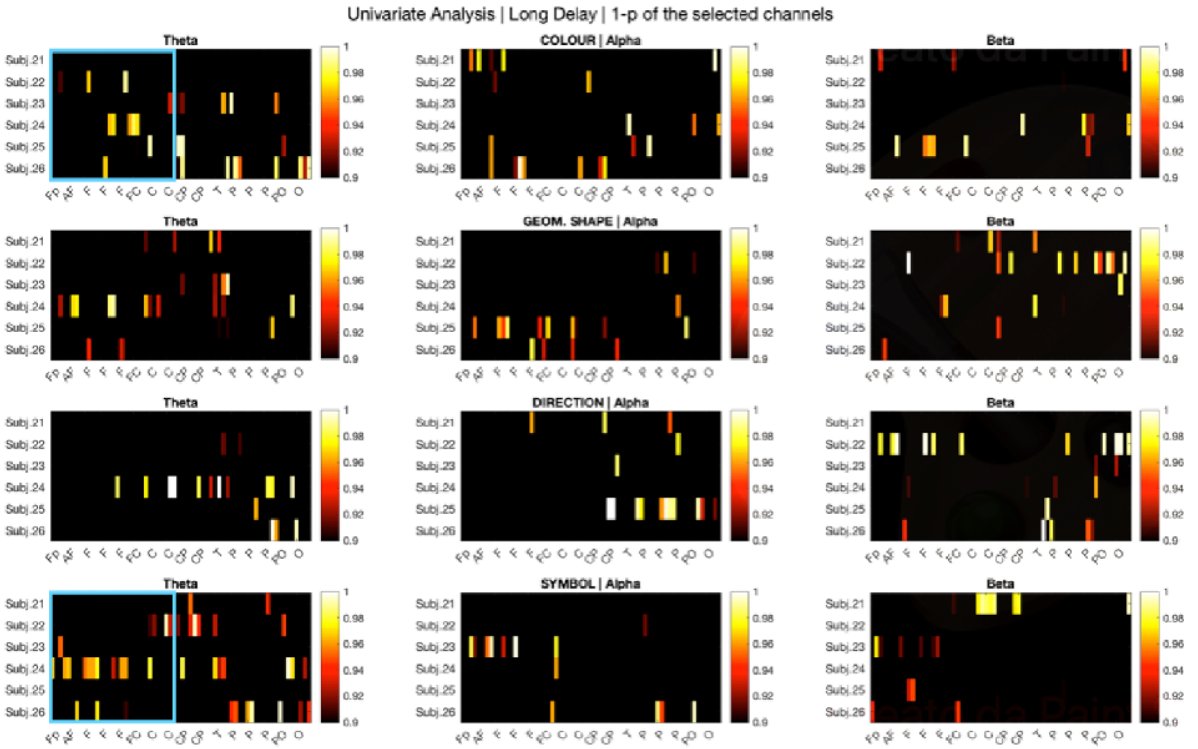

Figure 4.3.15: (1-p) of the selected channels from the univariate analysis for each subject and all together | Long Delay.

The description of the significant areas and bands for each participant and time interval have been reported in Table 4.3.1.

Table 4.3.1: Discriminative areas for each participant and time interval. (ST=Stimulus Presentation, SD=Short Delay, LD=Long Delay).

Subject ID	Time Interval	Session	Band	Brain Region
	SP	Direction	Alpha	Centro-Parietal
21	SD	Shapes	Theta	Parieto-Occipital
		Direction	Theta	Frontal
	LD	Symbols	Beta	Centro-Parietal
	SP	Symbols	Theta	Parieto-Occipital
22	SD	Direction	Theta	Frontal
		Symbols	Theta	Frontal
	LD	Symbols	Beta	Centro-Parietal
	SP	Symbols	Theta	Parieto-Occipital
23	SD	Colour	Alpha	Temporo-Parietal
	LD	Symbols	Alpha	Frontal
	SP	-	-	-
24	SD	Shapes	Theta	Frontal
	LD	Colour	Theta	Frontal
		Shapes	Theta	Frontal
	SP	-	-	-
25	SD	Colour	Alpha	Frontal
	LD	Colour	Theta	Frontal
		Direction	Alpha	Parieto-Occipital
	SP	Symbols	Beta	Frontal
26	SD	Colour	Theta	Frontal
		Symbols	Beta	Parieto-Occipital
	LD	Colour	Theta	Parieto-Occipital
		Symbols	Theta	Parieto-Occipital

Chapter 5

Discussion

5.1 Behavioural Performances

From a behavioural perspective, some individual differences have been highlighted across participants considering the accuracies, the number of non-responses, and the response time. On the other hand, these parameters can be considered enough stable across sessions, a symbol that can be interpreted as the similar perceived working memory load across the tasks. Moreover, no particular trends can be highlighted over time (such as a decrease in accuracies or an increase in response times). This absence can be considered proof that the total experimental time is not too long to wear out participants. Moreover, 5 of the 6 participants have declared to be favourable to repeat the experiment in the future. Therefore, considering all these factors, the experimental setup seems to be suitable enough to be used in real applications.

5.2 Cross Subjects Generalisation

5.2 Across and Within subjects decodifiability As expected, considering the high subject-to-subject variability, the averaged powers in the selected 8 brain regions were not able to generalise across subjects in none of the four sessions. On the other hand, individual activities managed to achieve above-chance performances during the stimulus maintenance in some participants, especially during the direction session, coherently with the results of *Bocincova A. and Johnson J. (2019)* [53] who found above-chance classification during the maintenance of direction stimuli

for task-relevant features through a time-frequency analysis. This comparison between individual and cross-individual performances highlights the importance of personalised approaches for each subject, even if the limited number of samples for this first analysis (at most 30 for each time interval) must be pointed out. Considering the classifier performances between the first and second stimulus presentation and the first and second short delay periods, no statistically significant median differences have been found, supporting the merging of similar datasets for the subsequent analysis. Moreover, also some differences in the results between the short and long delay periods can be highlighted, those differences were more expected considering the different duration, the cue-related effects, and possible anticipatory potentials.

5.3 Subject Specific Feature Selection

5.3 Identification of significant areas Considering the discriminative areas reported from the univariate and the multivariate (with filtering and wrapping) analyses, most of the wrapped features have been resulted in a subset of the ones chosen by the univariate reduction. The main difference between the two approaches is the drop in the test accuracies for the second one, probably linked to the overfitting of the models (also considering the limited number of samples for each class). On the other hand, the highlighted areas from the Frequency Spatial Common Pattern filters have been resulted to be enough different from the other approaches. Moreover, also in this case, the drop in the generalisability can be attributed to overfitting in the training set. Considering all these findings, the univariate analysis seems the best candidate to identify possible brain areas as targets for neurofeedback, considering its generalisability and its ease of interpretation.

The univariate analysis has permitted the identification, for each participant, of the best type of stimulus and brain area during the delayed periods (See *"A.2 Identification of significant areas"* - *"A. Appendix | Real experiment)*. Moreover, some clusters of common discriminative areas have been highlighted across participants, especially the Parieto-Occipital region during the stimulus presentation for the symbol, and the Frontal regions during the delayed periods. The greater significance of symbol stimulus encoding may be explained due to its lack of a direct verbal label. Differently from the obtained results, some previous work [42, 46, 51, 52] has shown the possibility of decoding specific colour content during stimulus encoding, especially from the

parieto-occipital regions. However, all these results have been achieved by averaging trials (due to the phased-locked nature of stimulus encoding). Therefore, *Teichmann et al. (2019)* [42] and *Sutterer et al. (2021)* [46] based their analysis on the Event-Related Potentials (in the time domain), while *Hajonides J. et al. (2021)* [51] and *Ratcliffe O. et al. (2022)* [52] relied on the Evoked EEG power. For what concerns the induced activity of WM maintenance instead, the obtained results are more coherent with previous findings. In fact, the role of frontal areas has been highlighted in an fMRI review by *Lee S. et al. (2016)* [49] for different visual stimuli (especially for the directions) and in an EEG study by *Ratcliffe O. et al (2022)* [52]; while the general role of Parieto-Occipital discriminant activities (as identified in the fMRI study of *Christophel T. et al. (2018)* [50] has been found only in some individuals.

5.4 Impact on Neurofeedback

Neurofeedback is a technique with a strong potential impact on some patients' lives. In fact, it has been applied for the therapeutical treatment of several psychiatric disorders (such as depression, schizophrenia, and anxiety) and as a rehabilitation tool to train or restore specific cognitive deficits (such as enhancing Attention Deficit in Hyperactivity Disorders (ADHD) [10]. To obtain these results, neurofeedback relies on humans' learning abilities and on brain plasticity by activating reinforcement learning networks [25], following the modulation of participants' brain activity in response to some informative feedback. Therefore, patients' cortical processes information is extracted through EEG acquisitions and refined through machine learning techniques to decode the information of a presented/maintained stimulus. Nevertheless, the high inter-subject variability of brain representations has led to at least 30% of participants to be not able to self-regulate their brain activities in response to a standardised protocol, even after several sessions [10].

In order to build individual-specific reliable classifiers for reducing this number of non-responder patients, the presented work has shown that a personalised treatment is more suited than a standardised one to highlight some EEG-related differences across subjects, during the working memory maintenance of an item. Especially, none of the tested visual stimuli has reached statistically significant generalisability through classifiers trained on across subjects EEG powers, showing that cerebral activity relies on different representations across subjects. On the other hand, the EEG powers

have resulted in some statistically significant generalisability within the same subject, depending on the visual stimulus. Therefore, indicating that specific stimuli are more decodable for each participant, an essential characteristic to build reliable classifiers. Moreover, through the statistical significance of the classifiers' test accuracies from the univariate analysis, some brain regions have been identified, for each participant, as the most discriminative areas for the specific stimulus. Consequently, the feedback representation during a clinical session could be constrained to that area, to shift its cerebral activity to a more physiological range. Finally, another possible implication of these findings could be a reduction in the number of neurofeedback sessions necessary to enhance the working memory capacity due to the a priori identification of individual-specific preferential stimuli and brain regions. This result could be very impactful for patients' rehabilitation journey, considering that neurofeedback treatment for WM enhancement can last months [75].

Chapter 6

Future Work

Some limitations of the current study are intrinsically linked to the experimental design. Firstly, the use of ICA decomposition to remove eye-related artefacts. This methodology cannot be used in real-time acquisitions, but it has been necessary due to the high number of participant blinks during the acquisition. This issue had been already considered during the experimental planning. In fact, during the pilot studies, a pre-trained participant had been able to not bink for all the sessions also with a longer trial (see "*"B.3 Eye-Artefact and ICA Component Removal" - "B. Appendix | Pilots)* and another one had reported that the blinking at the correct time becoming more automatic during sessions (in fact, it had corresponded in a decrease of the number of blinks per session). Therefore, this issue can be simply solved through repetitions.

Another important limitation is related to the number of trials per comparison. In fact, the low generalisability of the multivariate analyses is likely linked to the small number of samples. Moreover, for the stimulus presentation and the short delay, the data from different portions of trials have been pooled under the same comparison. For example, in the comparison of "red" vs "blue" during the stimulus presentation, all the data related to the "red" stimulus presentation have been pooled independently on if it was the first or the second stimulus and if the other stimulus, present during the trial, was "green" or "blue". To mitigate this increase in heterogeneity, the data have been split into a stratified way during the train-test division (and possible cross-validation), so that they were equally represented during feature selection and generalisability assessment. A final important limitation of this study is the lack of day-

by-day acquisitions to monitor the intra-day stability of the discriminative features. In fact, even if some areas are expected to be the most discriminative, for example, the Frontal and Occipital during the delays, a quantification of the stability of these areas is necessary to apply this methodology in real scenarios.

Future studies should investigate the generalisability in larger cohorts of participants and, more importantly, in the target groups (elderly, patients affected by strokes or brain injuries), considering that the examined group was composed of male, young participants. Moreover, future studies can investigate the changes in the discriminability of brain areas across stimuli during a neurofeedback experiment, investigating the time-frequency classification performances.

Chapter 7

Conclusions

The performed analysis has shown that it is possible to classify the specific object during the working memory maintenance at a single trial level (without averaging) within the same individual. Indeed, the generalisation across subjects has not achieved above-chance classifications, whilst it has been possible after considering each subject independently, and not as a part of a population. Therefore, the personalised approach has allowed defining for each participant the most discriminative stimulus and a target area. In fact, even if the Frontal and Occipital areas are the most highlighted by literature during the stimulus maintenance, individual target areas have sometimes moved away from this generalisation, depending on the optimal stimulus. Among the three tested classification methodologies to investigate the discriminative brain regions, the univariate analysis has been shown to be the most generalisable and easy to interpret. Another important result of this analysis is that the tested experimental setup resulted in no negative impact on the behavioural performances of the participants, and most of them reported to be favourable to repeating it in the future. Considering all these factors, the present study can be considered as an important step to achieving personalised neurofeedback. Future research should assess the impact of a such personalised approach, compared to a standardised one, on the decline of working memory in the elderly, stroke survivors, and other fragile groups.

Bibliography

[1] A. Baddeley, “Working memory,” *Science*, vol. 255, pp. 556–559, 1992.

[2] O. Matysiak, A. Kroemeke, and A. Brzezicka, “Working memory capacity as a predictor of cognitive training efficacy in the elderly population,” *Frontiers in Aging Neuroscience*, vol. 11, 2019.

[3] T. S.-S. Megan and Klingberg, “Benefits of a working memory training program for inattention in daily life: A systematic review and meta-analysis,” *PLOS ONE*, vol. 10, pp. 1–18, 5 2015.

[4] B. T. Baune, R. Miller, J. McAfoose, M. Johnson, F. Quirk, and D. Mitchell, “The role of cognitive impairment in general functioning in major depression,” *Psychiatry Research*, vol. 176, pp. 183–189, 2010.

[5] C. Cotrena, L. D. Branco, R. Kochhann, F. M. Shansis, and R. P. Fonseca, “Quality of life, functioning and cognition in bipolar disorder and major depression: A latent profile analysis,” *Psychiatry Research*, vol. 241, pp. 289–296, 2016.

[6] N. Revheim, I. Schechter, D. Kim, G. Silipo, B. Allingham, P. Butler, and D. C. Javitt, “Neurocognitive and symptom correlates of daily problem-solving skills in schizophrenia,” *Schizophrenia Research*, vol. 83, pp. 237–245, 2006.

[7] F. Fregni, P. S. Boggio, M. Nitsche, F. Bermpohl, A. Antal, E. Feredoes, M. A. Marcolin, S. P. Rigonatti, M. T. A. Silva, W. Paulus, and A. Pascual-Leone, “Anodal transcranial direct current stimulation of prefrontal cortex enhances working memory,” *Experimental Brain Research*, vol. 166, pp. 23–30, 2005.

[8] R. M. G. Reinhart and J. A. Nguyen, “Working memory revived in older adults by synchronizing rhythmic brain circuits,” *Nature Neuroscience*, vol. 22, pp. 820–827, 2019.

[9] M. Mirjalili, R. Zomorrodi, Z. Daskalakis, S. Hill, and T. Rajji, "Individualized real□time prediction of working memory performance by classifying electroencephalography signals," *International Journal of Imaging Systems and Technology*, vol. 32, 4 2022.

[10] C. Loriette, C. Ziane, and S. B. Hamed, "Neurofeedback for cognitive enhancement and intervention and brain plasticity," *Revue Neurologique*, vol. 177, pp. 1133–1144, 2021. THEMATIC SECTION: PLASTICITY.

[11] L. R. Trambaiolli, R. Cassani, D. M. A. Mehler, and T. H. Falk, "Neurofeedback and the aging brain: A systematic review of training protocols for dementia and mild cognitive impairment," *Frontiers in Aging Neuroscience*, vol. 13, 2021.

[12] S. J. Luck and E. K. Vogel, "Visual working memory capacity: from psychophysics and neurobiology to individual differences," *Trends in Cognitive Sciences*, vol. 17, pp. 391–400, 2013.

[13] J. Brockmole and R. Logie, "Age-related change in visual working memory: A study of 55,753 participants aged 8–75," *Frontiers in Psychology*, vol. 4, 2013.

[14] I. Pavisic, J. Nicholas, Y. Pertzov, A. O'Connor, Y. Liang, J. Collins, K. Lu, P. Weston, N. Ryan, M. Husain, S. Crutch, and N. Fox, "Visual short-term memory impairments in presymptomatic familial alzheimer's disease: a longitudinal observational study," 4 2020.

[15] S. Ferber, J. Ruppel, and J. Danckert, "Visual working memory deficits following right brain damage," *Brain and Cognition*, vol. 142, p. 105566, 2020.

[16] H. Arciniega, J. Shires, S. Furlong, A. Kilgore-Gomez, A. Cerreta, N. G. Murray, and M. E. Berryhill, "Impaired visual working memory and reduced connectivity in undergraduates with a history of mild traumatic brain injury," *Scientific Reports*, vol. 11, p. 2789, 2021.

[17] S. Lugtmeijer, N. A. Lammers, E. H. F. de Haan, F.-E. de Leeuw, and R. P. C. Kessels, "Post-stroke working memory dysfunction: A meta-analysis and systematic review," *Neuropsychology Review*, vol. 31, pp. 202–219, 2021.

[18] S. Lugtmeijer, S. Schneegans, N. A. Lammers, L. Geerligs, F. E. de Leeuw, E. H. F. de Haan, P. M. Bays, and R. P. C. Kessels, "Consequence of stroke for feature recall

and binding in visual working memory," *Neurobiology of Learning and Memory*, vol. 179, p. 107387, 2021.

[19] M. Liu, Z.-Y. Nie, R.-R. Li, W. Zhang, L.-H. Huang, J.-Q. Wang, W.-X. Xiao, J. C. Zheng, and Y.-X. Li, "Neural mechanism of repeated transcranial magnetic stimulation to enhance visual working memory in elderly individuals with subjective cognitive decline," *Frontiers in Neurology*, vol. 12, 2021.

[20] N. R. Polizzotto, N. Ramakrishnan, and R. Y. Cho, "Is it possible to improve working memory with prefrontal tdcs? bridging currents to working memory models," *Frontiers in Psychology*, vol. 11, 2020.

[21] H. Marzbani, H. Marateb, and M. Mansourian, "Methodological note: Neurofeedback: A comprehensive review on system design, methodology and clinical applications," *Basic and Clinical Neuroscience Journal*, vol. 7, pp. 143–158, 4 2016.

[22] V. K. da Paz, A. Garcia, A. da Paz Neto, and C. Tomaz, "Smr neurofeedback training facilitates working memory performance in healthy older adults: A behavioral and eeg study," *Frontiers in Behavioral Neuroscience*, vol. 12, 2018.

[23] S. Xiong, C. Cheng, X. wu, L. Yao, and J. Zhang, "Working memory training using eeg neurofeedback in normal young adults," *Bio-medical materials and engineering*, vol. 24, pp. 3637–3644, 4 2014.

[24] Y. Lavy, T. Dwolatzky, Z. Kaplan, J. Guez, and D. Todder, "Mild cognitive impairment and neurofeedback: A randomized controlled trial," *Frontiers in Aging Neuroscience*, vol. 13, 2021.

[25] J. V. Doren, H. Heinrich, M. Bezold, N. Reuter, O. Kratz, S. Horndasch, M. Berking, T. Ros, H. Gevensleben, G. H. Moll, and P. Studer, "Theta/beta neurofeedback in children with adhd: Feasibility of a short-term setting and plasticity effects," *International Journal of Psychophysiology*, vol. 112, pp. 80–88, 2017.

[26] A. Marinelli, N. Boccardo, F. Tessari, D. D. Domenico, G. Caserta, M. Canepa, G. Gini, G. Barresi, M. Laffranchi, L. D. Michieli, and M. Semprini, "Active upper limb prostheses: a review on current state and upcoming breakthroughs," *Progress in Biomedical Engineering*, vol. 5, p. 12001, 1 2023.

[27] L. Pessoa, E. Gutierrez, P. A. Bandettini, and L. G. Ungerleider, "Neural correlates of visual working memory: fmri amplitude predicts task performance," *Neuron*, vol. 35, pp. 975–987, 2002.

[28] M. Lundqvist, J. Rose, P. Herman, S. Brincat, T. Buschman, and E. Miller, "Gamma and beta bursts underlie working memory," *Neuron*, vol. 90, pp. 152–164, 2016.

[29] E. K. Miller, C. A. Erickson, and R. Desimone, "Neural mechanisms of visual working memory in prefrontal cortex of the macaque," *Journal of Neuroscience*, vol. 16, pp. 5154–5167, 1996.

[30] M. Stokes, M. Kusunoki, N. Sigala, H. Nili, D. Gaffan, and J. Duncan, "Dynamic coding for cognitive control in prefrontal cortex," *Neuron*, vol. 78, pp. 364–375, 2013.

[31] G. Mongillo, O. Barak, and M. Tsodyks, "Synaptic theory of working memory," *Science*, vol. 319, pp. 1543–1546, 2008.

[32] J. Parvizi and S. Kastner, "Promises and limitations of human intracranial electroencephalography," *Nature Neuroscience*, vol. 21, pp. 474–483, 2018.

[33] Z. J. Koles, "Trends in eeg source localization," *Electroencephalography and Clinical Neurophysiology*, vol. 106, pp. 127–137, 1998.

[34] M. G. Stokes, M. J. Wolff, and E. Spaak, "Decoding rich spatial information with high temporal resolution.," *Trends in cognitive sciences*, vol. 19, pp. 636–638, 11 2015.

[35] V. Changoluisa, C. Poch, P. Campo, and F. B. Rodriguez, "Predicting working memory performance based on specific individual eeg spatiotemporal features," *bioRxiv*, p. 2022.05.06.490941, 1 2022.

[36] S. Mirjalili, P. Powell, J. Strunk, T. James, and A. Duarte, "Evaluation of classification approaches for distinguishing brain states predictive of episodic memory performance from electroencephalography: Abbreviated title: Evaluating methods of classifying memory states from eeg," *NeuroImage*, vol. 247, p. 118851, 2022.

[37] T. Grootswagers, S. Wardle, and T. Carlson, "Decoding dynamic brain patterns from evoked responses: A tutorial on multivariate pattern analysis applied to time series neuroimaging data," *Journal of cognitive neuroscience*, vol. 29, 4 2016.

[38] F. Sandhaeger, C. von Nicolai, E. K. Miller, and M. Siegel, "Monkey eeg links neuronal color and motion information across species and scales," *eLife*, vol. 8, p. e45645, 2019.

[39] R. M. Cichy, F. M. Ramirez, and D. Pantazis, "Can visual information encoded in cortical columns be decoded from magnetoencephalography data in humans?," *NeuroImage*, vol. 121, pp. 193–204, 2015.

[40] P. Ramkumar, M. Jas, S. Pannasch, R. Hari, and L. Parkkonen, "Feature-specific information processing precedes concerted activation in human visual cortex," *The Journal of Neuroscience*, vol. 33, p. 7691, 5 2013.

[41] J. J. Foster, E. M. Bsales, R. J. Jaffe, and E. Awh, "Alpha-band activity reveals spontaneous representations of spatial position in visual working memory.," *Current biology : CB*, vol. 27, pp. 3216–3223.e6, 10 2017.

[42] L. Teichmann, T. Grootswagers, T. A. Carlson, and A. N. Rich, "Seeing versus knowing: The temporal dynamics of real and implied colour processing in the human brain," *NeuroImage*, vol. 200, pp. 373–381, 2019.

[43] L. Teichmann, G. L. Quek, A. K. Robinson, T. Grootswagers, T. A. Carlson, and A. N. Rich, "The influence of object-colour knowledge on emerging object representations in the brain," *bioRxiv*, p. 533513, 1 2020.

[44] Y. Wang, S. Wang, and M. Xu, "The function of color and structure based on eeg features in landscape recognition," *International Journal of Environmental Research and Public Health*, vol. 18, 2021.

[45] Y. Wu, X. Zeng, K. Feng, D. Wei, and L. Song, "Visual color decoding using brain-computer interfaces," pp. 269–273, 2021.

[46] D. Sutterer, A. Coia, V. Sun, S. Shevell, and E. Awh, "Decoding chromaticity and luminance from patterns of eeg activity," *Psychophysiology*, vol. 58, 4 2021.

[47] F. van Ede, S. R. Chekroud, and A. C. Nobre, "Human gaze tracks attentional focusing in memorized visual space," *Nature Human Behaviour*, vol. 3, pp. 462–470, 2019.

[48] P. Mostert, A. M. Albers, L. Brinkman, L. Todorova, P. Kok, and F. P. de Lange, "Eye movement-related confounds in neural decoding of visual working memory representations," *eneuro*, vol. 5, pp. ENEURO.0401–17.2018, 7 2018.

[49] S.-H. Lee and C. I. Baker, "Multi-voxel decoding and the topography of maintained information during visual working memory," *Frontiers in Systems Neuroscience*, vol. 10, 2016.

[50] T. B. Christophel, C. Allefeld, C. Endisch, and J.-D. Haynes, "View-independent working memory representations of artificial shapes in prefrontal and posterior regions of the human brain," *Cerebral Cortex*, vol. 28, pp. 2146–2161, 6 2018.

[51] J. E. Hajonides, A. C. Nobre, F. van Ede, and M. G. Stokes, "Decoding visual colour from scalp electroencephalography measurements," *NeuroImage*, vol. 237, p. 118030, 2021.

[52] O. Ratcliffe, K. Shapiro, and B. P. Staresina, "Fronto-medial theta coordinates posterior maintenance of working memory content," *Current Biology*, vol. 32, pp. 2121–2129.e3, 2022.

[53] A. Bocincova and J. S. Johnson, "The time course of encoding and maintenance of task-relevant versus irrelevant object features in working memory," *Cortex*, vol. 111, pp. 196–209, 2019.

[54] A. C. Nobre and F. van Ede, "Under the mind #039;s hood: What we have learned by watching the brain at work," *The Journal of Neuroscience*, vol. 40, p. 89, 1 2020.

[55] H. D. Zimmer and B. Fischer, "Visual working memory of chinese characters and expertise: The expert's memory advantage is based on long-term knowledge of visual word forms," *Frontiers in Psychology*, vol. 11, 2020.

[56] P. Zerr, S. Gayet, and S. Stigchel, "Retro-cue benefits across time," *Journal of Vision*, vol. 20, p. 689, 4 2020.

[57] J. Thielen, S. E. Bosch, T. M. van Leeuwen, M. A. J. van Gerven, and R. van Lier, "Evidence for confounding eye movements under attempted fixation and active viewing in cognitive neuroscience," *Scientific Reports*, vol. 9, p. 17456, 2019.

[58] S. C. Quax, N. Dijkstra, M. J. van Staveren, S. E. Bosch, and M. A. J. van Gerven, "Eye movements explain decodability during perception and cued attention in meg," *NeuroImage*, vol. 195, pp. 444–453, 2019.

[59] S. Teki and T. D. Griffiths, "Brain bases of working memory for time intervals in rhythmic sequences," *Frontiers in Neuroscience*, vol. 10, 2016.

[60] R. Watanabe and T. Higuchi, "Anticipatory action planning for stepping onto competing potential targets," *Frontiers in Human Neuroscience*, vol. 16, 2022.

[61] D. H. Brainard, "The psychophysics toolbox," *Spatial Vision*, vol. 10, pp. 433 – 436, 1997.

[62] P. Bak, C. Tang, and K. Wiesenfeld, "Bak, p., tang, c. & wiesenfeld, k. self-organized criticality: An explanation of 1/f noise. phys. rev. lett. 59, 381-384," *Physical Review Letters*, vol. 59, pp. 381–384, 4 1987.

[63] J. van Driel, C. N. L. Olivers, and J. J. Fahrenfort, "High-pass filtering artifacts in multivariate classification of neural time series data," *Journal of Neuroscience Methods*, vol. 352, p. 109080, 2021.

[64] M. Pontifex, K. Gwizdala, A. Parks, M. Billinger, and C. Brunner, "Variability of ica decomposition may impact eeg signals when used to remove eyeblink artifacts," *Psychophysiology*, vol. 54, 4 2016.

[65] P. Welch, "The use of fast fourier transform for the estimation of power spectra: A method based on time averaging over short, modified periodograms," *IEEE Transactions on Audio and Electroacoustics*, vol. 15, pp. 70–73, 1967.

[66] A. Skiadopoulos and N. Stergiou, "Chapter 5 - power spectrum and filtering," *Biomechanics and Gait Analysis*, pp. 99–148, 2020.

[67] B. Sen, M. Peker, A. Cavuşoğlu, and F. Celebi, "A comparative study on classification of sleep stage based on eeg signals using feature selection and classification algorithms," *Journal of medical systems*, vol. 38, p. 18, 4 2014.

[68] C. J. C. Burges, "A tutorial on support vector machines for pattern recognition," *Data Mining and Knowledge Discovery*, vol. 2, pp. 121–167, 1998.

[69] R. A. FISHER, "The use of multiple measurements in taxonomic problems," *Annals of Eugenics*, vol. 7, pp. 179–188, 1936.

[70] K. K. Ang, Z. Y. Chin, H. Zhang, and C. Guan, "Filter bank common spatial pattern (fbcsp) in brain-computer interface," pp. 2390–2397, 2008.

[71] E. Combrisson and K. Jerbi, "Exceeding chance level by chance: The caveat of theoretical chance levels in brain signal classification and statistical assessment of decoding accuracy," *Journal of Neuroscience Methods*, vol. 250, pp. 126–136, 2015. Cutting-edge EEG Methods.

[72] E. Maris and R. Oostenveld, "Nonparametric statistical testing of eeg- and meg-data," *Journal of neuroscience methods*, vol. 164, pp. 177–190, 5 2007.

[73] P. K. Saha, M. A. Rahman, M. K. Alam, A. Ferdowsi, and M. N. Mollah, "Common spatial pattern in frequency domain for feature extraction and classification of multichannel eeg signals," *SN Computer Science*, vol. 2, p. 149, 2021.

[74] S. Haufe, F. Meinecke, K. Görgen, S. Dähne, J.-D. Haynes, B. Blankertz, and F. Bießmann, "On the interpretation of weight vectors of linear models in multivariate neuroimaging," *NeuroImage*, vol. 87, pp. 96–110, 2014.

[75] W.-H. Yeh, J.-J. Hsueh, and F.-Z. Shaw, "Neurofeedback of alpha activity on memory in healthy participants: A systematic review and meta-analysis," *Frontiers in Human Neuroscience*, vol. 14, 2021.

[76] C. M. Bilacchi, E. V. P. Sirius, A. M. Cravo, and R. M. de Azevedo Neto, "Temporal dynamics of implicit memory underlying serial dependence," *Memory & Cognition*, vol. 50, pp. 449–458, 2022.

Appendix - Contents

Appendix A

Appendix | Real experiment

This supplementary section has been used to describe the reported mental strategies used by the participants during the real experiment in *"A.1 Mental Strategies"* and a detailed analysis of the discriminative areas for each participant in *"A.2 Subject Specific Feature Selection*.

A.1 Mental Strategies

Participants of the real experiment were asked to report their mental strategies used during the different sessions (Table A.1.1).

Table A.1.1: Mental strategies of participants | Real experiment.

Subject ID	Mental Strategies
21	For all the sessions, the participant imagined the first stimulus on the left of an imaginary panel, while the second on the right.
22	For all the sessions, the participant tried to memorise the object of the first stimulus and then both after the presentation of the second one. After the cue, only the cued item was kept in memory.
23	For the first session, the participant associated the colour with a continent (Green=Europe, Red=America, Blue=Asia); for the second one, he thought of the initial letter of the geometrical shape; for the third one he tried to memorise the shape; while for the final one he associated the symbol to some Greek letters.
24	For all the first three sessions, the participant associated the stimuli with their verbal labels. Only during the final one, he tried to memorise the shapes. He also reported that (sometimes during the second session, and frequently during the third one) he remembered only one stimulus after the cue, and he answered by exclusion.
25	For all the sessions, the participant tried to memorise the object, he reported only some fatigue to do it in the first one (colour).
26	For all the sessions, the participant tried to memorise the object, he reported only some fatigue to do it in the first and the second ones (colour and shapes).

A.2 Subject Specific Feature Selection

The following section reports only the results from the univariate analysis.

A.2.1 Subject 21

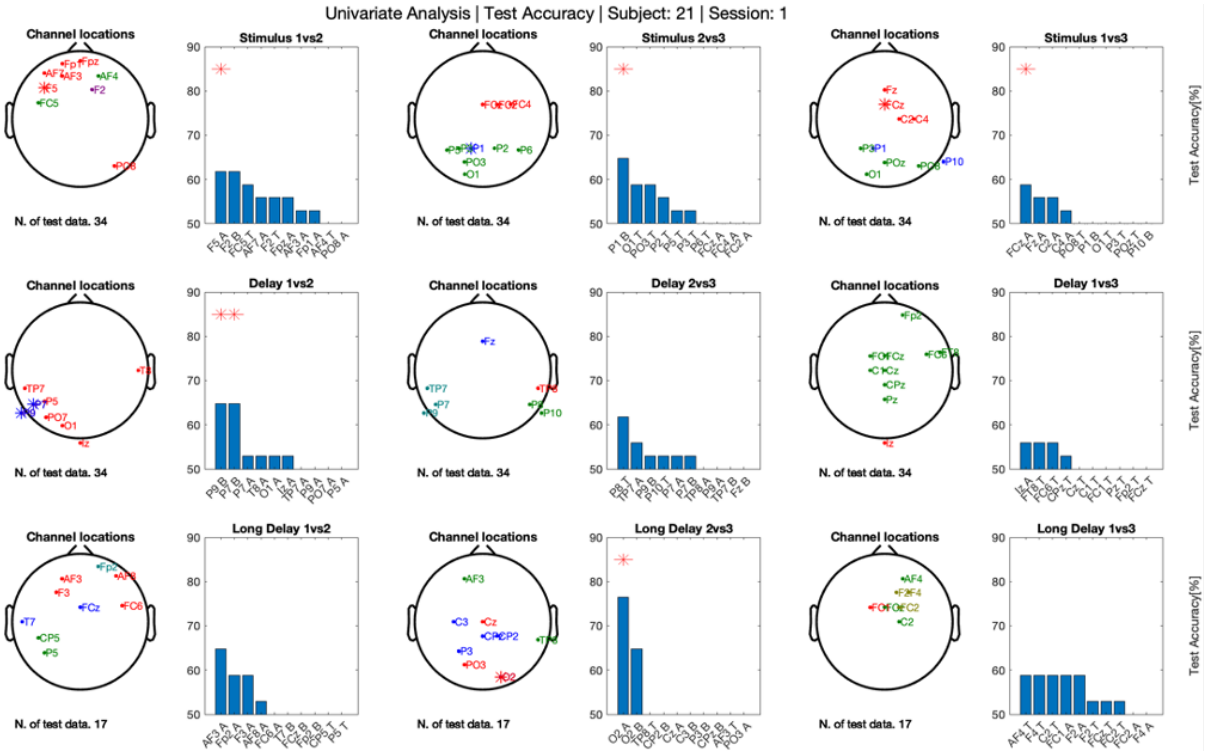

Figure A.2.1: Test Accuracy and Meaningful channel representation | Subject 21 | Session 1 | Univariate analysis.

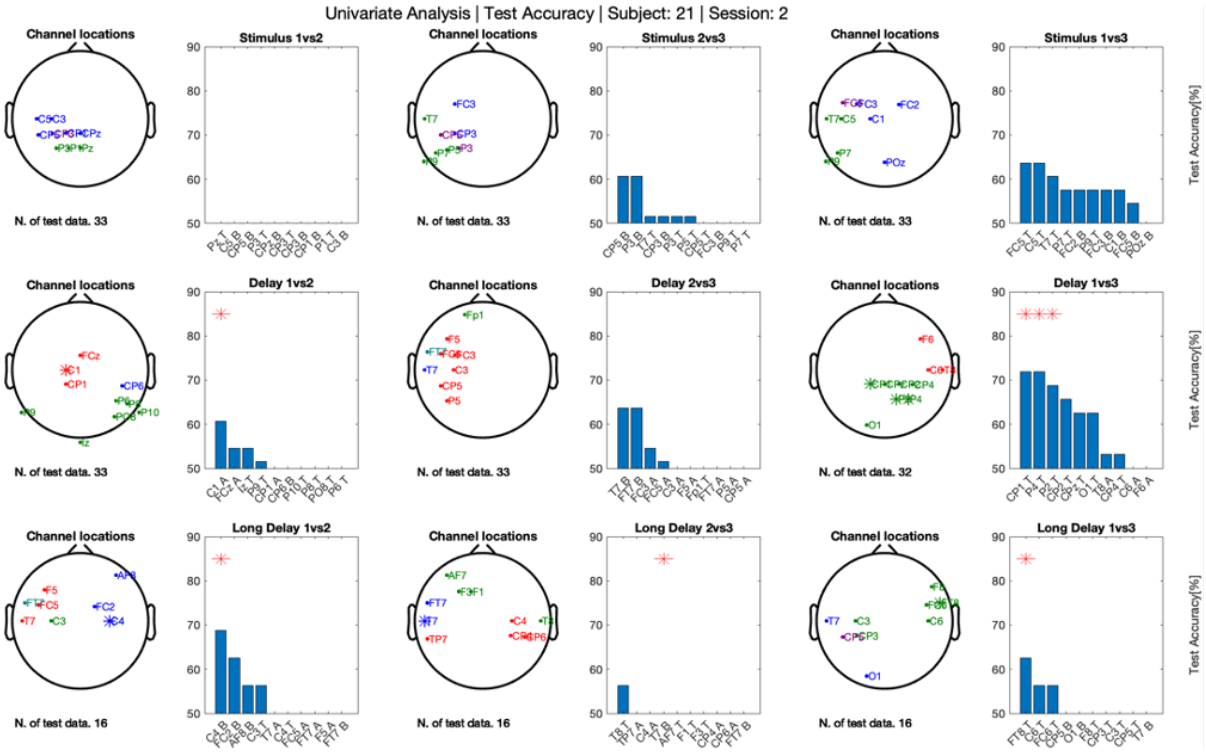

Figure A.2.2: Test Accuracy and Meaningful channel representation | Subject 21 | Session 2 | Univariate analysis.

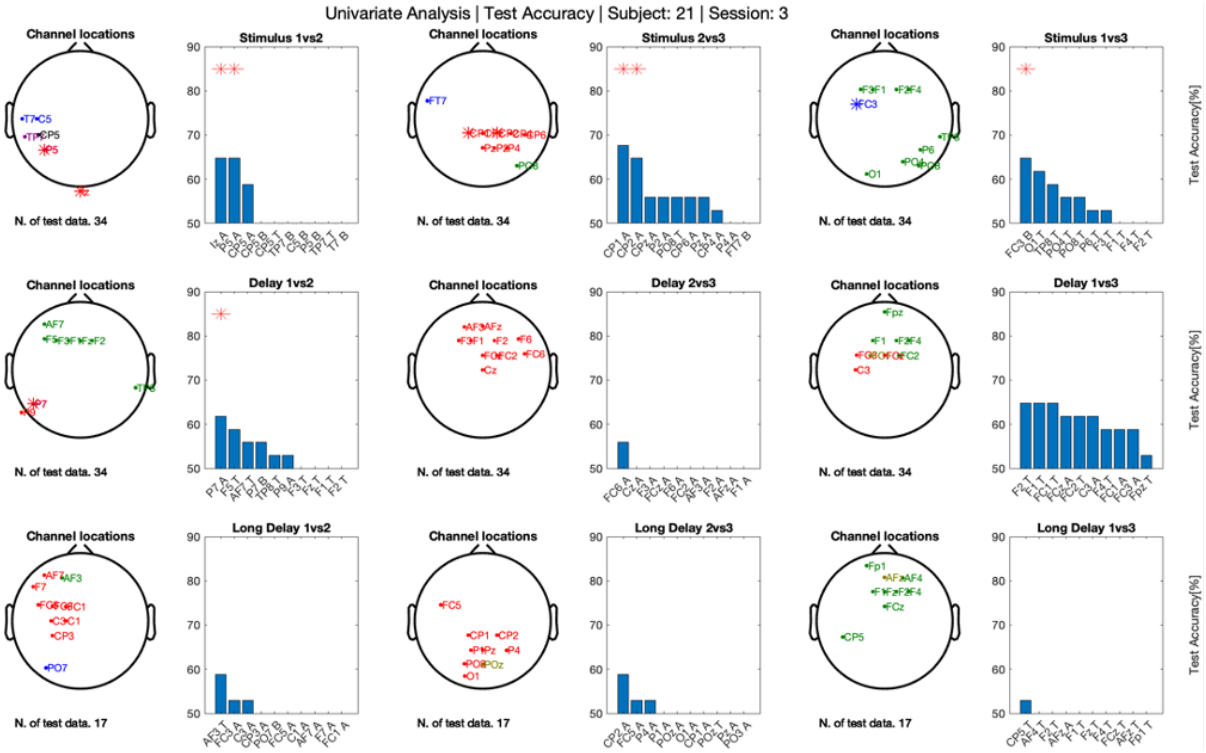

Figure A.2.3: Test Accuracy and Meaningful channel representation | Subject 21 | Session 3 | Univariate analysis.

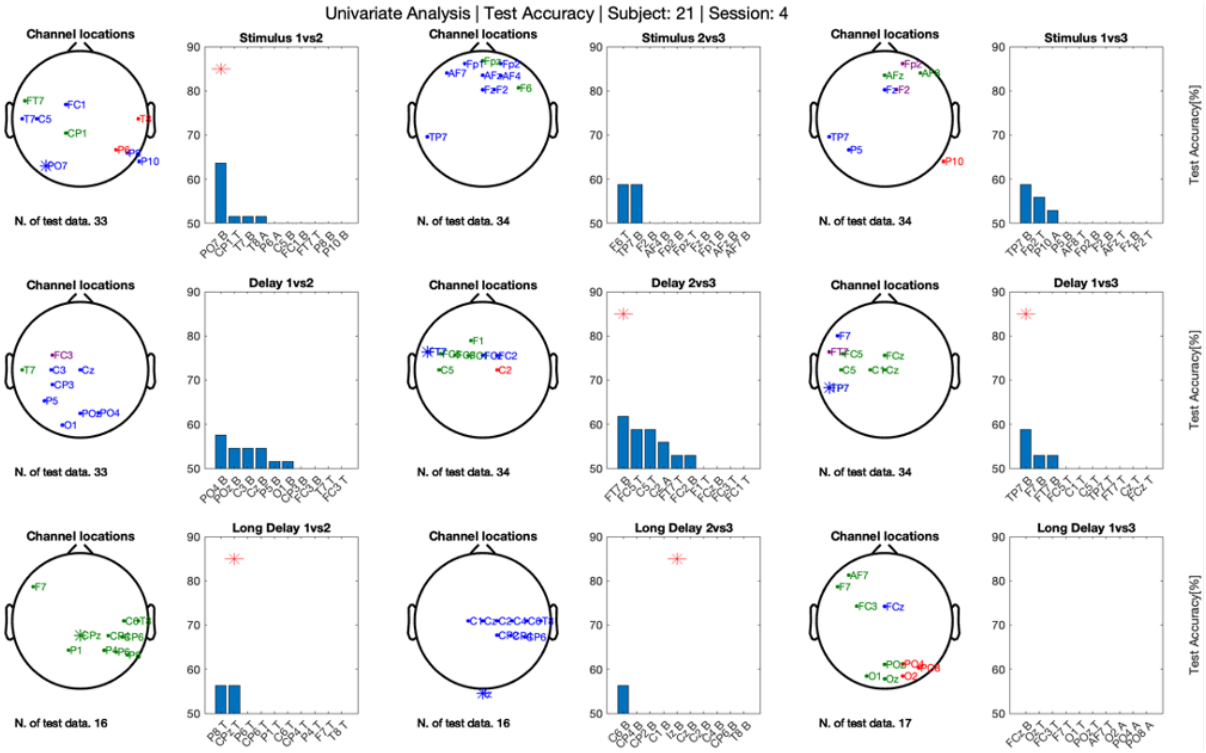

Figure A.2.4: Test Accuracy and Meaningful channel representation | Subject 21 | Session 4 | Univariate analysis.

A.2.2 Subject 22

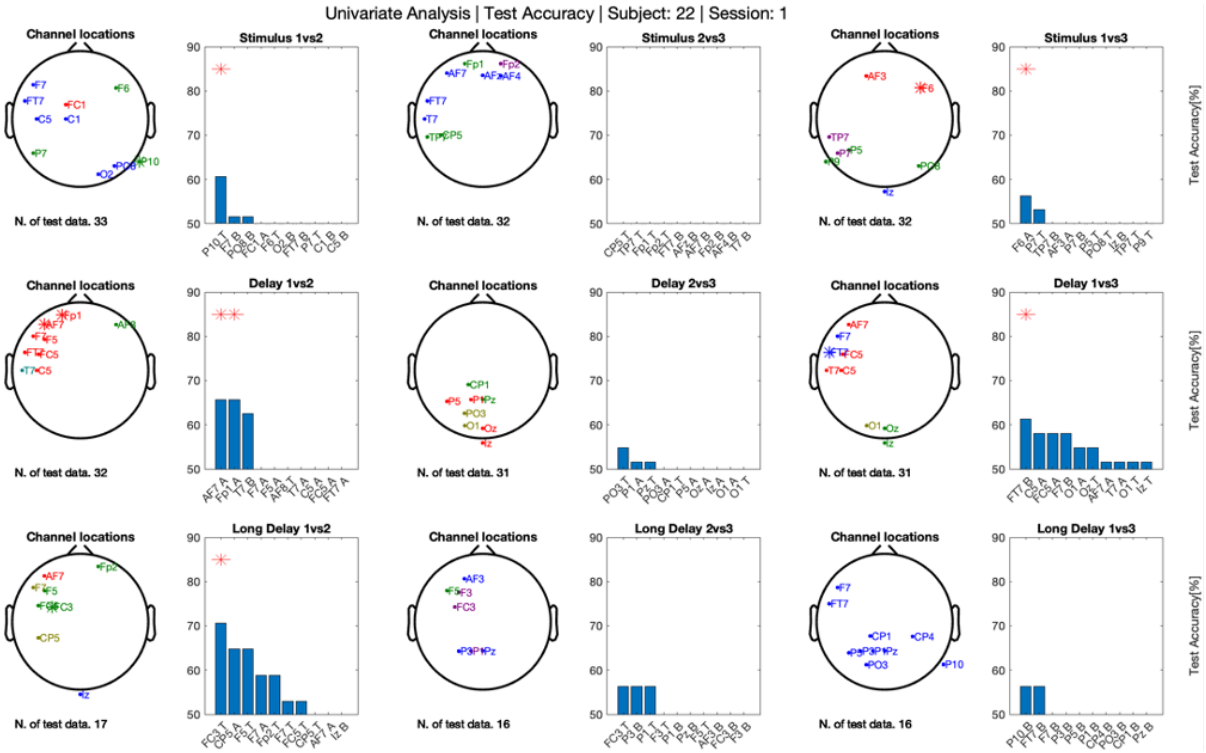

Figure A.2.5: Test Accuracy and Meaningful channel representation | Subject 22 | Session 1 | Univariate analysis.

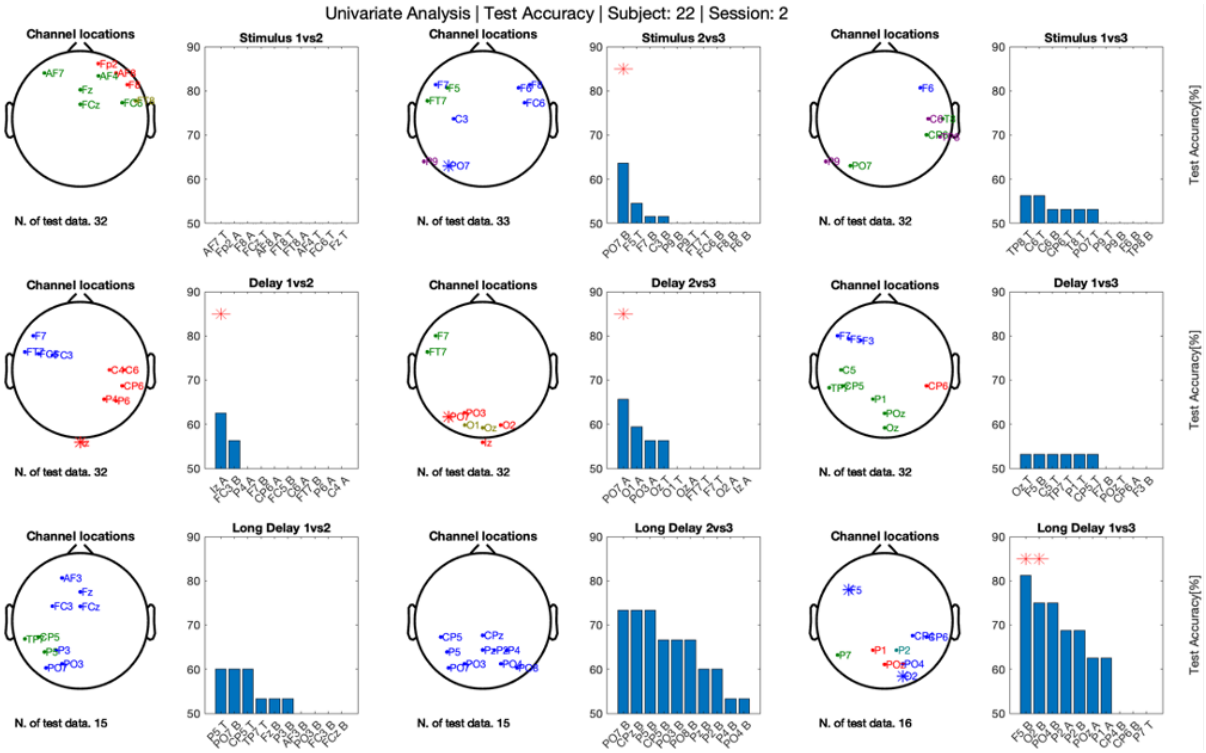

Figure A.2.6: Test Accuracy and Meaningful channel representation | Subject 22 | Session 2 | Univariate analysis.

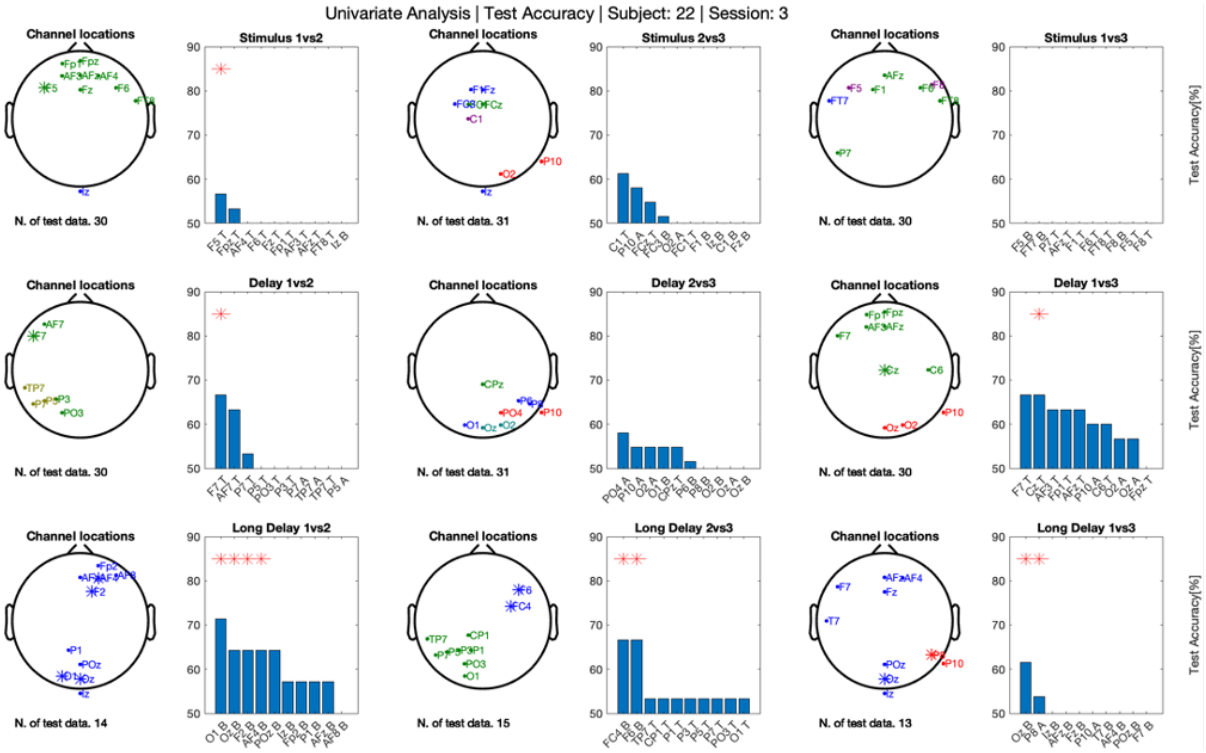

Figure A.2.7: Test Accuracy and Meaningful channel representation | Subject 22 | Session 3 | Univariate analysis.

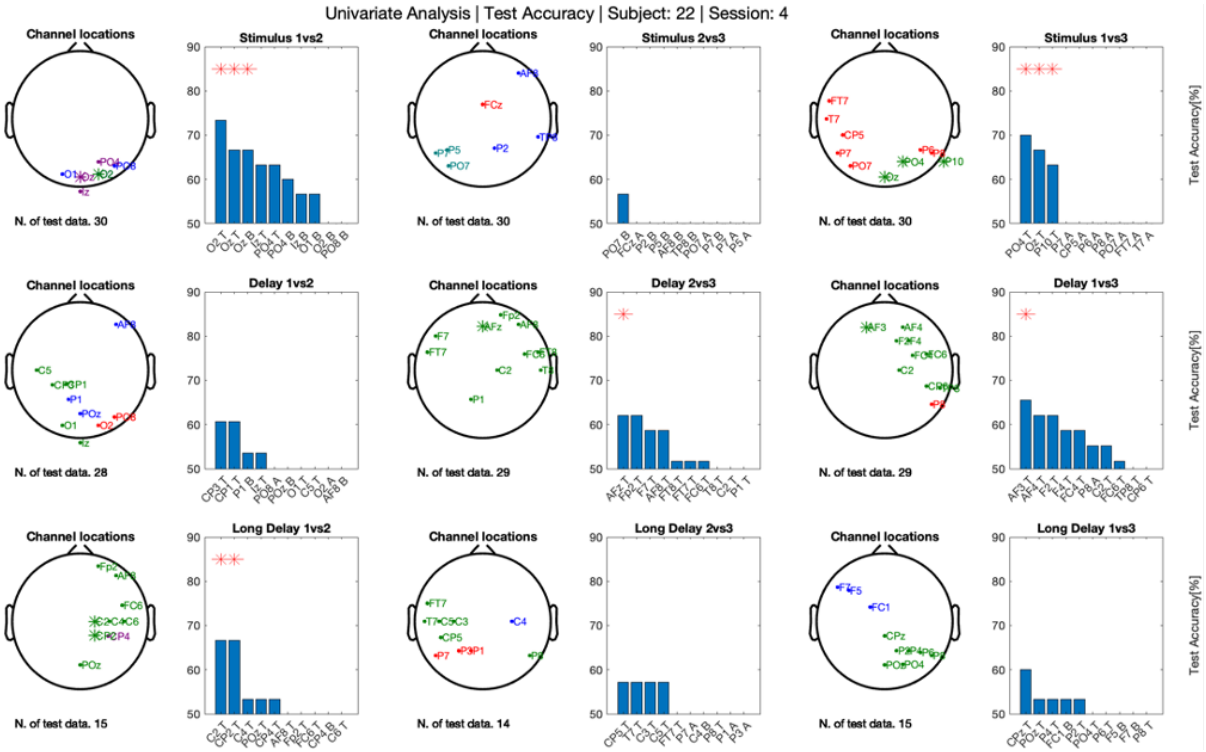

Figure A.2.8: Test Accuracy and Meaningful channel representation | Subject 22 | Session 4 | Univariate analysis.

A.2.3 Subject 23

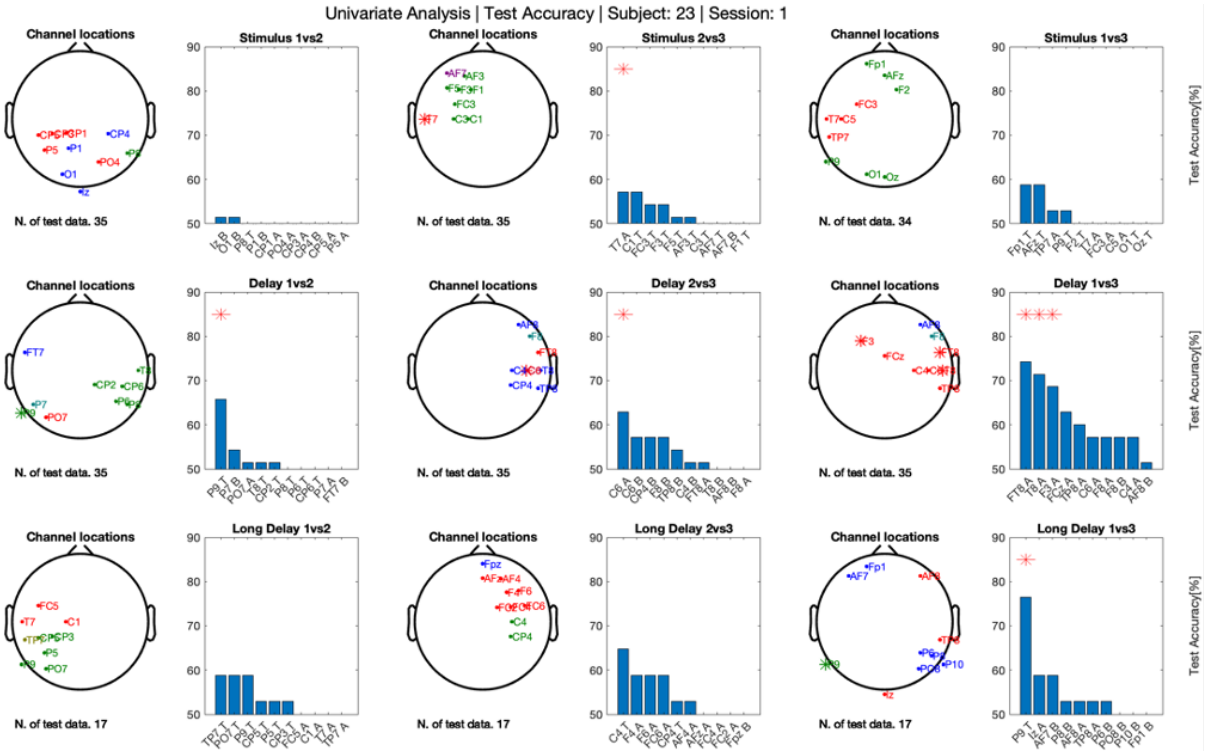

Figure A.2.9: Test Accuracy and Meaningful channel representation | Subject 23 | Session 1 | Univariate analysis.

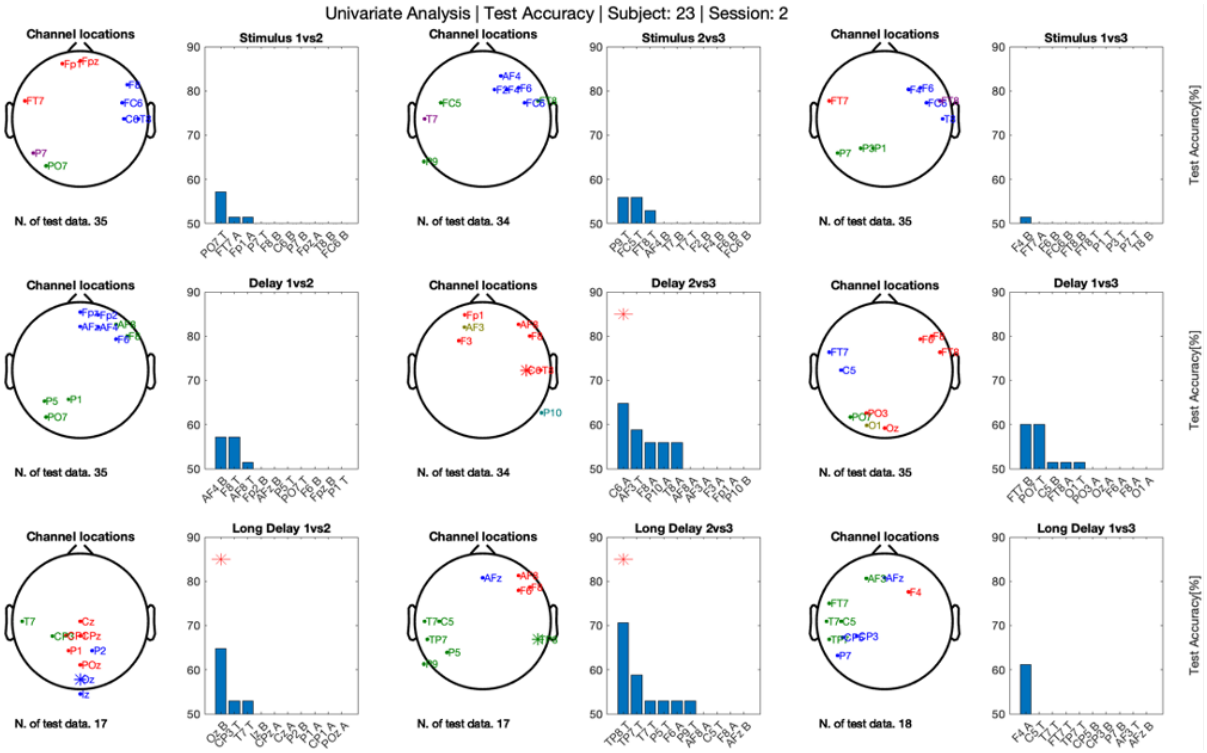

Figure A.2.10: Test Accuracy and Meaningful channel representation | Subject 23 | Session 2 | Univariate analysis.

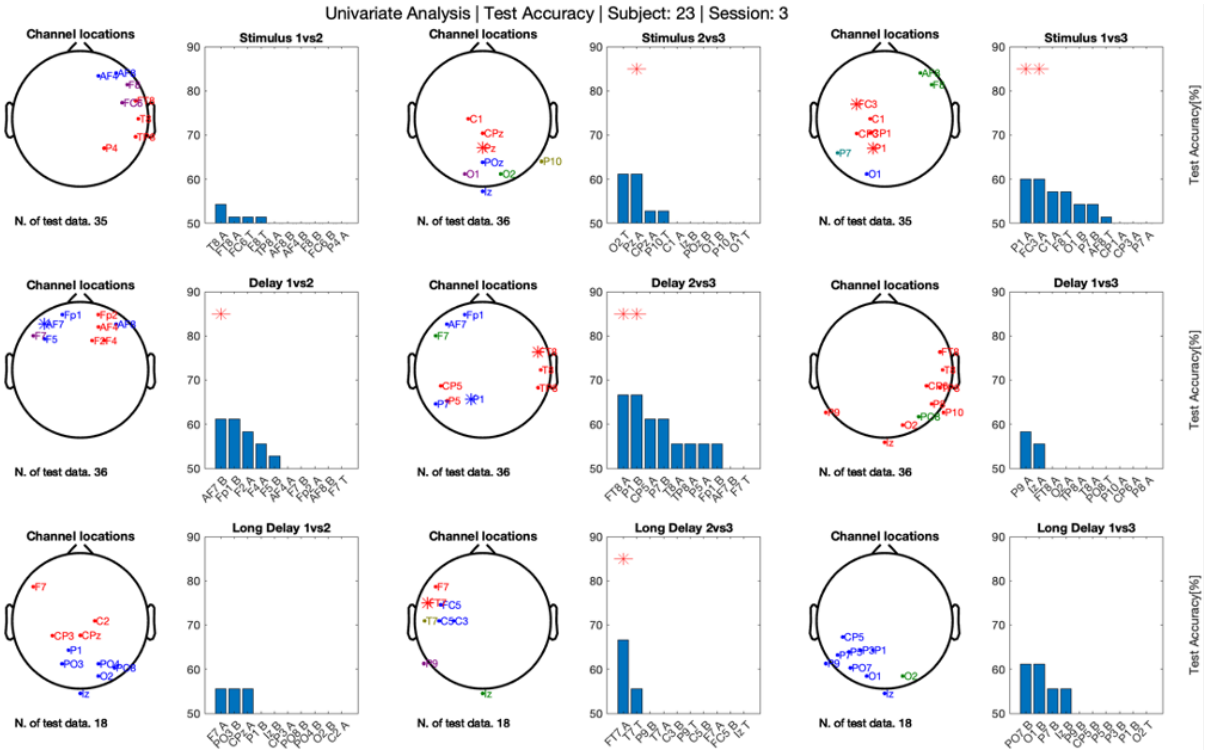

Figure A.2.11: Test Accuracy and Meaningful channel representation | Subject 23 | Session 3 | Univariate analysis.

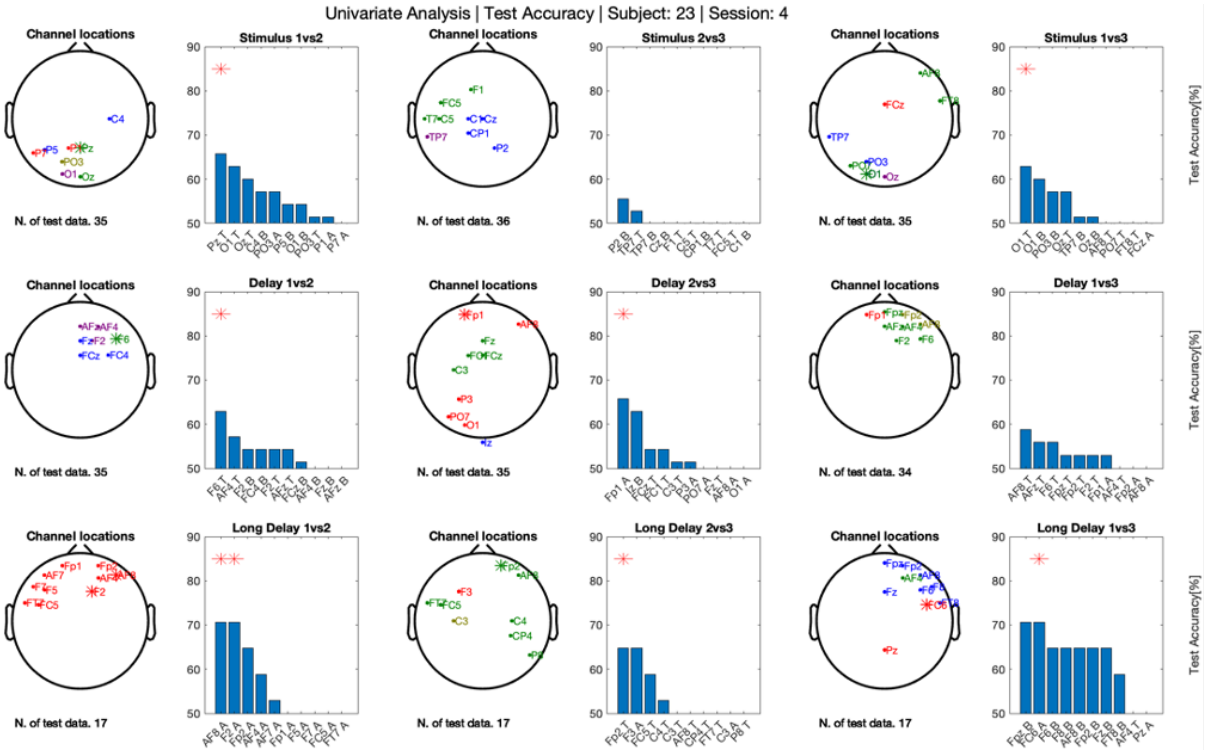

Figure A.2.12: Test Accuracy and Meaningful channel representation | Subject 23 | Session 4 | Univariate analysis.

A.2.4 Subject 24

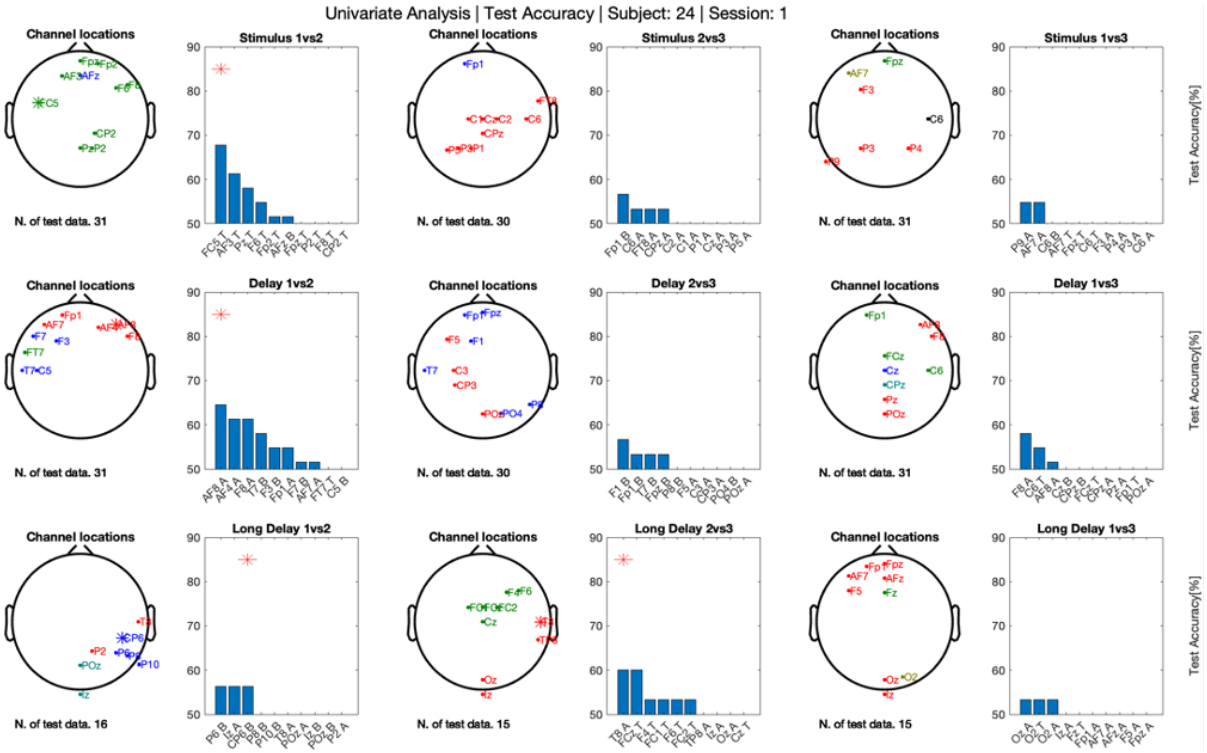

Figure A.2.13: Test Accuracy and Meaningful channel representation | Subject 24 | Session 1 | Univariate analysis.

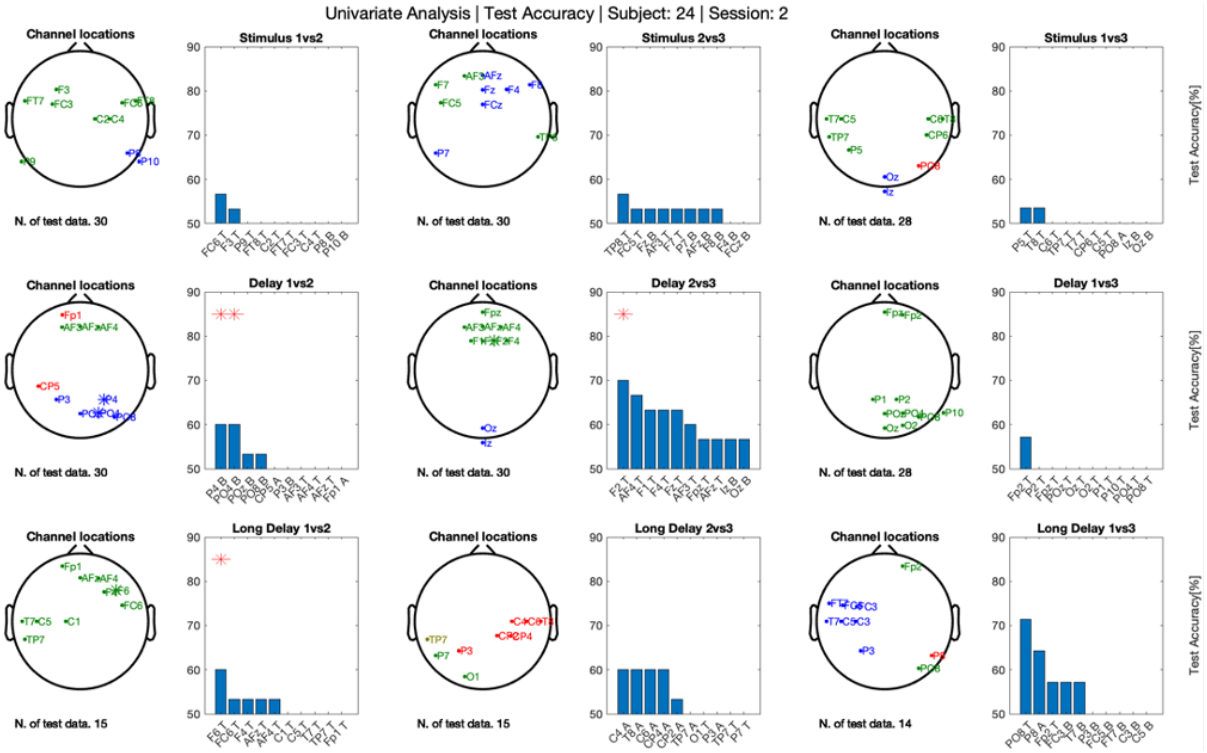

Figure A.2.14: Test Accuracy and Meaningful channel representation | Subject 24 | Session 2 | Univariate analysis.

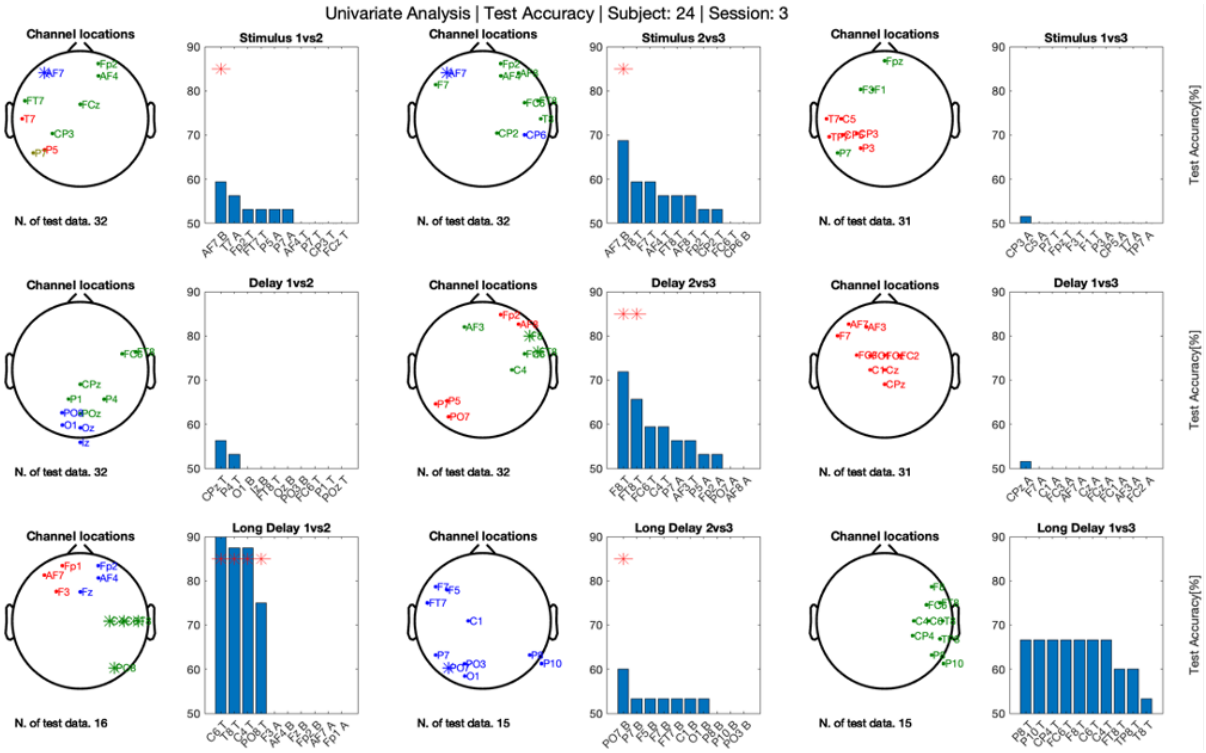

Figure A.2.15: Test Accuracy and Meaningful channel representation | Subject 24 | Session 3 | Univariate analysis.

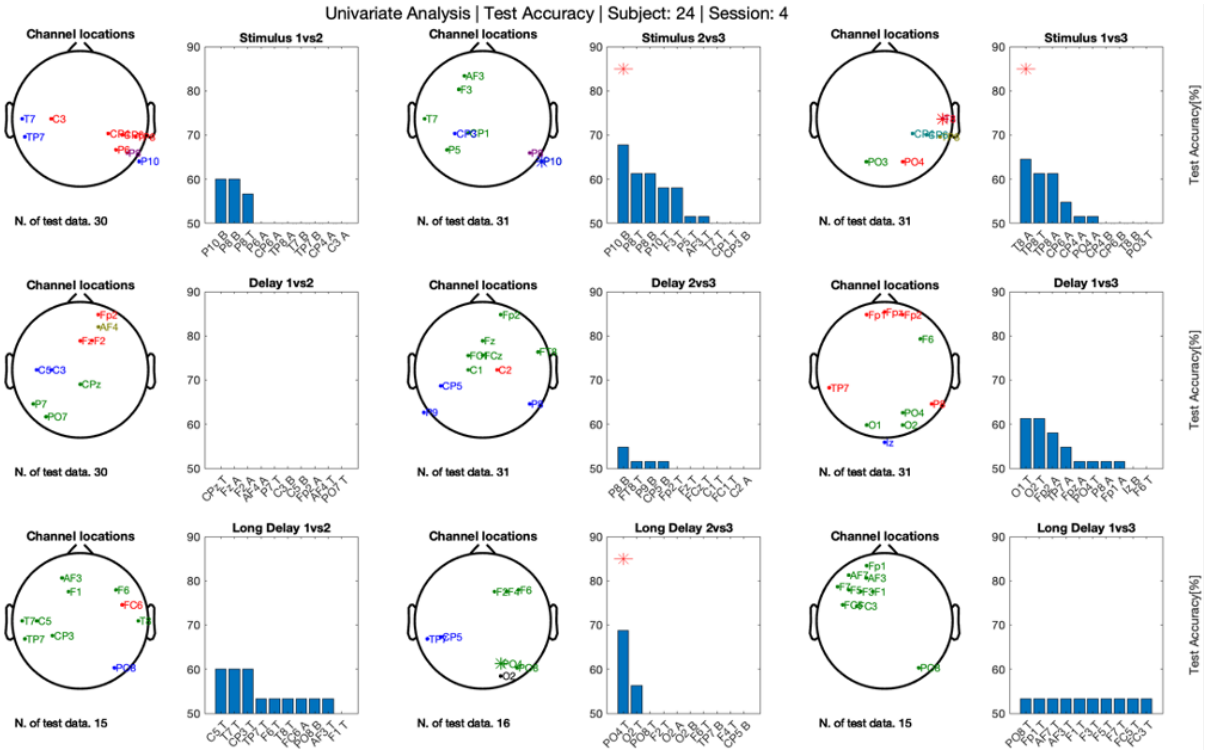

Figure A.2.16: Test Accuracy and Meaningful channel representation | Subject 24 | Session 4 | Univariate analysis.

A.2.5 Subject 25

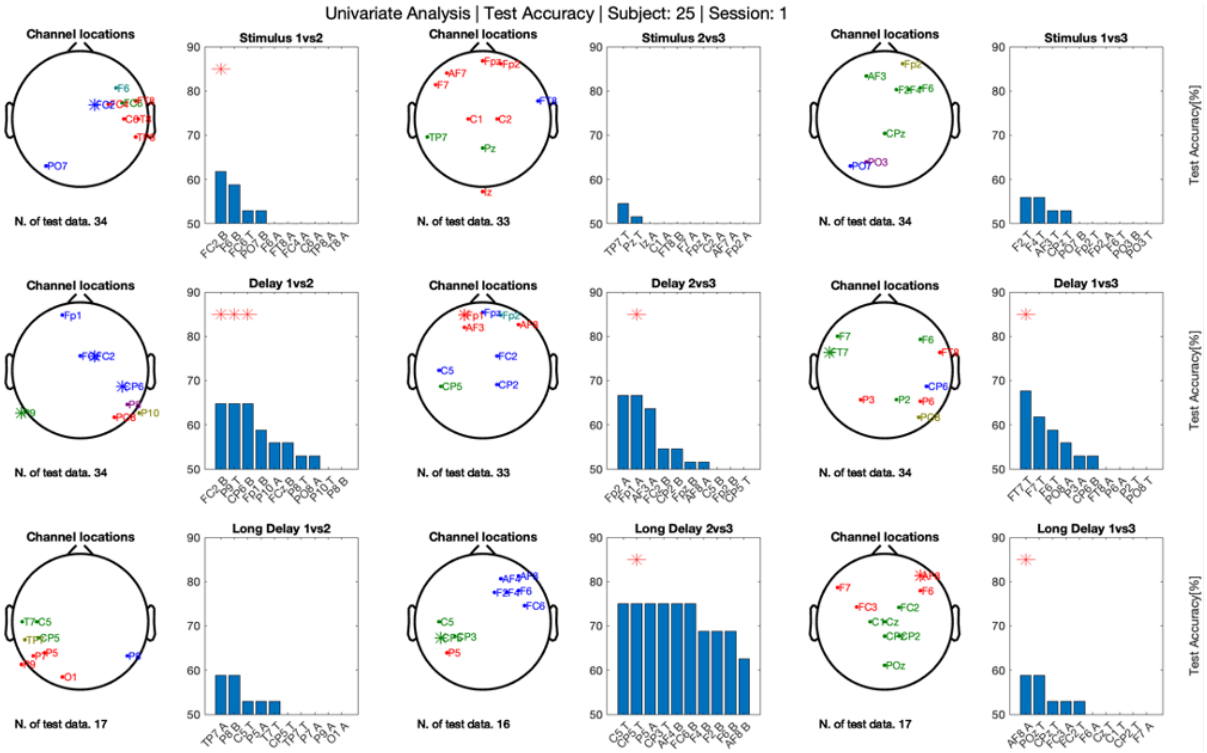

Figure A.2.17: Test Accuracy and Meaningful channel representation | Subject 25 | Session 1 | Univariate analysis.

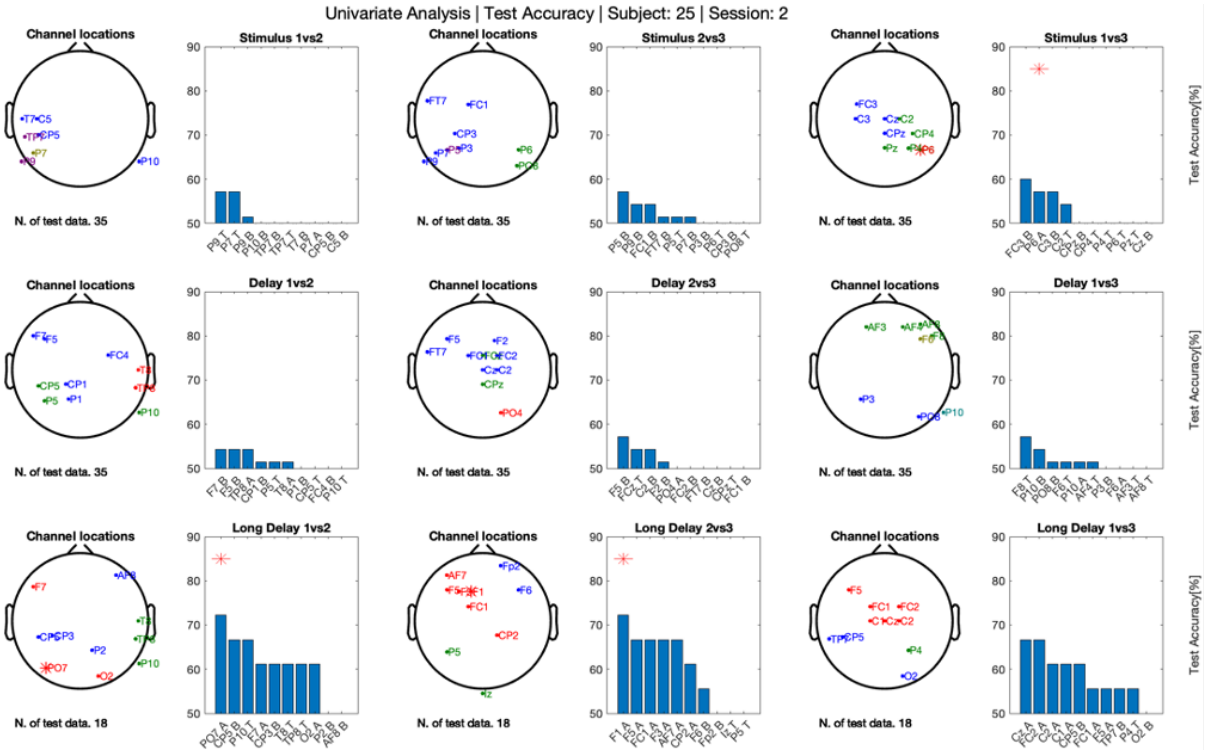

Figure A.2.18: Test Accuracy and Meaningful channel representation | Subject 25 | Session 2 | Univariate analysis.

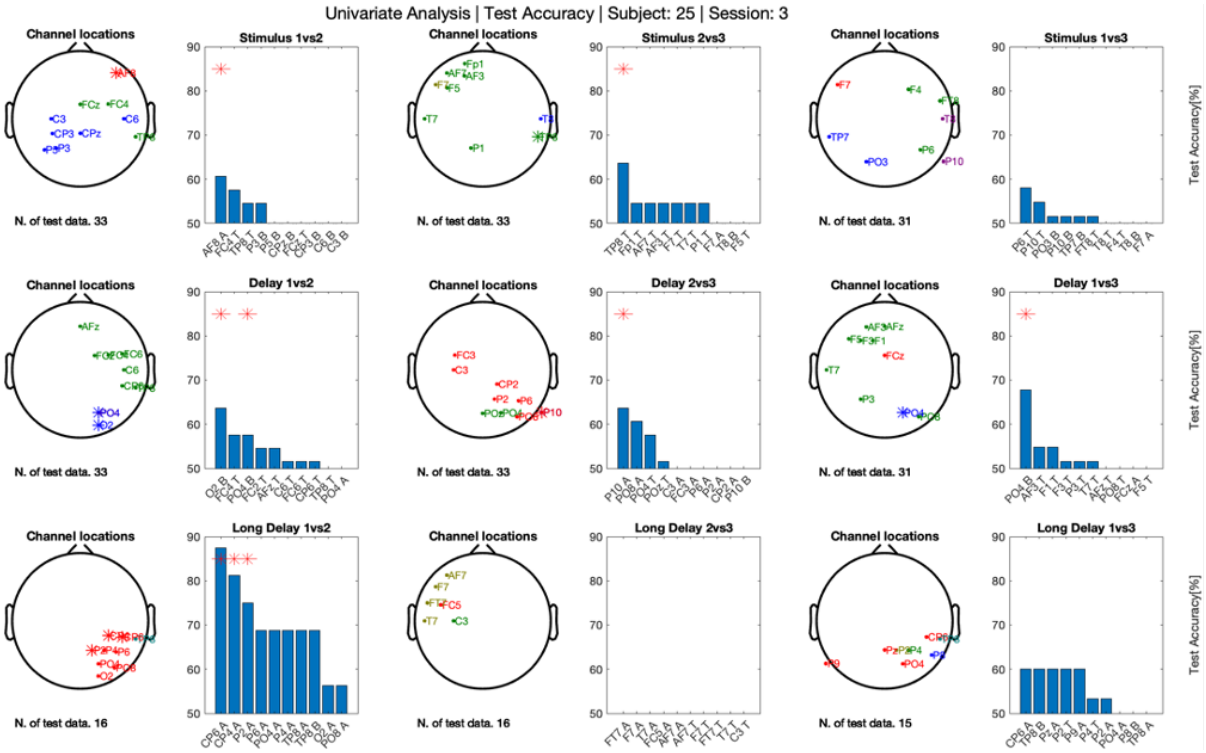

Figure A.2.19: Test Accuracy and Meaningful channel representation | Subject 25 | Session 3 | Univariate analysis.

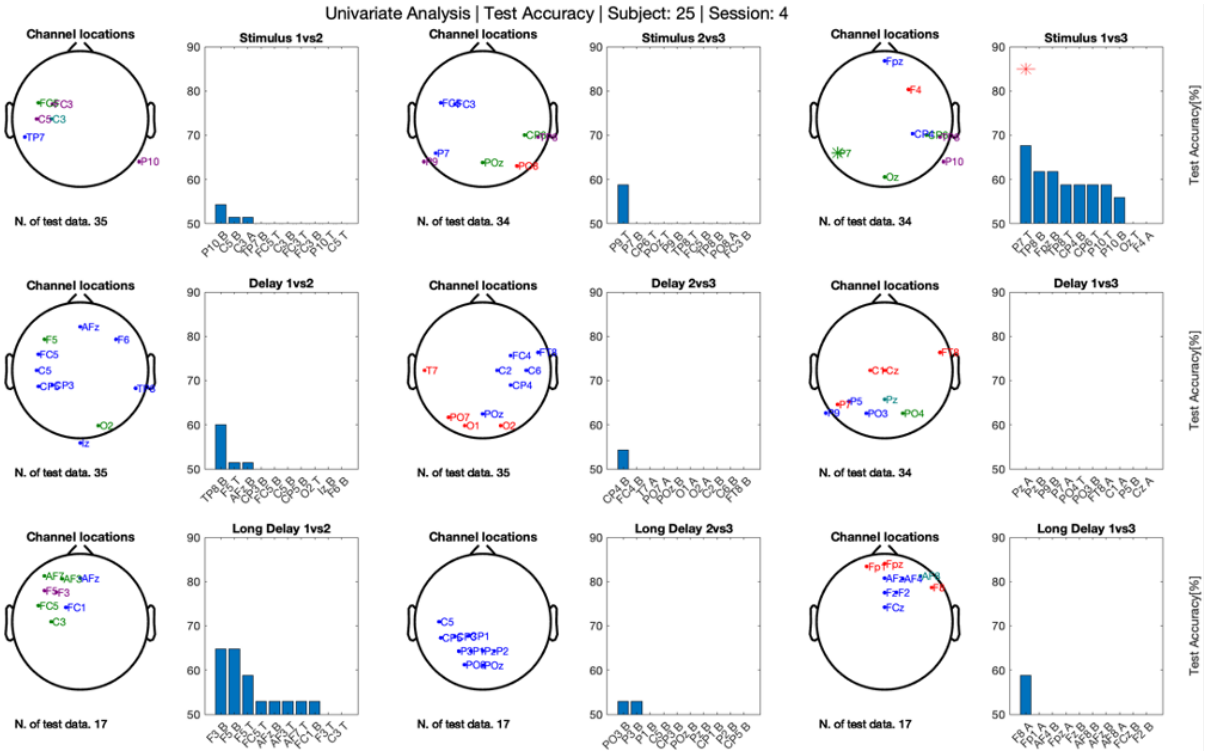

Figure A.2.20: Test Accuracy and Meaningful channel representation | Subject 25 | Session 4 | Univariate analysis.

Appendix B

Appendix | Pilots

This supplementary section has been used to precisely describe the pilot studies which have led to the final decisions for the experimental design. Firstly, in *"B.1 Interview on the Feasibility of the Experimental Design"* the interview with participant feedback about the feasibility of the protocol, especially in terms of fatigue and the protocol adjustments has been reported. Secondly, the behavioural performances of the three subjects have been described in *"B.2 Behavioural Performances"* highlighting the behavioural accuracies and the different response times over sessions. Moreover, the number of eye-related artefacts and the necessity of ICA-decomposition has been discussed in *"B.3 Eye-Artefact and ICA Components Removal"*, while the decision of trial rejection has been explained in *"B.4 Trial Rejection"*. Finally, the subjects-specific neurophysiological performances of subject 14 have been expressed in detail in *"B.5 Subject 14 – Effects of Different Mental Modalities - Univariate Analysis* to highlight the effect of different montal modalities on the performances.

B.1 Interview on the Feasibility of the Experimental Design

Considering the participants' feedback in (Table B.1.1), the adjustments seem a good trade-off between their well-being and the quality and quantity of the data.

Table B.1.1: Pilot Participant Interview..

Subject ID	**13**	**14**	**15**
Number of Sessions	2	3	4
Number of Trials per Session	90	90	90
Duration of a Trial	10 sec	10 sec	8 sec
Global Duration	$< 45\ min$	$< 1\ h$	$\sim\ 1\ h$
Presented Stimuli	**Colour:** RGB [255,0,0], [0,255,0], [0,0,255] on a black background [0,0,0].	**Colour:** RGB [255,0,0], [0,255,0], [0,0,255] on a black background [0,0,0]	**Colour:** RGB [230,80,80], [80,230,80], [80,80,230] on a grey background [0,0,0] **Orientation:** [60°, 180°, 300°]
Mental Memorisation Strategy	**Session 1:** Mainly Object. **Session 2:** Object and Verbal Label (repeated only once).	**Session 1:** Mainly Object. **Session 2:** Verbal Label (continuously repeated). **Session 3:** Object and Verbal Label (continuously repeated).	**All Sessions:** Mainly Object.
Level of Visual Fatigue	Before:4; After:5	Before:5; After:9.5	Before:4; After:6.5

Considerations	Blinking only at the response time is not hard with some home training.	The experiment should be shrunk. (Not so easy to blink only at the response time). The contrast of the colour over the background is too high. This condition has led to an increase in blinks during the trials. Thinking about a specific characteristic (object, label, or both) is not too hard, but with some training is better.	Over trials the blink at the right time is more mechanical. This shortened trial is not trivial, this led to: Confusion about objects of previous trials; Less capability to focus on the object (more use of verbal labels); Reconstruction of the first or second object by exclusion.
Adjustments	5 trials of preparation for each different stimulus (20 trials).	Reduction of the contrast between colour and background. Reduction of the trial duration from 10 sec to 8 sec.	Increase rest time for a total duration of the trial of 8.5 sec, to reduce the serial-dependence effect [76]

B.2 Behavioural Performances

The response accuracies (Figure B.2.1, Left) and response times (Figure B.2.1, right) are enough stable among sessions, this could be considered proof of the not excessive tiredness of the participants. Subject 13 had an improvement in time responses (especially a decrease in the standard deviation) and a little decrement in accuracy;

Subject 14 had a constant reduction of time responses and enhancement of accuracy (probably linked to task learning [56]); Subject 15 had a higher response time and a lot of non-answers compared to the previous participants. This could be linked to an excessive shrinkage of the trial duration.

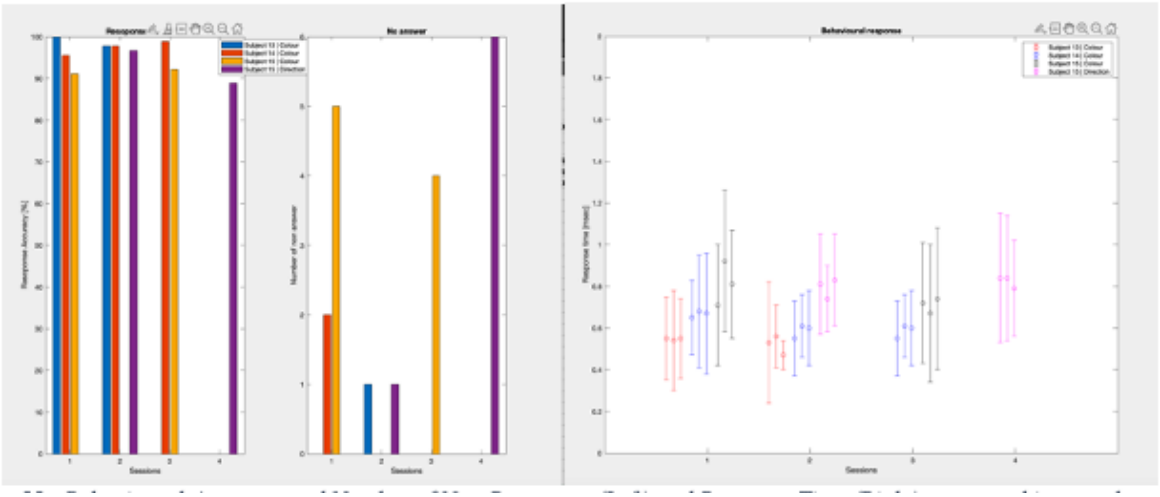

Figure B.2.1: Behavioural Accuracy and Number of Non-Responses (Left) and Response Time (Right) among subjects and sessions.

B.3 Eye-Artefact and ICA Components Removal

The number of trials affected by eye-related artefacts is very different across subjects and sessions (Table B.3.1). Subject 13 had a very limited number of eye-related artefacts because he was trained before the experiment to blink only at the correct timing. This result is very important because demonstrates that with some practice the ICA decomposition is not necessary. Therefore, the entire algorithm can be applied in real applications. On the other hand, the number of trials affected by eye-related artefacts is very high for subjects 14 and 15, who were not trained before. Considering the trends, it is possible to note the effects of fatigue for subject 14 (with a constant slight increase over sessions), and the opposite effects of learning and fatigue for subject 15, in which a strong initial decrease from session 1 to 2 is followed by a slow increase until the final one. It is important to note that Participant 15 reported that the blinks become more automatic over sessions, another promising symbol that eye-blink artefacts can be naturally mitigated with some practice.

Table B.3.1: Trials with Ocular Artefacts.

Subject ID	**Session**	**Number of Correct Trials**	**Number of Trials with Ocular Artefacts**	**Percentage of Trials with Ocular Artefacts**
13	1	90	1	1.1
	2	89	2	2.3
	1	86	47	54.7
14	2	88	55	62.5
	3	89	60	67.4
	1	82	62	75.6
15	2	87	33	37.9
	3	83	36	43.4
	4	80	45	56.3

The ICA components of the first session of subject 13 (Figure B.3.1) and the second session of subject 14 (Figure B.3.2) have been reported sorted by the variance of the components and classified by the EEGLAB toolbox ICA Labels. In the first case, eye-related components (4, 18, and 49) explained only 7.8% of the variance; while in the second one, components 1, 9, and 42 explained 70% of the variance. In the end, from the first dataset, components 4 18 25 32 38 44 45 47 49 52 54 55 56 58 59 63 have been discarded, while components 1 9 15 23 24 36 38 40 42 44 48 54 57 59 62 63 have been excluded from the second one. It is important to note, that all the rejected non-eye-related components have been mainly caused by muscular activity or small deviations in the channel signals. These components are temporally very localised, and a simple trial removal could have removed them, but it has been decided to remove them with ICA in order to maximise the number of residual trials.

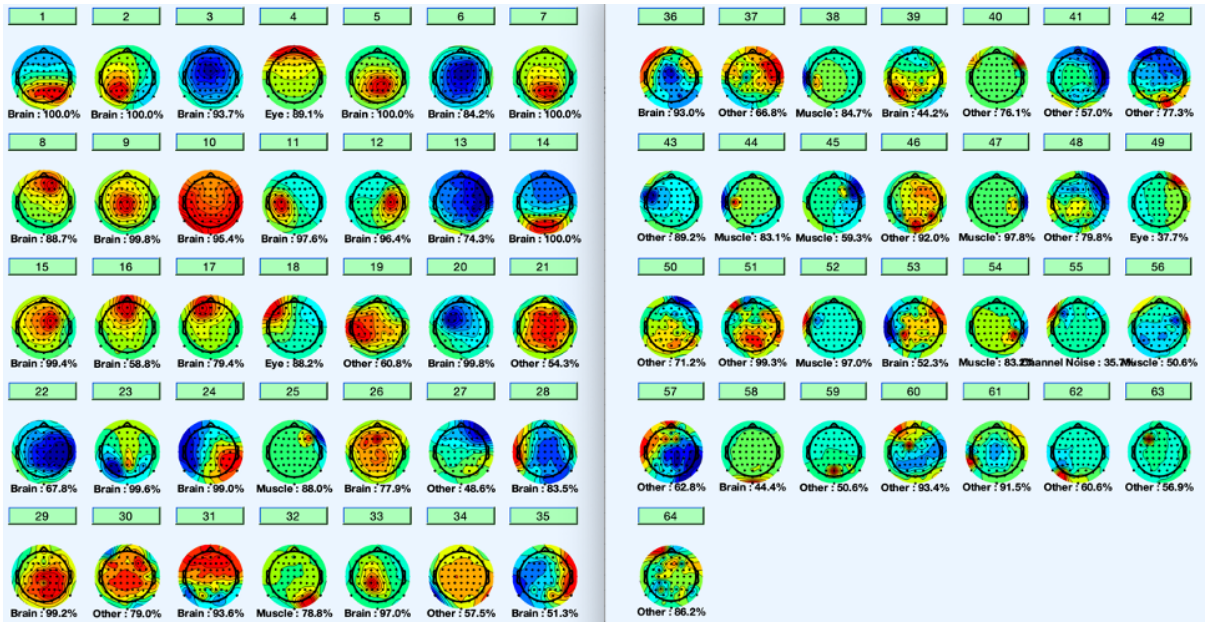

Figure B.3.1: ICA components | Subject 13 | Session 1.

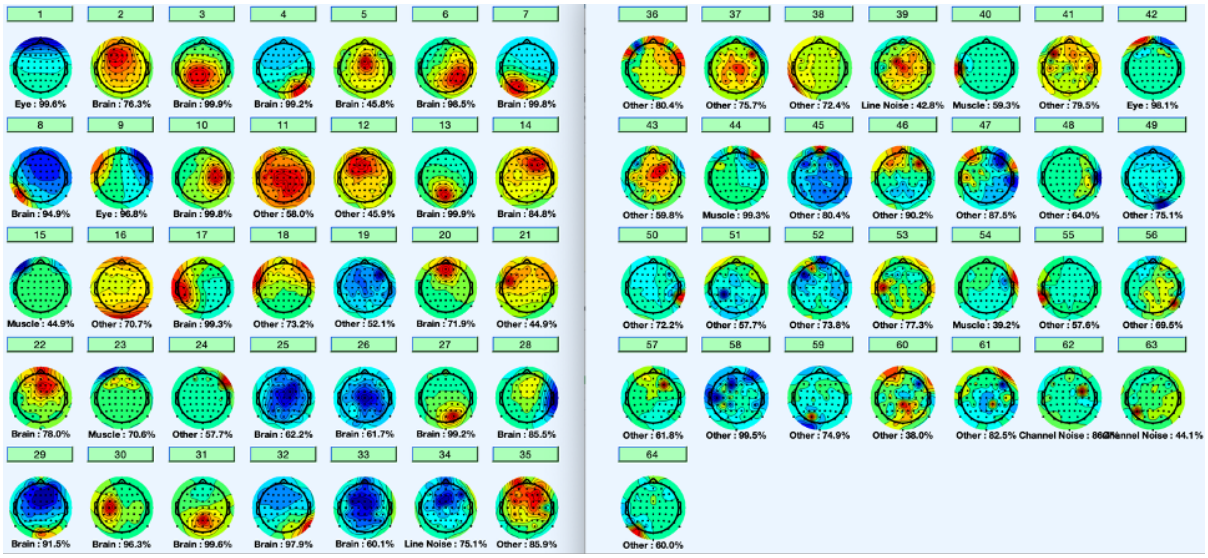

Figure B.3.2: ICA components | Subject 14 | Session 2.

B.4 Trial Rejection

Despite the use of ICA decomposition, some trials have persistent high-frequency artefacts (probably linked to muscle contraction) even after ICA reconstruction. To examine these undesired components all the trials have been visually inspected before and after ICA reconstruction. Figure B.4.1 shows an example of persistent high-frequency artefact in trial 36 (enumerated as 136) that was present in all the interest subparts (2,3,4,5,7), compared to trial 37 (enumerated as 137) of the second session of

subject 14. Therefore, the whole trial 36 has been discarded before ICA decomposition (in the figure it is shown before ICA decomposition).

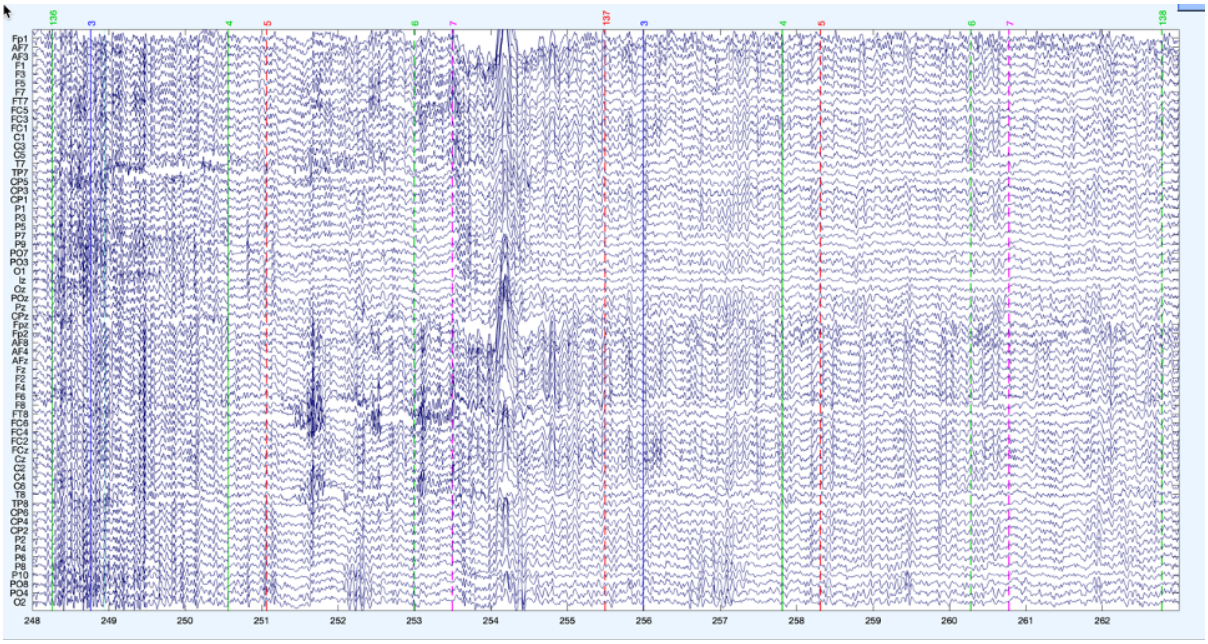

Figure B.4.1: Example of artefact resistant to ICA decomposition | Trial 36 compared to Trial 37 | Subject 14 | Session 2.

B.5 Subject 14 – Effects of Different Mental Modalities - Univariate Analysis

The results of the univariate analysis for subject 14, session 1, session 2, and session 3 have been reported in Figure B.5.1, Figure B.5.2, Figure B.5.3 respectively. Stimulus presentation discriminability is similar enough among different mental representations, driven by Posterior-Occipital alpha activities. The short delay is very discriminant in sessions 1 and 3 by Fronto-Central and Parieto-Occipital theta and alpha bands, while only a spurious Central beta channel is significant in the second session. Finally, the long delay is enough different across modalities, Centro-Parietal in beta and theta for sessions 1 and 2, while Frontal theta and beta and Parieto-Occipital theta for session 3.

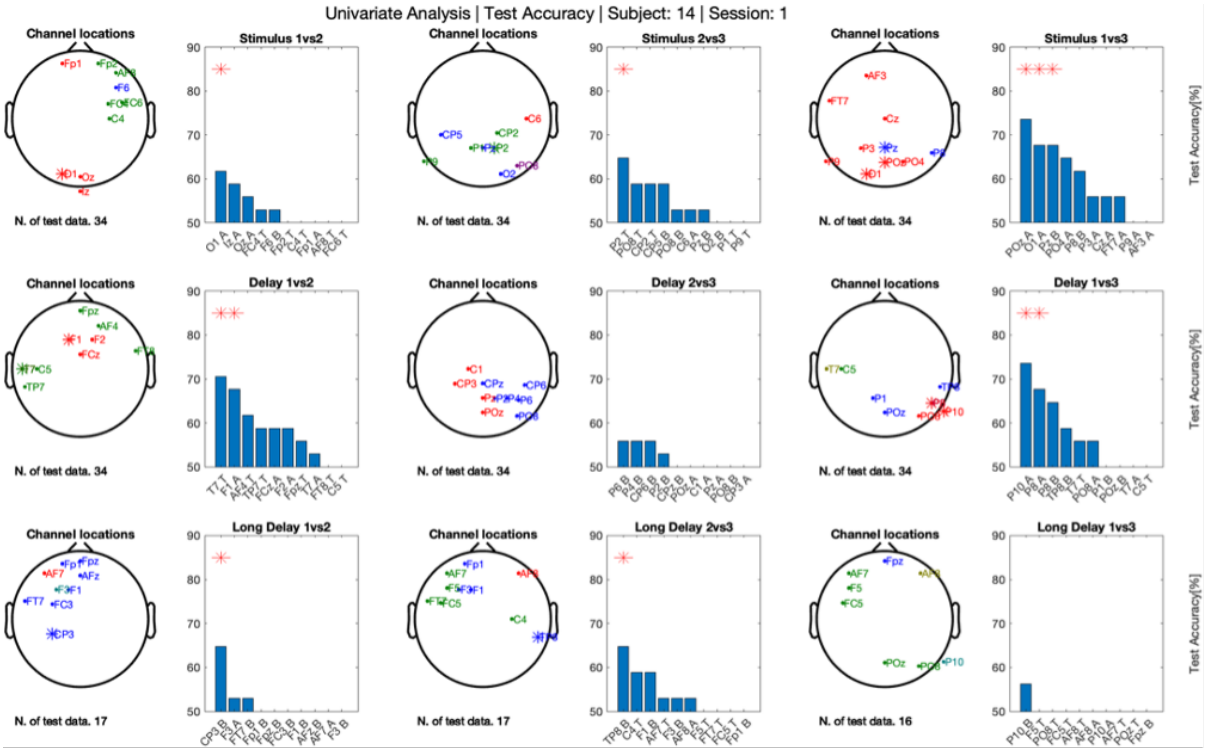

Figure B.5.1: Test Accuracy and Meaningful channel representation | Subject 14 | Session 1 | Univariate analysis.

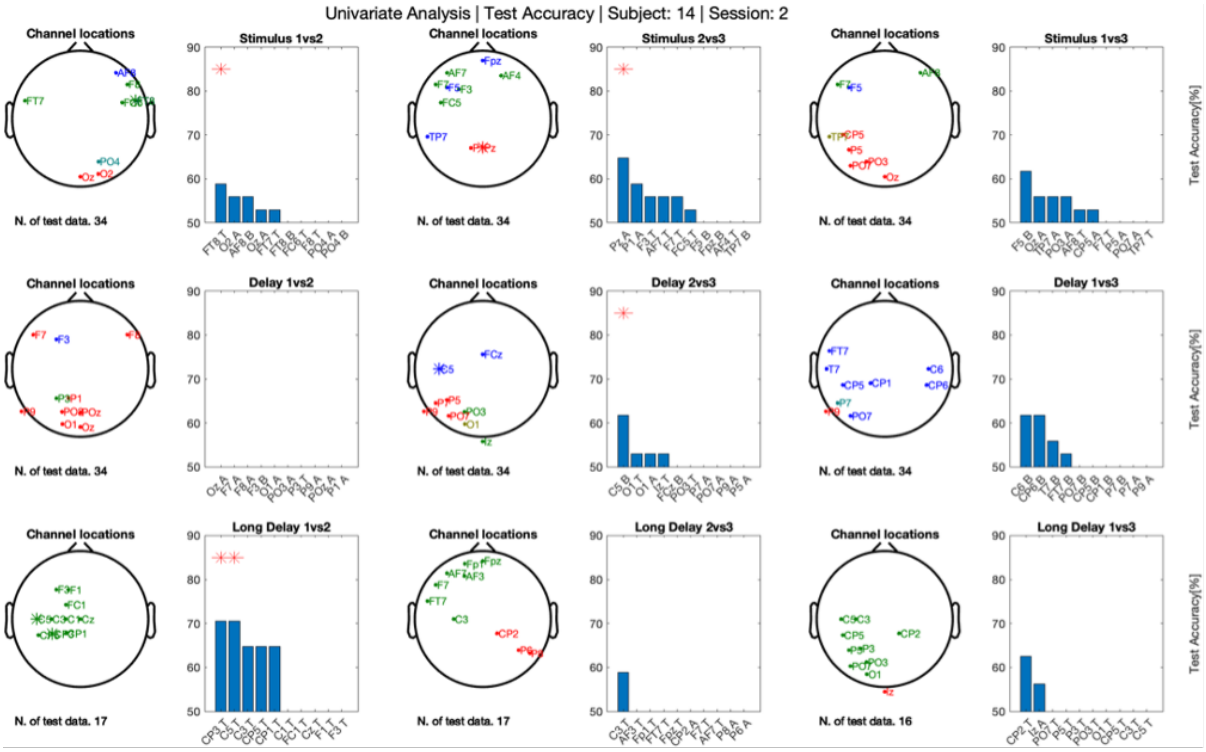

Figure B.5.2: Test Accuracy and Meaningful channel representation | Subject 14 | Session 2 | Univariate analysis.

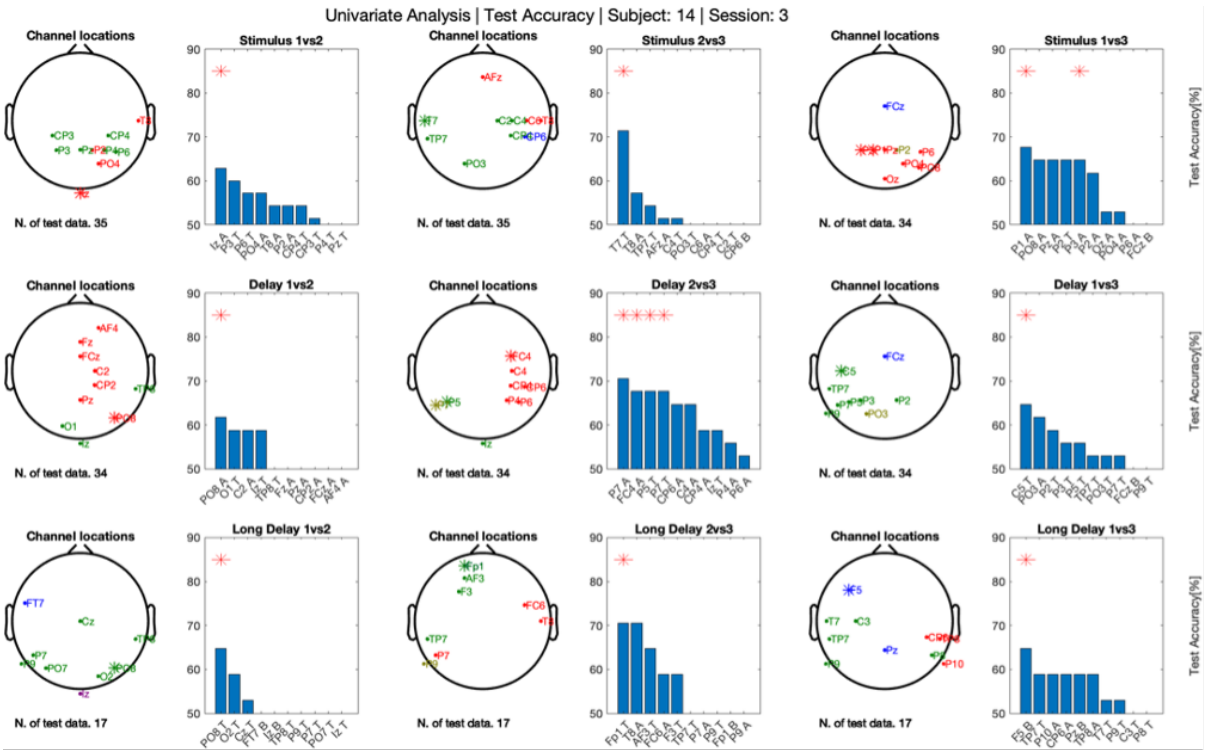

Figure B.5.3: Test Accuracy and Meaningful channel representation | Subject 14 | Session 3 | Univariate analysis.

From this analysis of subject 14 seems that the different modalities of thinking about the object are very influential on the performances and on the discriminable areas. It seems that stimulus presentation and the short delay are more identifiable when the subject tries to remember the object or the object and its verbal label; while the long delay is more identifiable when there is not only the object memorisation. Therefore, during the real experiment, all the subjects were asked to memorise mainly the object.